

A 3D cutaway diagram of the Mu2e experiment detector. The diagram shows a long, cylindrical detector structure with various internal components, including a central beam pipe and surrounding shielding. The detector is shown in a perspective view, with a green translucent outer shell and a yellow translucent inner shell. A red dashed line indicates the path of a particle beam through the detector. The detector is mounted on a complex support structure.

# Mu2e : Searching for $\mu^- N \rightarrow e^- N$ at Fermilab

*Presented by Sophie Charlotte Middleton  
Research Associate at Caltech  
University of Michigan  
October 2021*

*\*smidd@caltech.edu*

# Outline



CHARGED LEPTON FLAVOR VIOLATION (CLFV)



THE GLOBAL SEARCH FOR CLFV AND COMPLEMENTARITY



HOW CAN MU2E HELP US UNDERSTAND BEYOND STANDARD MODEL PHYSICS?



THE MU2E EXPERIMENT



THE MU2E-II EXPERIMENT



SUMMARY



Mu2e: Searching for  $\mu^- N \rightarrow e^- N$  at Fermilab

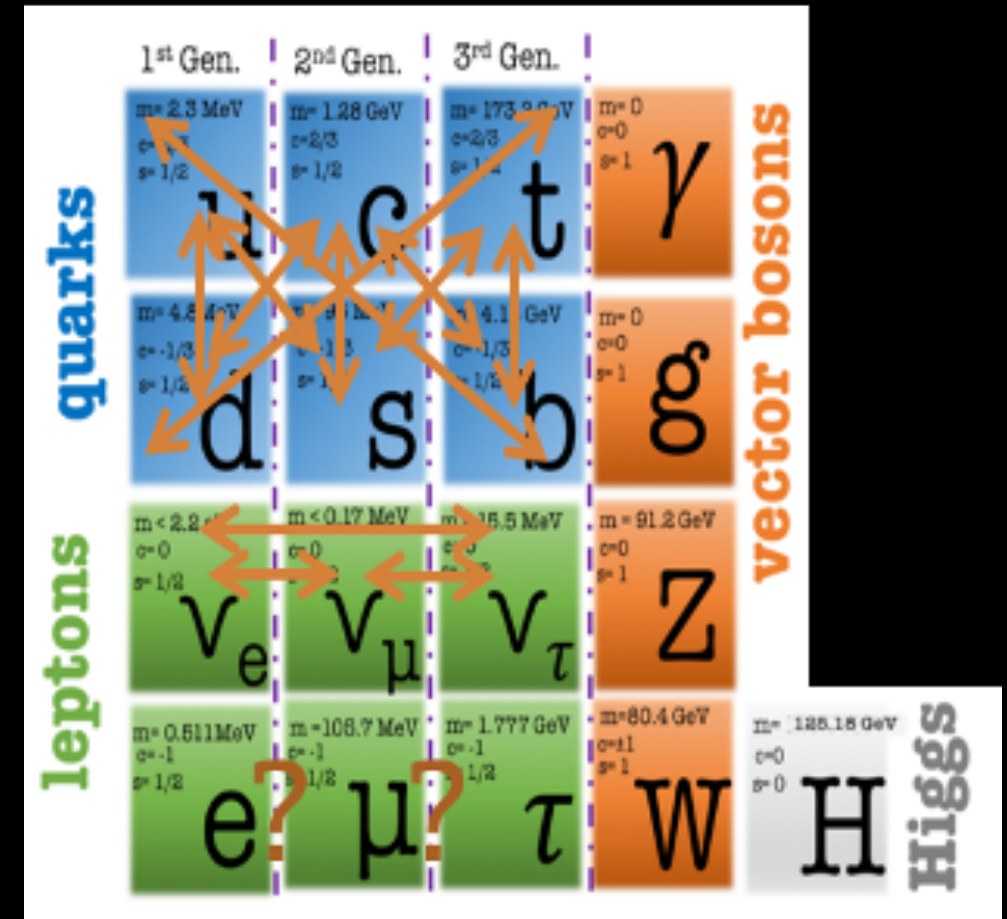


# Quark Flavor Violation



- The quarks commit Flavour Violation -

*Mixing strengths are parameterized by Cabibbo–Kobayashi–Maskawa (CKM) matrix:*



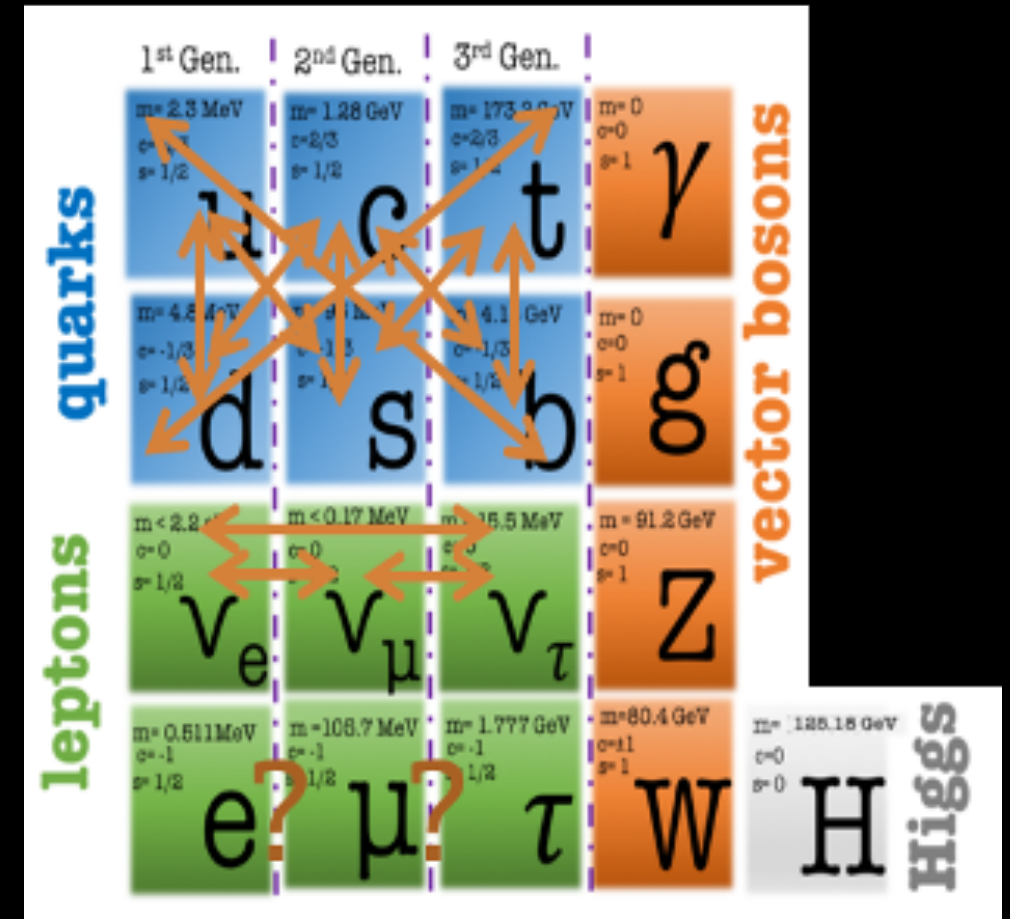
# Quark Flavor Violation



- The quarks commit Flavour Violation -

*Mixing strengths are parameterized by Cabibbo–Kobayashi–Maskawa (CKM) matrix:*

$$(d', s', b') = \begin{pmatrix} V_{ud} & V_{us} & V_{ub} \\ V_{cd} & V_{cs} & V_{cb} \\ V_{td} & V_{ts} & V_{tb} \end{pmatrix} \begin{pmatrix} d \\ s \\ b \end{pmatrix}$$



# Quark Flavor Violation

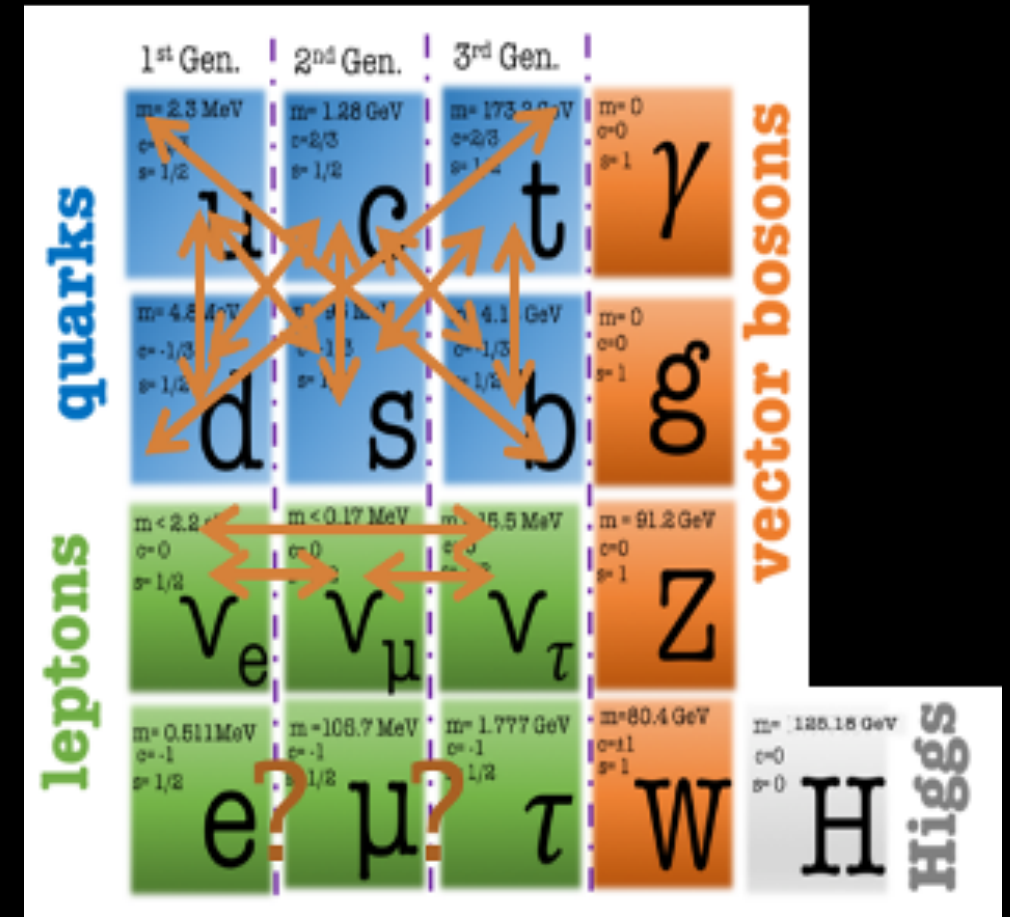


- The quarks commit Flavour Violation -

*Mixing strengths are parameterized by Cabibbo–Kobayashi–Maskawa (CKM) matrix:*

$$(d', s', b') = \begin{pmatrix} V_{ud} & V_{us} & V_{ub} \\ V_{cd} & V_{cs} & V_{cb} \\ V_{td} & V_{ts} & V_{tb} \end{pmatrix} \begin{pmatrix} d \\ s \\ b \end{pmatrix}$$

→ almost diagonal.

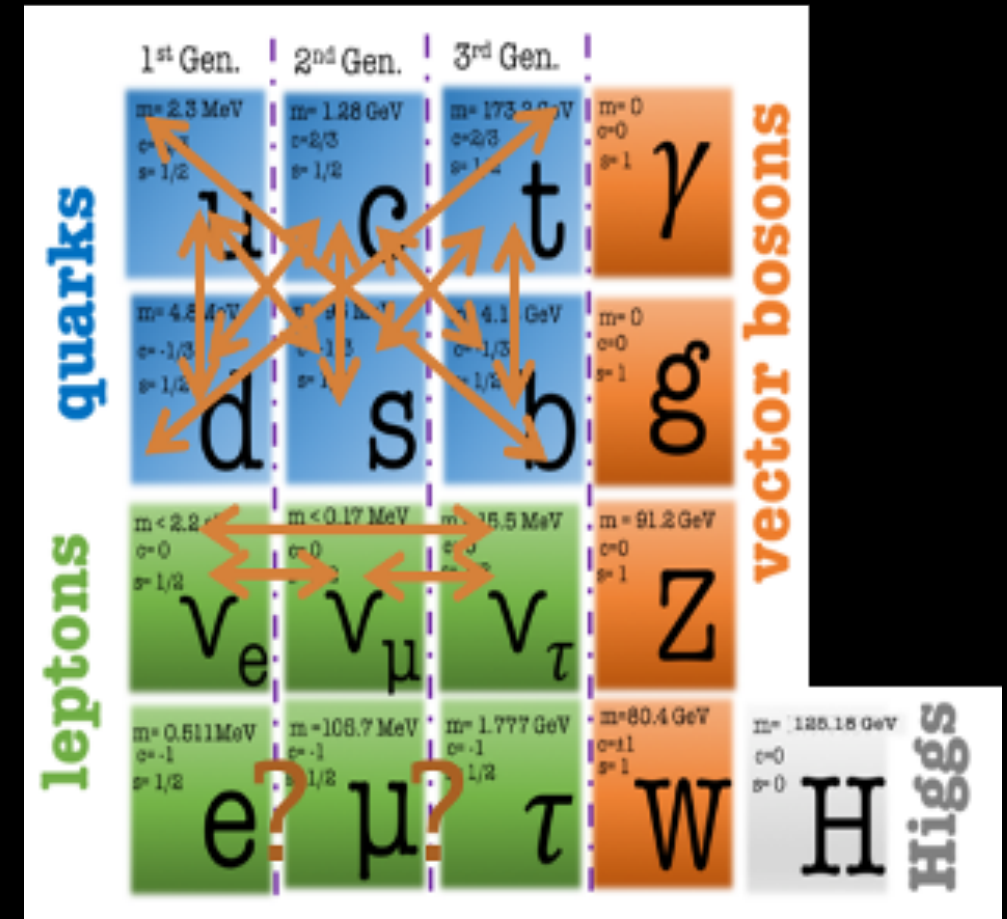


# Neutral Lepton Flavor Violations



- $\nu$  oscillations  $\rightarrow$  Lepton Flavour Violation (LFV)

*Mixing strengths parameterised by the Pontecorvo–Maki–Nakagawa–Sakata matrix (PMNS) matrix:*





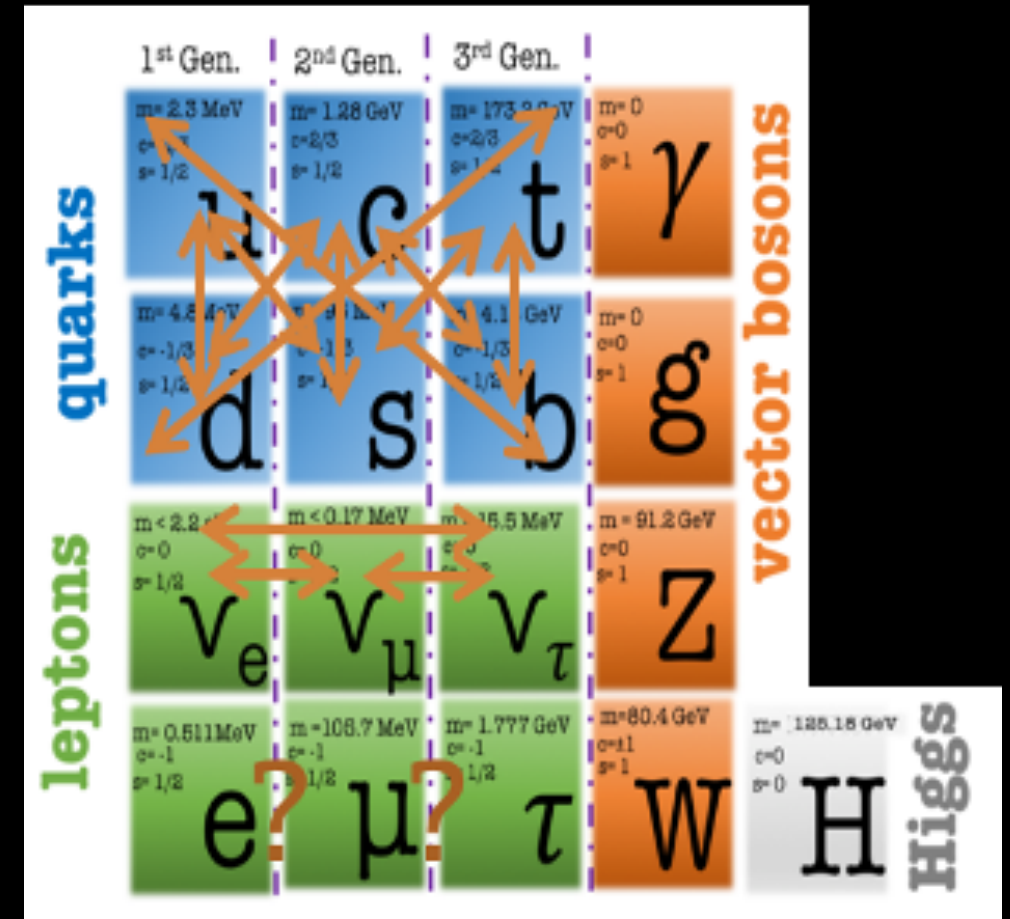


# Neutral Lepton Flavor Violations

- $\nu$  oscillations  $\rightarrow$  Lepton Flavour Violation (LFV)

**Mixing strengths parameterised by the Pontecorvo–Maki–Nakagawa–Sakata matrix (PMNS) matrix:**

$$(\nu_e, \nu_\mu, \nu_\tau) = \begin{pmatrix} U_{e1} & U_{e2} & U_{e3} \\ U_{\mu 1} & U_{\mu 2} & U_{\mu 3} \\ U_{\tau 1} & U_{\tau 2} & U_{\tau 3} \end{pmatrix} \begin{pmatrix} \nu_1 \\ \nu_2 \\ \nu_3 \end{pmatrix}$$





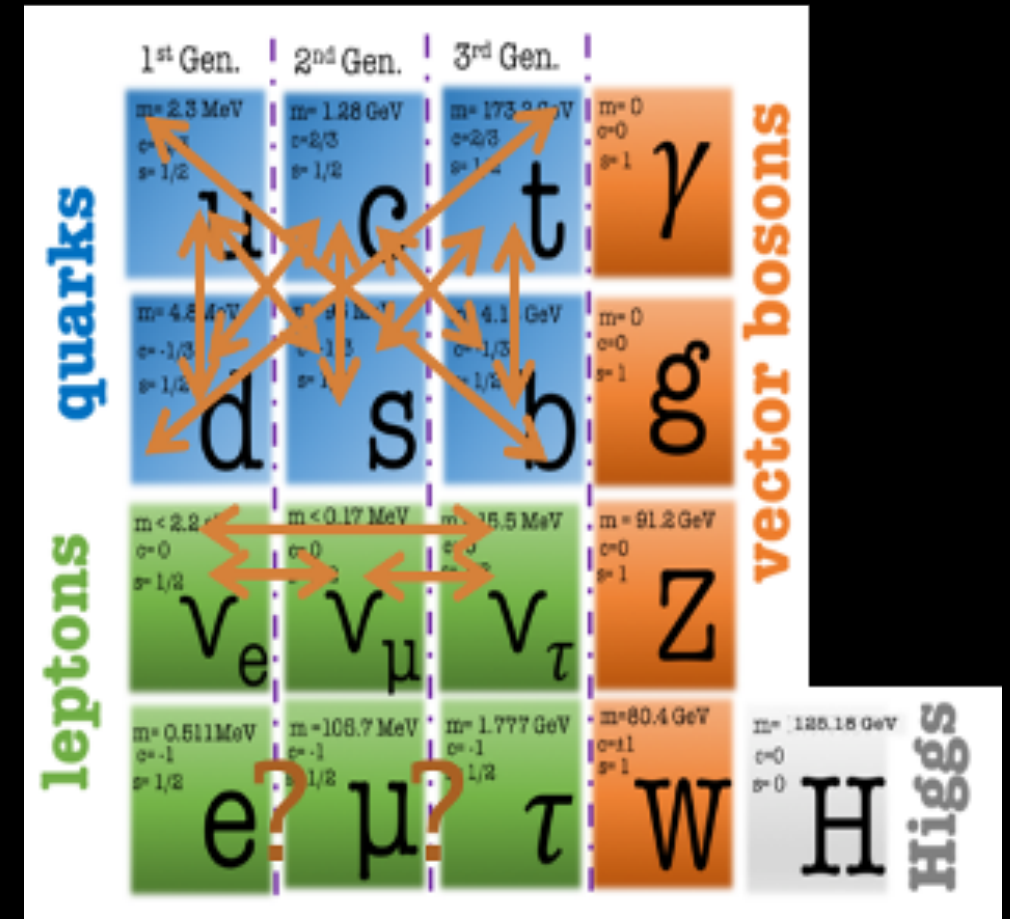
# Neutral Lepton Flavor Violations

- $\nu$  oscillations  $\rightarrow$  Lepton Flavour Violation (LFV)

**Mixing strengths parameterised by the Pontecorvo–Maki–Nakagawa–Sakata matrix (PMNS) matrix:**

$$(\nu_e, \nu_\mu, \nu_\tau) = \begin{pmatrix} U_{e1} & U_{e2} & U_{e3} \\ U_{\mu 1} & U_{\mu 2} & U_{\mu 3} \\ U_{\tau 1} & U_{\tau 2} & U_{\tau 3} \end{pmatrix} \begin{pmatrix} \nu_1 \\ \nu_2 \\ \nu_3 \end{pmatrix}$$

$\rightarrow$  The current best fit values imply that there is much more neutrino mixing than there is mixing between the quark flavours in the CKM matrix.



# Charged Lepton Flavor Violation (CLFV)

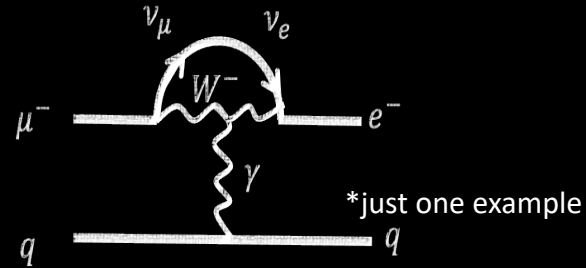
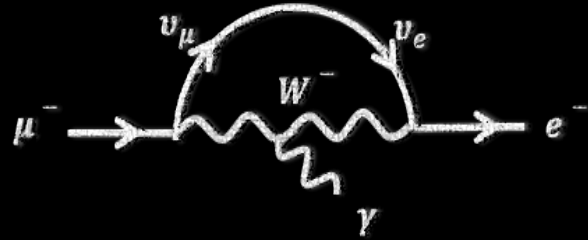


- The minimal extension of the Standard Model, including Dirac masses of neutrinos, allows for CLFV at loop level, mediated by  $W$  bosons.



# Charged Lepton Flavor Violation (CLFV)

- The minimal extension of the Standard Model, including Dirac masses of neutrinos, allows for CLFV at loop level, mediated by  $W$  bosons.

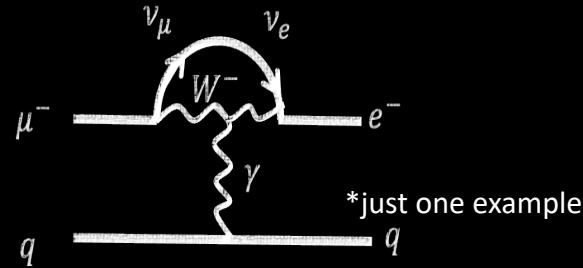
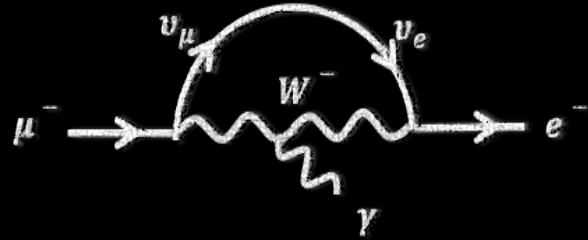






# Charged Lepton Flavor Violation (CLFV)

- The minimal extension of the Standard Model, including Dirac masses of neutrinos, allows for CLFV at loop level, mediated by  $W$  bosons.

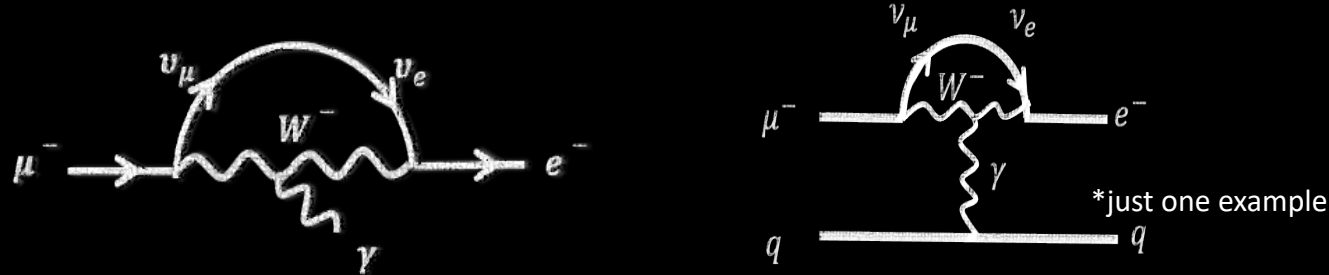


- Rates heavily suppressed by GIM suppression and are far below any conceivable experiment could measure:



# Charged Lepton Flavor Violation (CLFV)

- The minimal extension of the Standard Model, including Dirac masses of neutrinos, allows for CLFV at loop level, mediated by  $W$  bosons.



- Rates heavily suppressed by GIM suppression and are far below any conceivable experiment could measure:

$$B(\mu \rightarrow e\gamma) = \frac{3\alpha}{32\pi} \left| \sum_{i=2,3} U_{\mu i}^* U_{ei} \frac{\Delta m_{1i}^2}{M_W^2} \right|^2$$

$$B(\mu \rightarrow e\gamma) = \frac{3\alpha}{32\pi} \left( \frac{1}{4} \right) \sin^2 2\theta_{13} \sin^2 \theta_{23} \left| \frac{\Delta m_{13}^2}{M_W^2} \right|^2$$

$$B(\mu \rightarrow e\gamma) \approx \mathcal{O}(10^{-54})$$

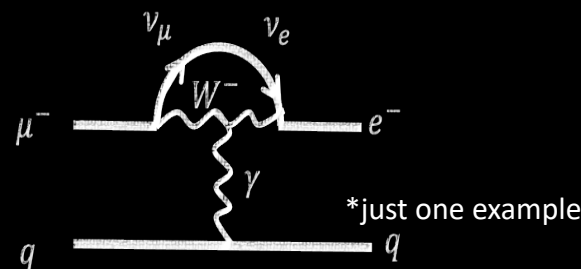
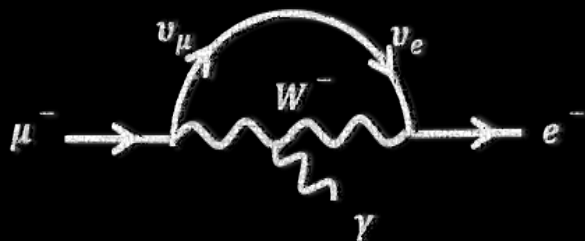
[1-4]

using best-fit values for neutrino data ( $m_{\nu j}$  for the neutrino mass and  $U_{ij}$  for the element of the PMNS matrix).



# Charged Lepton Flavor Violation (CLFV)

- The minimal extension of the Standard Model, including Dirac masses of neutrinos, allows for CLFV at loop level, mediated by W bosons.



- Rates heavily suppressed by GIM suppression and are far below any conceivable experiment could measure:

$$B(\mu \rightarrow e\gamma) = \frac{3\alpha}{32\pi} \left| \sum_{i=2,3} U_{\mu i}^* U_{ei} \frac{\Delta m_{1i}^2}{M_W^2} \right|^2$$

$$B(\mu \rightarrow e\gamma) = \frac{3\alpha}{32\pi} \left( \frac{1}{4} \right) \sin^2 2\theta_{13} \sin^2 \theta_{23} \left| \frac{\Delta m_{13}^2}{M_W^2} \right|^2$$

$$B(\mu \rightarrow e\gamma) \approx \mathcal{O}(10^{-54})$$

[1-4]

using best-fit values for neutrino data ( $m_{\nu j}$  for the neutrino mass and  $U_{ij}$  for the element of the PMNS matrix).

***If observed at Mu2e or Mu2e-II → this would be an unambiguous sign of physics beyond the Standard Model (BSM).***

# BSM Scenarios

Nice overview: Lorenzo Calibbi, Giovanni Signorelli  
arXiv:1709.00294 (2018)



There are many well-motivated BSM theories which invoke CLFV mediated by (pseudo) scalar, (axial) vector, or tensor currents at rates close to current experimental limits i.e.  $B \approx 10^{-15} - 10^{-17}$ :

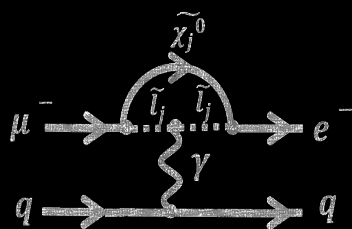


# BSM Scenarios

Nice overview: Lorenzo Calibbi, Giovanni Signorelli  
arXiv:1709.00294 (2018)

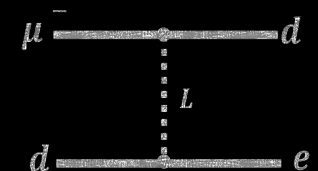


There are many well-motivated BSM theories which invoke CLFV mediated by (pseudo) scalar, (axial) vector, or tensor currents at rates close to current experimental limits i.e.  $B \approx 10^{-15} - 10^{-17}$ :



**SO(10) SUSY :**  
L. Calibbi *et al.*, Phys. Rev. D **74**, 116002 (2006), L. Calibbi *et al.*, JHEP **1211**, 40 (2012).

**Scalar Leptoquarks:**  
J.M. Arnold *et al.*, Phys. Rev D **88**, 035009 (2013).



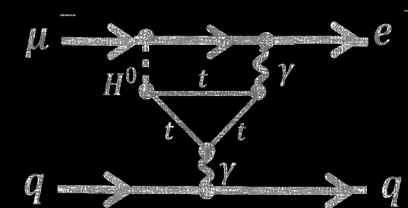
**Different neutrino mass-generating Lagrangians lead to very different rates for CLFV :**

Nuclear Physics B (Proc. Suppl.) **248–250** (2014) 13–19

**Extended Higgs/Gauge sector:**

Left-Right Symmetric Models  
C.-H. Lee *et al.*, Phys. Rev D **88**, 093010 (2013).

Littlest Higgs Blanke *et al* Phys.Polon.B41:657, 2010, arXiv:0906.5454v2 [hep-ph]

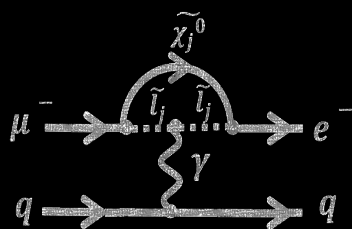


# BSM Scenarios

Nice overview: Lorenzo Calibbi, Giovanni Signorelli  
arXiv:1709.00294 (2018)

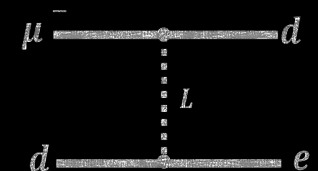


There are many well-motivated BSM theories which invoke CLFV mediated by (pseudo) scalar, (axial) vector, or tensor currents at rates close to current experimental limits i.e.  $B \approx 10^{-15} - 10^{-17}$ :



**SO(10) SUSY :**  
L. Calibbi *et al.*, Phys. Rev. D **74**, 116002 (2006), L. Calibbi *et al.*, JHEP **1211**, 40 (2012).

**Scalar Leptoquarks:**  
J.M. Arnold *et al.*, Phys. Rev D **88**, 035009 (2013).



A few examples – not an exclusive list!

Important point:

Mu2e is an indirect search for new physics, with sensitivity to lots of models. Even a null result would have huge implications!

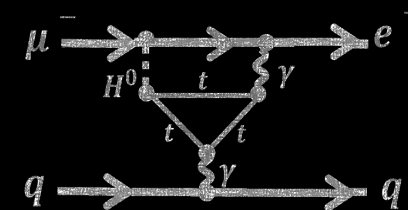
**Different neutrino mass-generating Lagrangians lead to very different rates for CLFV :**

Nuclear Physics B (Proc. Suppl.) **248–250** (2014) 13–19

**Extended Higgs/Gauge sector:**

Left-Right Symmetric Models  
C.-H. Lee *et al.*, Phys. Rev D **88**, 093010 (2013).

Littlest Higgs Blanke *et al* Phys.Polon.B41:657, 2010, arXiv:0906.5454v2 [hep-ph]

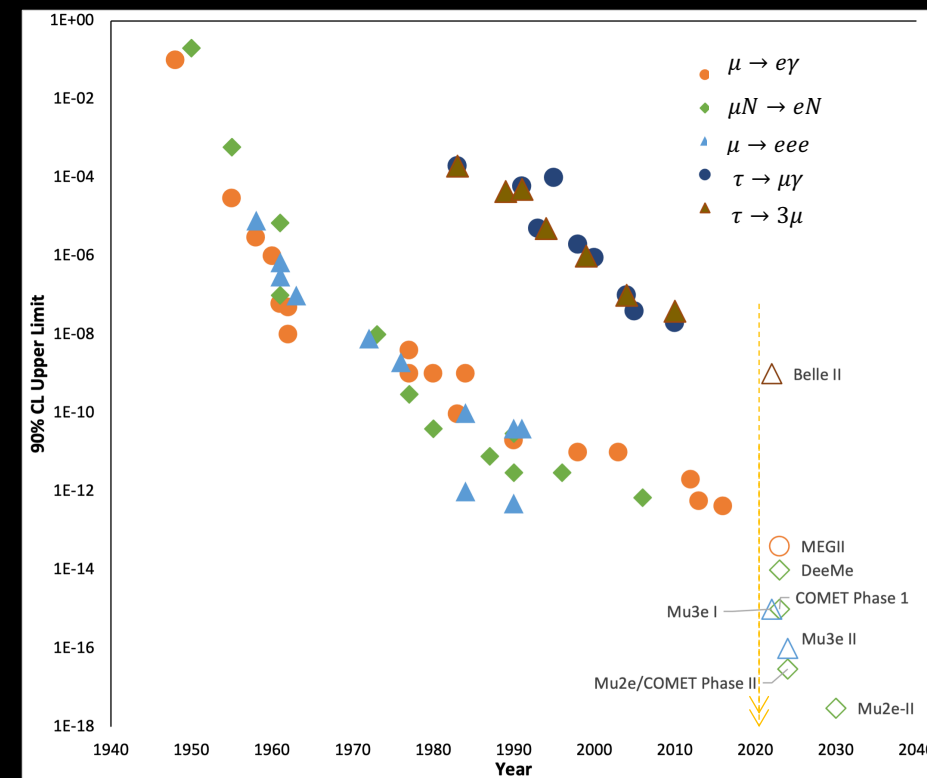


# Experimental Searches for CLFV



- $\mu^- N \rightarrow e^- N$  searches are crucial part of global program searching for CLFV.
- Muons offer more powerful probe for CLFV compared to taus.
- To elucidate the mechanism responsible for any CLFV – must look at relative rates (if any) in different muon channels.

Mode	Current Limit (at 90% CL)	Future Proposed Limit	Future Experiment/s
$\mu^\pm \rightarrow e^\pm \gamma$	$4.2 \times 10^{-13}$ [5]	$4 \times 10^{-14}$	MEG II [8]
$\mu^- N \rightarrow e^- N$	$7 \times 10^{-13}$ [6]	$10^{-15}$ $10^{-17}$ $10^{-18}$	COMET Phase-I Mu2e [10] & COMET Phase-II [9] Mu2e-II
$\mu^+ \rightarrow e^+ e^+ e^-$	$\sim 10^{-12}$ [7]	$10^{-15} \sim 10^{-16}$	Mu3e



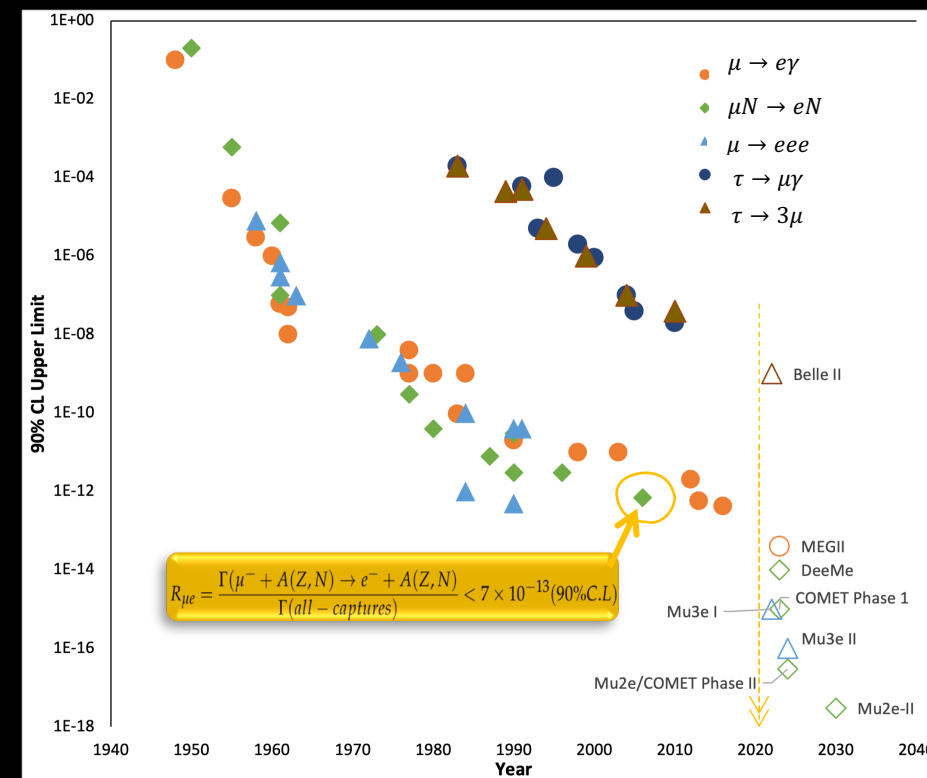
- Muon-to-electron sector provides powerful probes and complements collider searches for  $\tau \rightarrow e\gamma$  or  $\mu\gamma$  and  $H \rightarrow e\tau$ ,  $\mu\tau$ , or  $\mu e$ .

# Experimental Searches for CLFV



- $\mu^- N \rightarrow e^- N$  searches are crucial part of global program searching for CLFV.
- Muons offer more powerful probe for CLFV compared to taus.
- To elucidate the mechanism responsible for any CLFV – must look at relative rates (if any) in different muon channels.

Mode	Current Limit (at 90% CL)	Future Proposed Limit	Future Experiment/s
$\mu^\pm \rightarrow e^\pm \gamma$	$4.2 \times 10^{-13}$ [5]	$4 \times 10^{-14}$	MEG II [8]
$\mu^- N \rightarrow e^- N$	$7 \times 10^{-13}$ [6]	$10^{-15}$ $10^{-17}$ $10^{-18}$	COMET Phase-I Mu2e [10] & COMET Phase-II [9] Mu2e-II
$\mu^+ \rightarrow e^+ e^+ e^-$	$\sim 10^{-12}$ [7]	$10^{-15} \sim 10^{-16}$	Mu3e



- Muon-to-electron sector provides powerful probes and complements collider searches for  $\tau \rightarrow e\gamma$  or  $\mu\gamma$  and  $H \rightarrow e\tau$ ,  $\mu\tau$ , or  $\mu e$ .

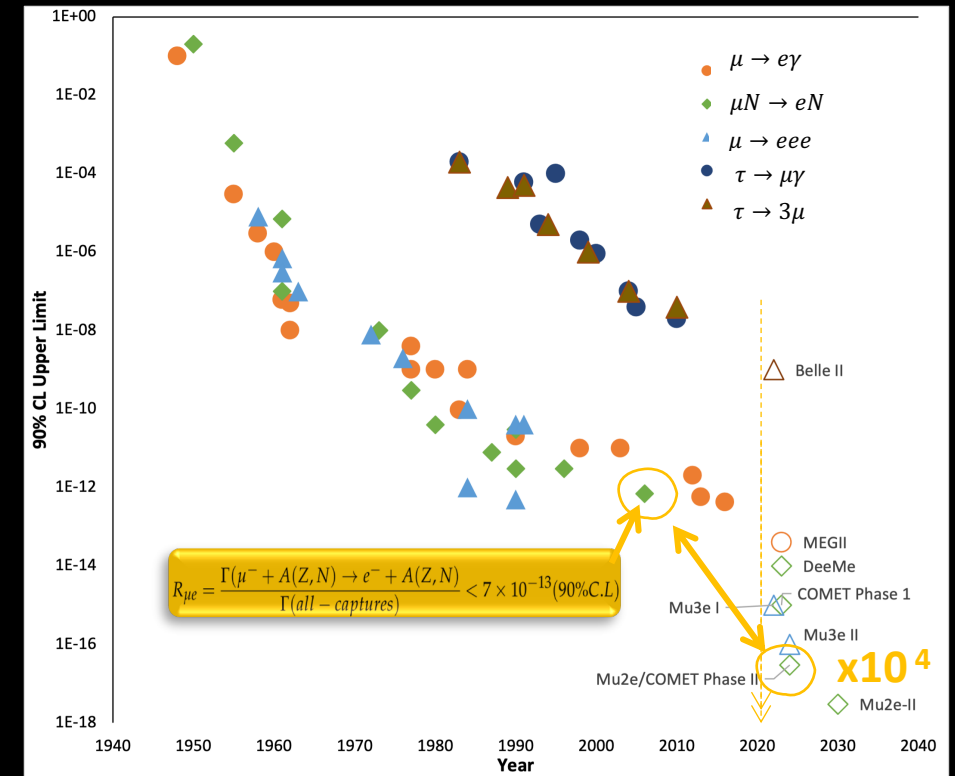


# Experimental Searches for CLFV



- $\mu^- N \rightarrow e^- N$  searches are crucial part of global program searching for CLFV.
- Muons offer more powerful probe for CLFV compared to taus.
- To elucidate the mechanism responsible for any CLFV – must look at relative rates (if any) in different muon channels.

Mode	Current Limit (at 90% CL)	Future Proposed Limit	Future Experiment/s
$\mu^\pm \rightarrow e^\pm \gamma$	$4.2 \times 10^{-13}$ [5]	$4 \times 10^{-14}$	MEG II [8]
$\mu^- N \rightarrow e^- N$	$7 \times 10^{-13}$ [6]	$10^{-15}$ $10^{-17}$ $10^{-18}$	COMET Phase-I Mu2e [10] & COMET Phase-II [9] Mu2e-II
$\mu^+ \rightarrow e^+ e^+ e^-$	$\sim 10^{-12}$ [7]	$10^{-15} \sim 10^{-16}$	Mu3e



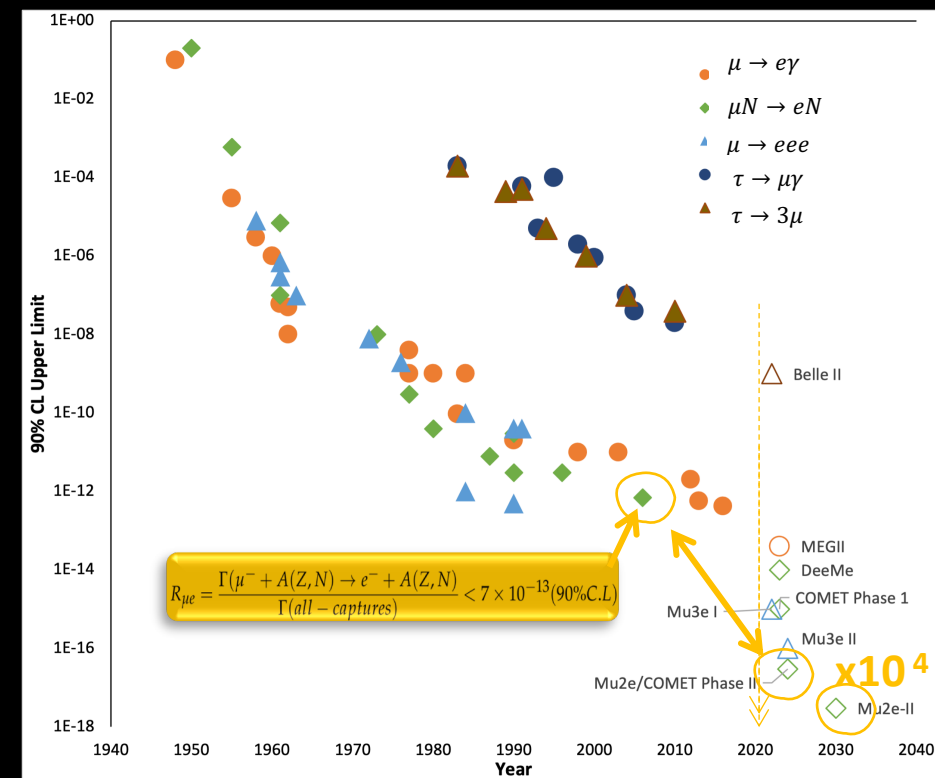
- Muon-to-electron sector provides powerful probes and complements collider searches for  $\tau \rightarrow e\gamma$  or  $\mu\gamma$  and  $H \rightarrow e\tau$ ,  $\mu\tau$ , or  $\mu e$ .

# Experimental Searches for CLFV



- $\mu^- N \rightarrow e^- N$  searches are crucial part of global program searching for CLFV.
- Muons offer more powerful probe for CLFV compared to taus.
- To elucidate the mechanism responsible for any CLFV – must look at relative rates (if any) in different muon channels.

Mode	Current Limit (at 90% CL)	Future Proposed Limit	Future Experiment/s
$\mu^\pm \rightarrow e^\pm \gamma$	$4.2 \times 10^{-13}$ [5]	$4 \times 10^{-14}$	MEG II [8]
$\mu^- N \rightarrow e^- N$	$7 \times 10^{-13}$ [6]	$10^{-15}$ $10^{-17}$ $10^{-18}$	COMET Phase-I Mu2e [10] & COMET Phase-II [9] Mu2e-II
$\mu^+ \rightarrow e^+ e^+ e^-$	$\sim 10^{-12}$ [7]	$10^{-15} \sim 10^{-16}$	Mu3e



**Mu2e-II will use PIP-II, Snowmass Proposal in progress!**

- Muon-to-electron sector provides powerful probes and complements collider searches for  $\tau \rightarrow e\gamma$  or  $\mu\gamma$  and  $H \rightarrow e\tau$ ,  $\mu\tau$ , or  $\mu e$ .

# Aside: Tau CLFV Searches

Taus Past/Present/Future:

<https://indico.fnal.gov/event/44457/?print=1>

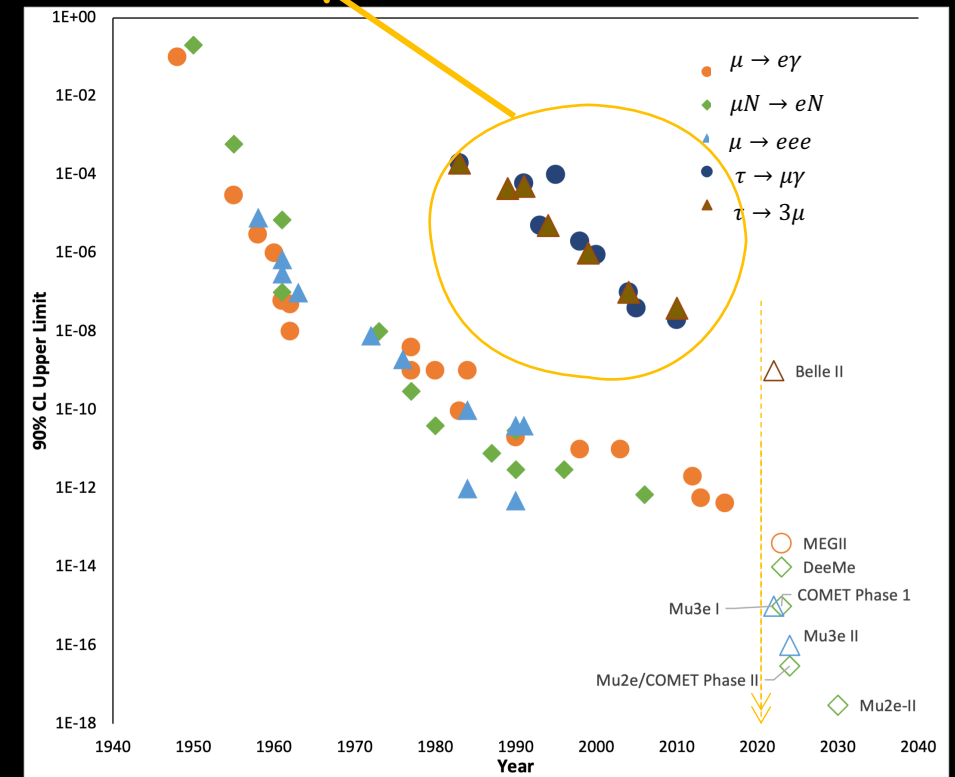


- Less stringent limits in 3rd generation, but here BSM effects may be higher.

Mode	Current Limit (at 90% CL)	Future Proposed Limit	Future Experiment/s
$\tau \rightarrow \mu\mu\mu$	Belle – $2.1 \times 10^{-8}$ BaBar – $3.3 \times 10^{-8}$ LHCb – $4.6 \times 10^{-8}$	$< 1 \times 10^{-9}$ (arXiv:1011.0352 arXiv:1808.10567)	Belle II, LHCb HL-LHC TauFV?
$\tau \rightarrow \mu\gamma$	$4.4 \times 10^{-8}$	$\sim 1 \times 10^{-9}$	Belle II
$\tau \rightarrow e\gamma$	$3.3 \times 10^{-8}$	$\sim 3 \times 10^{-9}$	Belle II

- $\tau$  LFV searches at Belle II will be extremely clean, with very little background (if any), thanks to pair production and double-tag analysis technique.

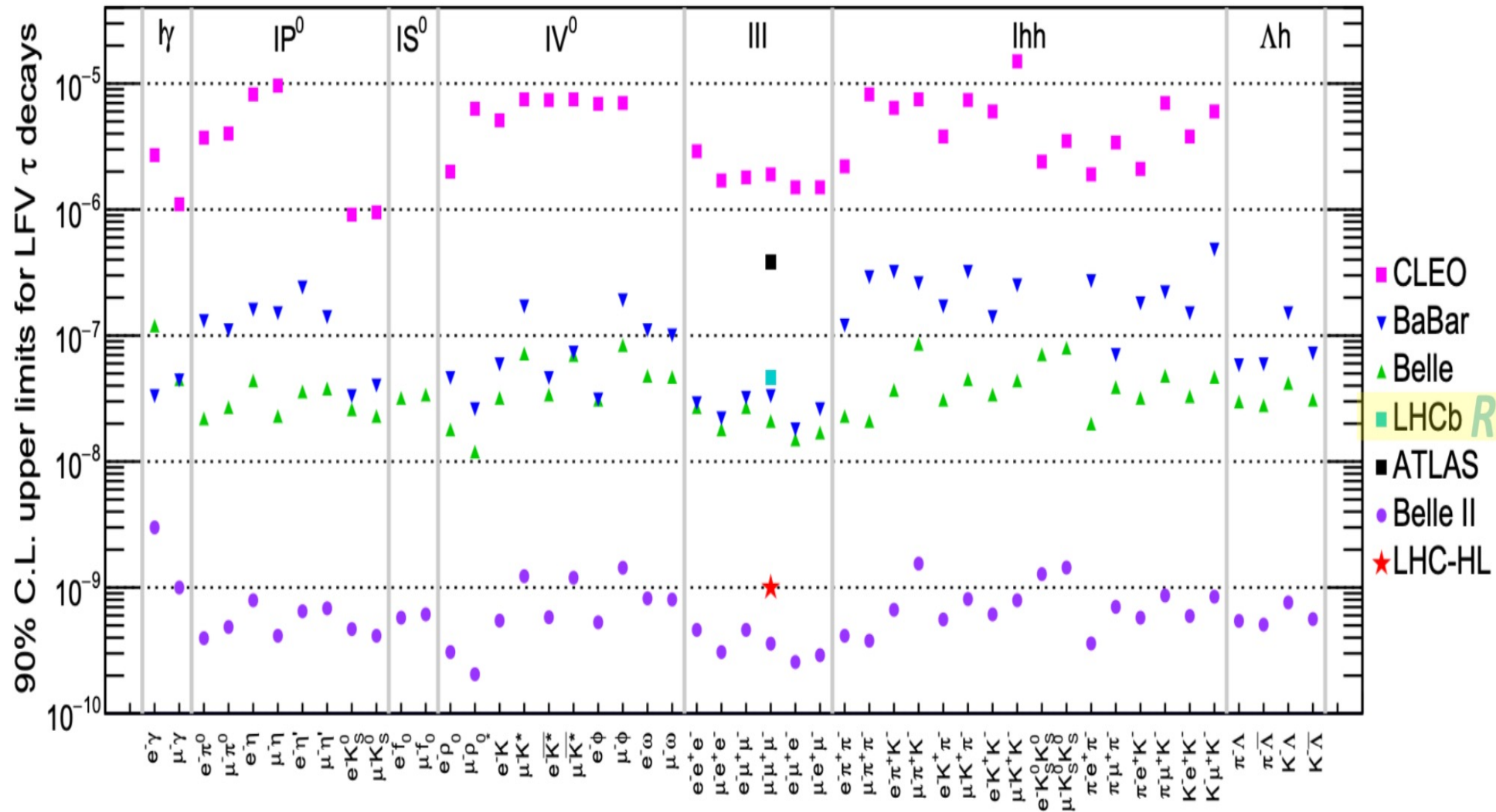
- Type of mediator:
  - Compare muon channels to each other
- Source of flavor violation:
  - Compare muons to other leptons i.e. taus



# Aside: Tau CLFV Searches



Time Past/Present/Future





# Simplistic Explanation of Physics Reach

A. de Gouvêa, P. Vogel  
arXiv:1303.4097

- For the purposes of discussion we can build a Toy Lagrangian which consists of 2 terms representing 2 types of physics process:

$$\mathcal{L}_{CLFV} = \frac{m_\mu}{(1+\kappa)\Lambda^2} \bar{\mu}_R \sigma_{\mu\nu} e_L F^{\mu\nu} + \frac{\kappa}{(1+\kappa)\Lambda^2} \bar{\mu}_L \gamma_\mu e_L \left( \sum_{q=u,d} \bar{q}_L \gamma_\mu q_L \right)$$



# Simplistic Explanation of Physics Reach

A. de Gouvêa, P. Vogel  
arXiv:1303.4097

- For the purposes of discussion we can build a Toy Lagrangian which consists of 2 terms representing 2 types of physics process:

$$\mathcal{L}_{CLFV} = \frac{m_\mu}{(1+\kappa)\Lambda^2} \bar{\mu}_R \sigma_{\mu\nu} e_L F^{\mu\nu} + \frac{\kappa}{(1+\kappa)\Lambda^2} \bar{\mu}_L \gamma_\mu e_L \left( \sum_{q=u,d} \bar{q}_L \gamma_\mu q_L \right)$$

“Photonic”



$\Lambda$  : effective mass scale of New Physics (NP),

$\kappa$  : determines to what extent NP is photonic ( $\kappa \ll 1$ ) or 4-fermion ( $\kappa \gg 1$ )



# Simplistic Explanation of Physics Reach

A. de Gouvêa, P. Vogel  
arXiv:1303.4097

- For the purposes of discussion we can build a Toy Lagrangian which consists of 2 terms representing 2 types of physics process:

$$\mathcal{L}_{CLFV} = \frac{m_\mu}{(1+\kappa)\Lambda^2} \bar{\mu}_R \sigma_{\mu\nu} e_L F^{\mu\nu} + \frac{\kappa}{(1+\kappa)\Lambda^2} \bar{\mu}_L \gamma_\mu e_L \left( \sum_{q=u,d} \bar{q}_L \gamma_\mu q_L \right)$$

**“Photonic”**  
**i.e. Dipole terms:**  
 $\mu^\pm \rightarrow e^\pm \gamma, \mu \rightarrow eee$   
 $\mu^- N \rightarrow e^- N$



$\Lambda$  : effective mass scale of New Physics (NP),  
 $\kappa$  : determines to what extent NP is photonic ( $\kappa \ll 1$ ) or 4-fermion ( $\kappa \gg 1$ )





# Simplistic Explanation of Physics Reach

A. de Gouvêa, P. Vogel  
arXiv:1303.4097

- For the purposes of discussion we can build a Toy Lagrangian which consists of 2 terms representing 2 types of physics process:

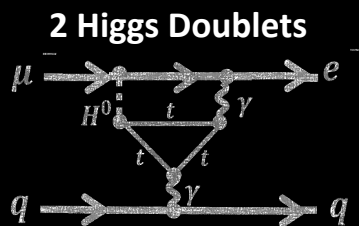
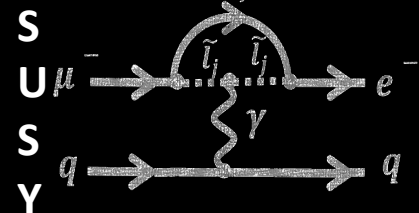
$$\mathcal{L}_{CLFV} = \frac{m_\mu}{(1 + \kappa)\Lambda^2} \bar{\mu}_R \sigma_{\mu\nu} e_L F^{\mu\nu} + \frac{\kappa}{(1 + \kappa)\Lambda^2} \bar{\mu}_L \gamma_\mu e_L \left( \sum_{q=u,d} \bar{q}_L \gamma_\mu q_L \right)$$

**“Photonic”**

i.e. Dipole terms:

$\mu^\pm \rightarrow e^\pm \gamma, \mu \rightarrow eee$

$\mu^- N \rightarrow e^- N$



$\Lambda$  : effective mass scale of New Physics (NP),

$\kappa$  : determines to what extent NP is photonic ( $\kappa \ll 1$ ) or 4-fermion ( $\kappa \gg 1$ )



# Simplistic Explanation of Physics Reach

A. de Gouvêa, P. Vogel  
arXiv:1303.4097

- For the purposes of discussion we can build a Toy Lagrangian which consists of 2 terms representing 2 types of physics process:

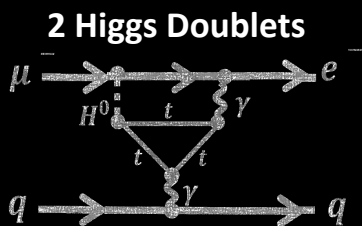
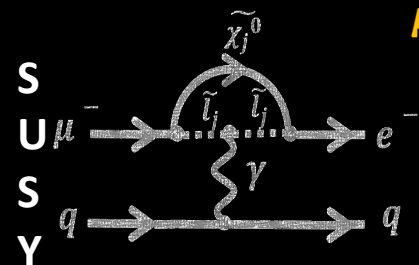
$$\mathcal{L}_{CLFV} = \frac{m_\mu}{(1 + \kappa)\Lambda^2} \bar{\mu}_R \sigma_{\mu\nu} e_L F^{\mu\nu} + \frac{\kappa}{(1 + \kappa)\Lambda^2} \bar{\mu}_L \gamma_\mu e_L \left( \sum_{q=u,d} \bar{q}_L \gamma_\mu q_L \right)$$

**“Photonic”**

i.e. Dipole terms:

$$\mu^\pm \rightarrow e^\pm \gamma, \mu \rightarrow eee$$

$$\mu^- N \rightarrow e^- N$$



**“Contact”**

$\Lambda$  : effective mass scale of New Physics (NP),

$\kappa$  : determines to what extent NP is photonic ( $\kappa \ll 1$ ) or 4-fermion ( $\kappa \gg 1$ )



# Simplistic Explanation of Physics Reach

A. de Gouvêa, P. Vogel  
arXiv:1303.4097

- For the purposes of discussion we can build a Toy Lagrangian which consists of 2 terms representing 2 types of physics process:

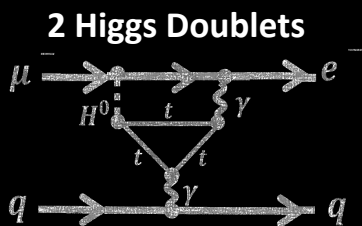
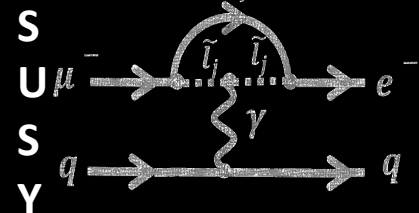
$$\mathcal{L}_{CLFV} = \frac{m_\mu}{(1 + \kappa)\Lambda^2} \bar{\mu}_R \sigma_{\mu\nu} e_L F^{\mu\nu} + \frac{\kappa}{(1 + \kappa)\Lambda^2} \bar{\mu}_L \gamma_\mu e_L \left( \sum_{q=u,d} \bar{q}_L \gamma_\mu q_L \right)$$

**“Photonic”**

i.e. Dipole terms:

$\mu^\pm \rightarrow e^\pm \gamma, \mu \rightarrow eee$

$\mu^- N \rightarrow e^- N$



**“Contact”**

i.e. 4 fermion terms

Only  $\mu^+ \rightarrow e^+ e^+ e^-$

And  $\mu^- N \rightarrow e^- N$

$\Lambda$  : effective mass scale of New Physics (NP),

$\kappa$  : determines to what extent NP is photonic ( $\kappa \ll 1$ ) or 4-fermion ( $\kappa \gg 1$ )



# Simplistic Explanation of Physics Reach

A. de Gouvêa, P. Vogel  
arXiv:1303.4097

- For the purposes of discussion we can build a Toy Lagrangian which consists of 2 terms representing 2 types of physics process:

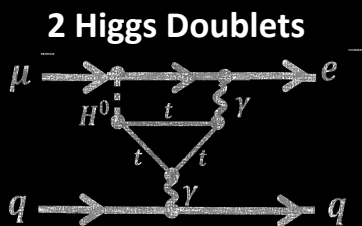
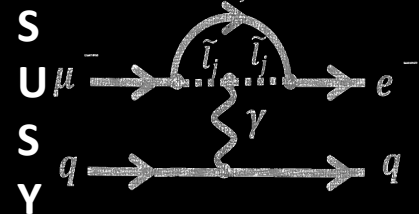
$$\mathcal{L}_{CLFV} = \frac{m_\mu}{(1 + \kappa)\Lambda^2} \bar{\mu}_R \sigma_{\mu\nu} e_L F^{\mu\nu} + \frac{\kappa}{(1 + \kappa)\Lambda^2} \bar{\mu}_L \gamma_\mu e_L \left( \sum_{q=u,d} \bar{q}_L \gamma_\mu q_L \right)$$

**“Photonic”**

i.e. Dipole terms:

$$\mu^\pm \rightarrow e^\pm \gamma, \mu \rightarrow eee$$

$$\mu^- N \rightarrow e^- N$$

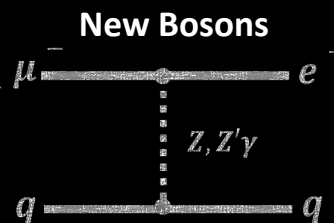
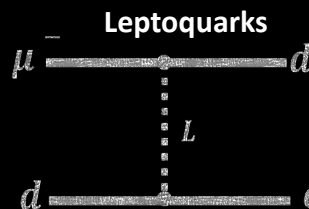


**“Contact”**

i.e. 4 fermion terms

$$\text{Only } \mu^+ \rightarrow e^+ e^+ e^-$$

$$\text{And } \mu^- N \rightarrow e^- N$$



$\Lambda$  : effective mass scale of New Physics (NP),

$\kappa$  : determines to what extent NP is photonic ( $\kappa \ll 1$ ) or 4-fermion ( $\kappa \gg 1$ )

# Simplistic Explanation of Physics Reach

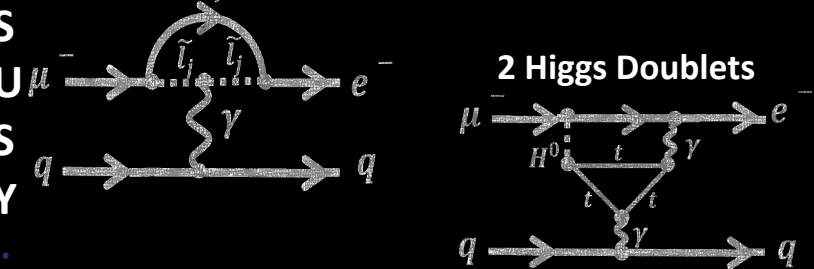


A. de Gouvêa, P. Vogel  
arXiv:1303.4097

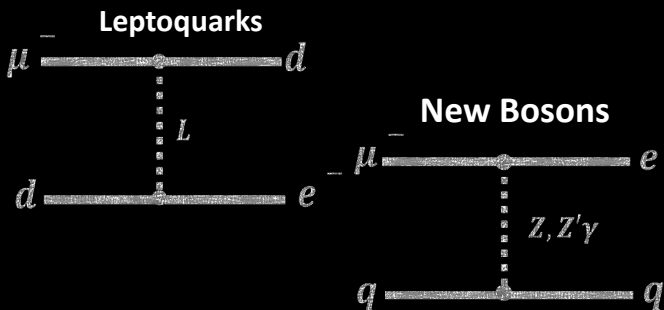
- For the purposes of discussion we can build a Toy Lagrangian which consists of 2 terms representing 2 types of physics process:

$$\mathcal{L}_{CLFV} = \frac{m_\mu}{(1 + \kappa)\Lambda^2} \bar{\mu}_R \sigma_{\mu\nu} e_L F^{\mu\nu} + \frac{\kappa}{(1 + \kappa)\Lambda^2} \bar{\mu}_L \gamma_\mu e_L \left( \sum_{q=u,d} \bar{q}_L \gamma_\mu q_L \right)$$

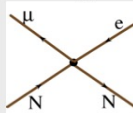
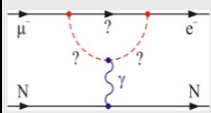
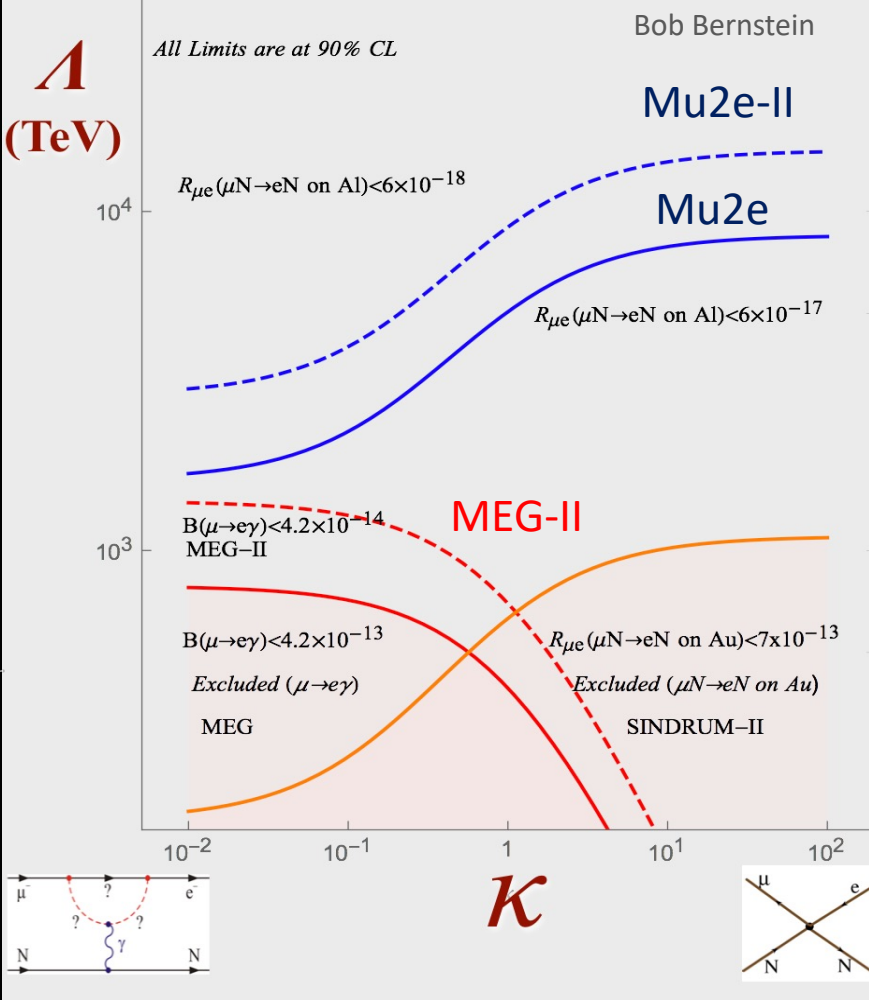
**“Photonic”**  
i.e. Dipole terms:  
 $\mu^\pm \rightarrow e^\pm \gamma, \mu \rightarrow eee$   
 $\mu^- N \rightarrow e^- N$



**“Contact”**  
i.e. 4 fermion terms  
Only  $\mu^+ \rightarrow e^+ e^+ e^-$   
And  $\mu^- N \rightarrow e^- N$



$\Lambda$  : effective mass scale of New Physics (NP),  
 $\kappa$  : determines to what extent NP is photonic ( $\kappa \ll 1$ ) or 4-fermion ( $\kappa \gg 1$ )



# Complementarity



Taken from: arXiv:0909.1333[hep-ph]

Table 8: “DNA” of flavour physics effects for the most interesting observables in a selection of SUSY and non-SUSY models ★★★ signals large effects, ★★ visible but small effects and ★ implies that the given model does not predict sizable effects in that observable.

	AC	RVV2	AKM	$\delta$ LL	FBMSSM	LHT	RS
$D^0 - \bar{D}^0$	★★★	★	★	★	★	★★★	?
$\epsilon_K$	★	★★★	★★★	★	★	★★	★★★
$S_{\psi\phi}$	★★★	★★★	★★★	★	★	★★★	★★★
$S_{\phi K_S}$	★★★	★★	★	★★★	★★★	★	?
$A_{CP}(B \rightarrow X_s \gamma)$	★	★	★	★★★	★★★	★	?
$A_{7,8}(B \rightarrow K^* \mu^+ \mu^-)$	★	★	★	★★★	★★★	★★	?
$A_9(B \rightarrow K^* \mu^+ \mu^-)$	★	★	★	★	★	★	?
$B \rightarrow K^{(*)} \nu \bar{\nu}$	★	★	★	★	★	★	★
$B_s \rightarrow \mu^+ \mu^-$	★★★	★★★	★★★	★★★	★★★	★	★
$K^+ \rightarrow \pi^+ \nu \bar{\nu}$	★	★	★	★	★	★★★	★★★
$K_L \rightarrow \pi^0 \nu \bar{\nu}$	★	★	★	★	★	★★★	★★★
$\mu \rightarrow e \gamma$	★★★	★★★	★★★	★★★	★★★	★★★	★★★
$\tau \rightarrow \mu \gamma$	★★★	★★★	★	★★★	★★★	★★★	★★★
$\mu + N \rightarrow e + N$	★★★	★★★	★★★	★★★	★★★	★★★	★★★

★★★ = Discovery Sensitivity



# Complementarity



Taken from: arXiv:0909.1333[hep-ph]

Table 8: “DNA” of flavour physics effects for the most interesting observables in a selection of SUSY and non-SUSY models ★★★ signals large effects, ★★ visible but small effects and ★ implies that the given model does not predict sizable effects in that observable.

Discovery sensitivity across the board.  
Relative Rates however will be model dependent.

	AC	RVV2	AKM	$\delta$ LL	FBMSSM	LHT	RS
$D^0 - \bar{D}^0$	★★★	★	★	★	★	★★★	?
$\epsilon_K$	★	★★★	★★★	★	★	★★	★★★
$S_{\psi\phi}$	★★★	★★★	★★★	★	★	★★★	★★★
$S_{\phi K_S}$	★★★	★★	★	★★★	★★★	★	?
$A_{CP}(B \rightarrow X_s \gamma)$	★	★	★	★★★	★★★	★	?
$A_{7,8}(B \rightarrow K^* \mu^+ \mu^-)$	★	★	★	★★★	★★★	★★	?
$A_9(B \rightarrow K^* \mu^+ \mu^-)$	★	★	★	★	★	★	?
$B \rightarrow K^{(*)} \nu \bar{\nu}$	★	★	★	★	★	★	★
$B_s \rightarrow \mu^+ \mu^-$	★★★	★★★	★★★	★★★	★★★	★	★
$K^+ \rightarrow \pi^+ \nu \bar{\nu}$	★	★	★	★	★	★★★	★★★
$K_L \rightarrow \pi^0 \nu \bar{\nu}$	★	★	★	★	★	★★★	★★★
$\mu \rightarrow e \gamma$	★★★	★★★	★★★	★★★	★★★	★★★	★★★
$\tau \rightarrow \mu \gamma$	★★★	★★★	★	★★★	★★★	★★★	★★★
$\mu + N \rightarrow e + N$	★★★	★★★	★★★	★★★	★★★	★★★	★★★

★★★ = Discovery Sensitivity



# Complementarity



Taken from: arXiv:0909.1333[hep-ph]

Table 8: “DNA” of flavour physics effects for the most interesting observables in a selection of SUSY and non-SUSY models ★★★ signals large effects, ★★ visible but small effects and ★ implies that the given model does not predict sizable effects in that observable.

Discovery sensitivity across the board.  
Relative Rates however will be model dependent.

Model	$\mu \rightarrow eee$	$\mu N \rightarrow eN$	$\frac{\text{BR}(\mu \rightarrow eee)}{\text{BR}(\mu \rightarrow e\gamma)}$	$\frac{\text{CR}(\mu N \rightarrow eN)}{\text{BR}(\mu \rightarrow e\gamma)}$
MSSM	Loop	Loop	$\approx 6 \times 10^{-3}$	$10^{-3} - 10^{-2}$
Type-I seesaw	Loop*	Loop*	$3 \times 10^{-3} - 0.3$	$0.1 - 10$
Type-II seesaw	Tree	Loop	$(0.1 - 3) \times 10^3$	$\mathcal{O}(10^{-2})$
Type-III seesaw	Tree	Tree	$\approx 10^3$	$\mathcal{O}(10^3)$
LFV Higgs	Loop†	Loop*†	$\approx 10^{-2}$	$\mathcal{O}(0.1)$
Composite Higgs	Loop*	Loop*	$0.05 - 0.5$	$2 - 20$

from L. Calibbi and G. Signorelli, Riv. Nuovo Cimento, 41 (2018) 71

	AC	RVV2	AKM	$\delta\text{LL}$	FBMSSM	LHT	RS
$D^0 - \bar{D}^0$	★★★	★	★	★	★	★★★	?
$\epsilon_K$	★	★★★	★★★	★	★	★★	★★★
$S_{\psi\phi}$	★★★	★★★	★★★	★	★	★★★	★★★
$S_{\phi K_S}$	★★★	★★	★	★★★	★★★	★	?
$A_{\text{CP}}(B \rightarrow X_s \gamma)$	★	★	★	★★★	★★★	★	?
$A_{7,8}(B \rightarrow K^* \mu^+ \mu^-)$	★	★	★	★★★	★★★	★★	?
$A_9(B \rightarrow K^* \mu^+ \mu^-)$	★	★	★	★	★	★	?
$B \rightarrow K^{(*)} \nu \bar{\nu}$	★	★	★	★	★	★	★
$B_s \rightarrow \mu^+ \mu^-$	★★★	★★★	★★★	★★★	★★★	★	★
$K^+ \rightarrow \pi^+ \nu \bar{\nu}$	★	★	★	★	★	★★★	★★★
$K_L \rightarrow \pi^0 \nu \bar{\nu}$	★	★	★	★	★	★★★	★★★
$\mu \rightarrow e \gamma$	★★★	★★★	★★★	★★★	★★★	★★★	★★★
$\tau \rightarrow \mu \gamma$	★★★	★★★	★	★★★	★★★	★★★	★★★
$\mu + N \rightarrow e + N$	★★★	★★★	★★★	★★★	★★★	★★★	★★★

★★★ = Discovery Sensitivity

# Complementarity



Taken from: arXiv:0909.1333[hep-ph]

Table 8: “DNA” of flavour physics effects for the most interesting observables in a selection of SUSY and non-SUSY models ★★★ signals large effects, ★★ visible but small effects and ★ implies that the given model does not predict sizable effects in that observable.

Discovery sensitivity across the board.  
Relative Rates however will be model dependent.

Theory on complementarity →  
<http://arxiv.org/abs/2010.00317v2>

Model	$\mu \rightarrow eee$	$\mu N \rightarrow eN$	$\frac{\text{BR}(\mu \rightarrow eee)}{\text{BR}(\mu \rightarrow e\gamma)}$	$\frac{\text{CR}(\mu N \rightarrow eN)}{\text{BR}(\mu \rightarrow e\gamma)}$
MSSM	Loop	Loop	$\approx 6 \times 10^{-3}$	$10^{-3} - 10^{-2}$
Type-I seesaw	Loop*	Loop*	$3 \times 10^{-3} - 0.3$	$0.1 - 10$
Type-II seesaw	Tree	Loop	$(0.1 - 3) \times 10^3$	$\mathcal{O}(10^{-2})$
Type-III seesaw	Tree	Tree	$\approx 10^3$	$\mathcal{O}(10^3)$
LFV Higgs	Loop†	Loop*†	$\approx 10^{-2}$	$\mathcal{O}(0.1)$
Composite Higgs	Loop*	Loop*	$0.05 - 0.5$	$2 - 20$

from L. Calibbi and G. Signorelli, Riv. Nuovo Cimento, 41 (2018) 71

	AC	RVV2	AKM	$\delta\text{LL}$	FBMSSM	LHT	RS
$D^0 - \bar{D}^0$	★★★	★	★	★	★	★★★	?
$\epsilon_K$	★	★★★	★★★	★	★	★★	★★★
$S_{\psi\phi}$	★★★	★★★	★★★	★	★	★★★	★★★
$S_{\phi K_S}$	★★★	★★	★	★★★	★★★	★	?
$A_{\text{CP}}(B \rightarrow X_s \gamma)$	★	★	★	★★★	★★★	★	?
$A_{7,8}(B \rightarrow K^* \mu^+ \mu^-)$	★	★	★	★★★	★★★	★★	?
$A_9(B \rightarrow K^* \mu^+ \mu^-)$	★	★	★	★	★	★	?
$B \rightarrow K^{(*)} \nu \bar{\nu}$	★	★	★	★	★	★	★
$B_s \rightarrow \mu^+ \mu^-$	★★★	★★★	★★★	★★★	★★★	★	★
$K^+ \rightarrow \pi^+ \nu \bar{\nu}$	★	★	★	★	★	★★★	★★★
$K_L \rightarrow \pi^0 \nu \bar{\nu}$	★	★	★	★	★	★★★	★★★
$\mu \rightarrow e \gamma$	★★★	★★★	★★★	★★★	★★★	★★★	★★★
$\tau \rightarrow \mu \gamma$	★★★	★★★	★	★★★	★★★	★★★	★★★
$\mu + N \rightarrow e + N$	★★★	★★★	★★★	★★★	★★★	★★★	★★★

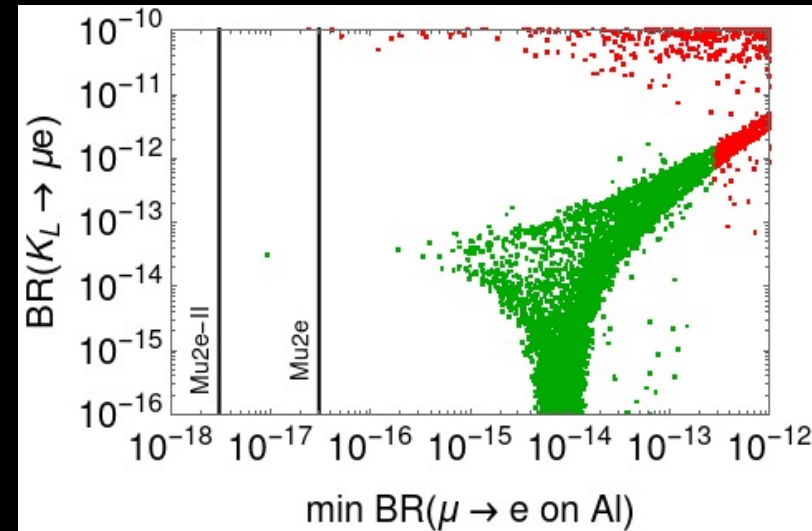
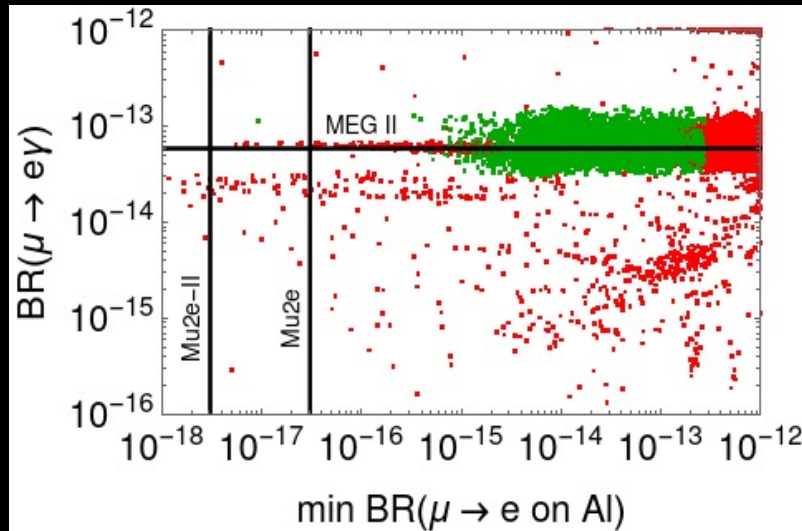
★★★ = Discovery Sensitivity

# Example: Leptoquarks

Heeck & Teresi, 1808.07492



- Pati-Salam Leptoquarks: B-meson anomalies could be explained by two scalar leptoquarks, whose couplings enter neutrino masses as well. Type-II seesaw dominance is favored.

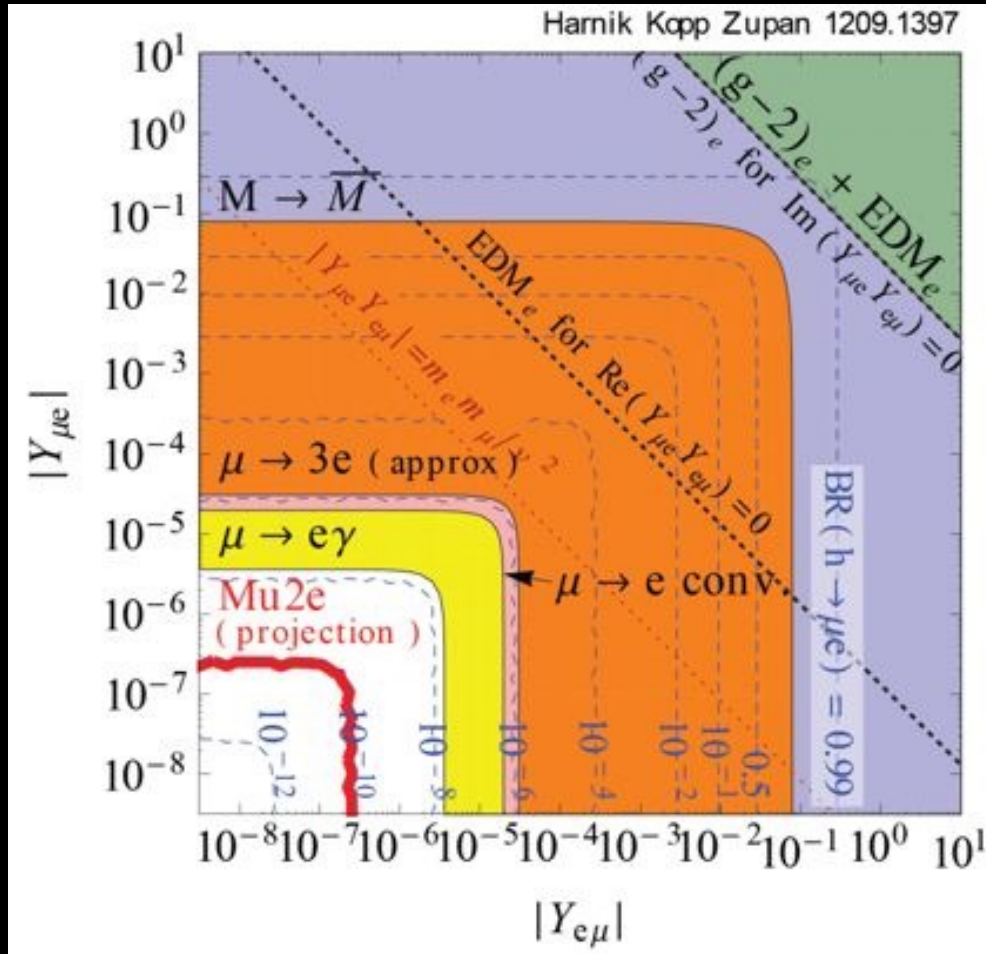


Plots: Julian Heck

- Flavor structure fixed by neutrino mass/mixing; scale  $\Lambda$  fixed to explain B-meson anomaly  $R(K)$ .
- Predicts testable rates in Mu2e!
- Explain B meson anomalies through adding 2 scalar leptoquarks: Bigaran, Gargalionis, Volkas, 1906.01870  $\rightarrow B(\mu N \rightarrow e N) < 3 \times 10^{-13}$

# Example: Constraining Flavor Violating Higgs Decays

Harnik, J. Kopp and J. Zupan, JHEP **3**, 26 (2013).



- Can also help constrain flavor violating Higgs decays.
- Higgs LFV decays arise in many frameworks of New Physics at the electroweak scale such as two Higgs doublet models, extra dimensions, or models of compositeness.
- Current  $\mu \rightarrow e$  conversion implies:

$$\sqrt{|Y_{\mu e}|^2 + |Y_{e\mu}|^2} < 4.6 \times 10^{-5}$$

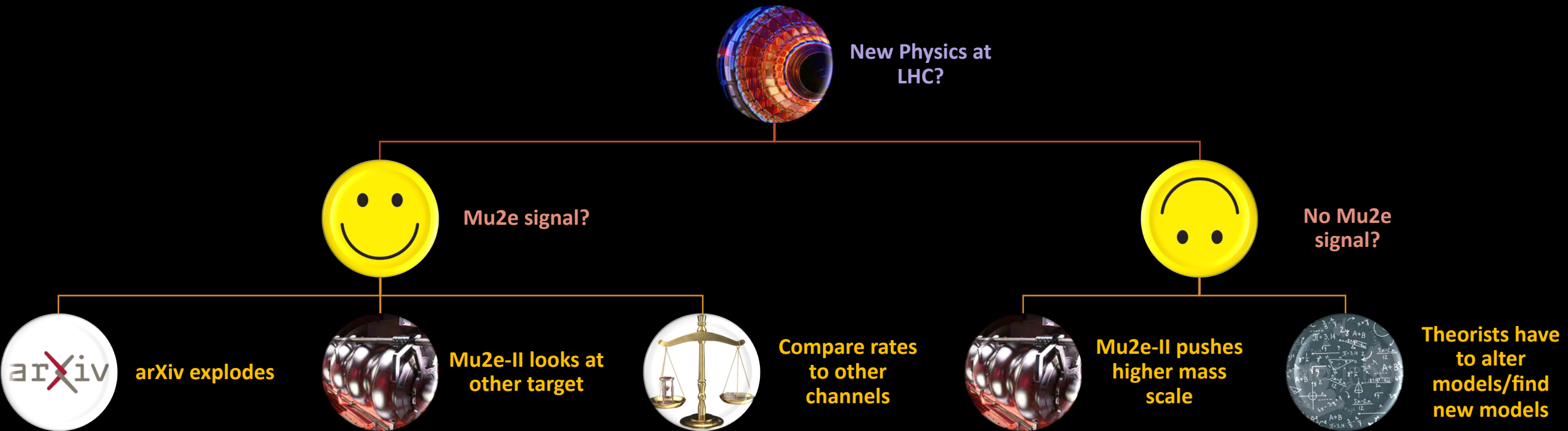
- Mu2e is expected to be sensitive to:

$$\sqrt{|Y_{\mu e}|^2 + |Y_{e\mu}|^2} > \text{few} \times 10^{-7}.$$

- Where  $|Y_{\mu e}|$  and  $|Y_{e\mu}|$  are flavor-violating Yukawa couplings for a 125 GeV Higgs boson i.e.  $h \rightarrow \mu e$ .
- Very strong limits on LFV Higgs decays for 1st-2nd generation**



# Possibilities



# Complementarity in Target Materials

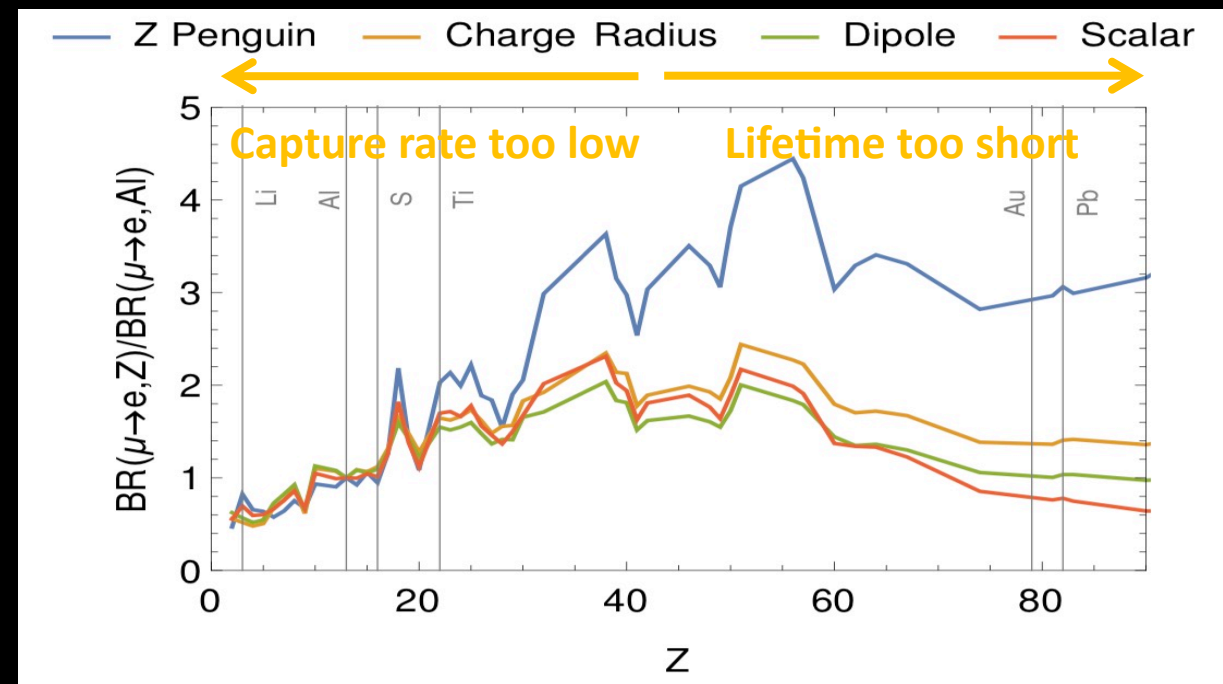
$$\text{BR}(\mu \rightarrow e) \propto |\text{DC}_{\text{DL}} + S^p C_{S,L}^p + V^p C_{V,R}^p + S^n C_{S,L}^n + V^n C_{V,R}^n|^2 + (\text{L} \leftrightarrow \text{R})$$

	S	D	V <sup>1</sup>	V <sup>2</sup>
$\frac{B(\mu \rightarrow e, \text{Ti})}{B(\mu \rightarrow e, \text{Al})}$	$1.70 \pm 0.005_y$	1.55	1.65	2.0
$\frac{B(\mu \rightarrow e, \text{Pb})}{B(\mu \rightarrow e, \text{Al})}$	$0.69 \pm 0.02_{\rho_n}$	1.04	1.41	$2.67 \pm 0.06_{\rho_n}$

$y$  = nuclear scalar form factor,  $\rho_n$  = nuclear neutron density

If we do see a signal in Al at Mu2e, what can we do?:

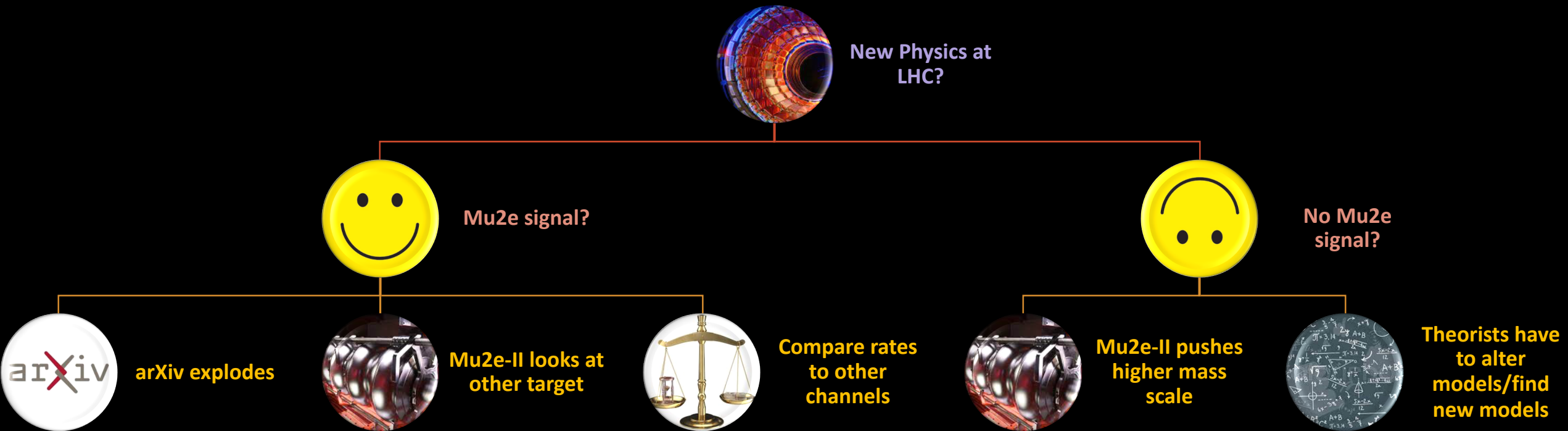
- Various operator coefficients add coherently in the amplitude.
  - Weighted by nucleus-dependent functions.
- Requires measurements of conversion rate in other target materials!
- Need to choose a target which is sensitive to directions Al is “blind” to



This is something we need to think about for Mu2e-II – our extended program (see final slide).

V. Cirigliano, S. Davidson, Y. Kuno, Phys. Lett. B 771 (2017) 242  
 S. Davidson, Y. Kuno, A. Saporta, Eur. Phys. J. C 78 (2018) 109  
 Kitano et al 2002

# Possibilities







# Other Physics Searches at Mu2e

$\mu^- N \rightarrow e^+ N'$

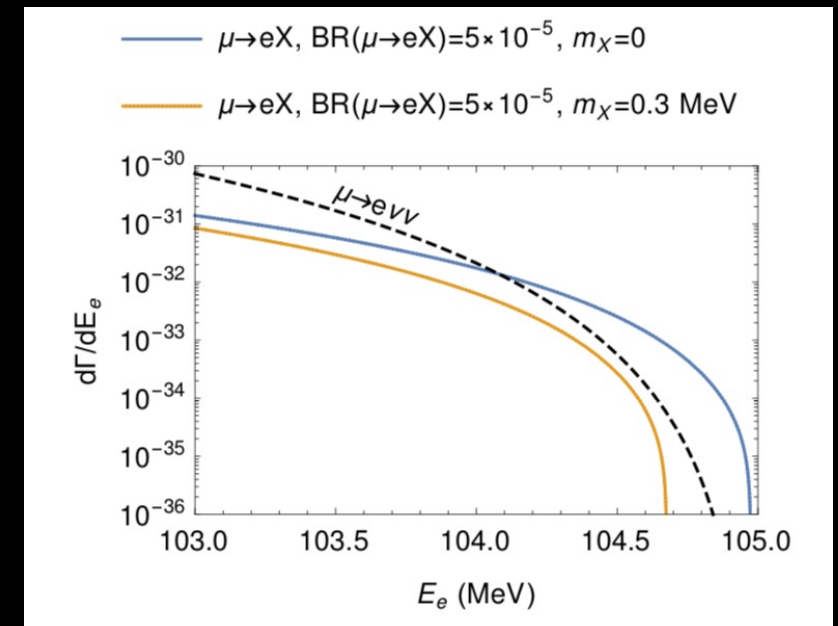
$$R_{\mu^- e^+}^{\text{Ti}} \equiv \frac{\Gamma(\mu^- + \text{Ti} \rightarrow e^+ + \text{Ca})}{\Gamma(\mu^- + \text{Ti} \rightarrow \nu_\mu + \text{Sc})} < \begin{cases} 1.7 \times 10^{-12} \text{ (GS, 90\% CL)} \\ 3.6 \times 10^{-11} \text{ (GDR, 90\% CL)} \end{cases}$$

- This conversion violates both lepton number ( $\Delta L = 2$ ) and lepton flavor conservation, and can be mediated by Majorana neutrinos through a type-1 see saw mechanism or new particle at  $> \text{TeV}$  scale.
- The Mu2e sensitivity to  $\mu^- \rightarrow e^+$  extends beyond the current best limit: [Phys Rev Lett B 412 p 334-338 \[13\]](#)
- $< m_{e\mu} >$  effective Majorana neutrino mass scale sensitivity down to the MeV region, surpassing the  $< m_{\mu\mu} >$  sensitivity in the kaon sector which is limited to the GeV region

Yeo et al 2017 <https://arxiv.org/abs/1705.07464>

$\mu^- N \rightarrow e X N$

- Where X is a new light boson (or axion).
- Currently understanding feasibility
- Example parameterization: [arXiv: 1110.2874](#)





# Experimental Strategy

How will Mu2e try to measure this process?

# Muonic Atoms



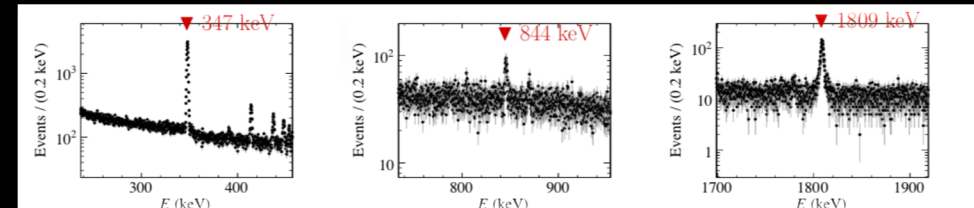
- The  $\mu \rightarrow e$  conversion rate is measured as a ratio to the muon capture rate on the same nucleus:

$$R_{\mu e} = \frac{\Gamma(\mu^- + A(Z, N) \rightarrow e^- + A(Z, N))}{\Gamma(\text{all-captures})}$$

- Low momentum (-) muons are captured in the target atomic orbit and quickly ( $\sim$ fs) cascades to 1s state.
- Lifetime of muonic aluminium = 864 ns
- In aluminum:

**Normalization = from X-rays emitted when muon stops in Al.**

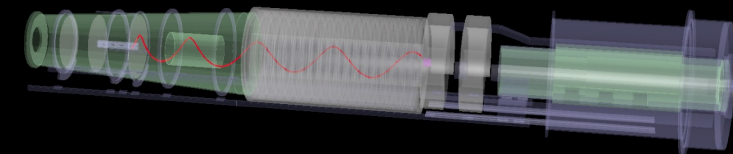
- 39 % Decay :**  $\mu + N \rightarrow e + \bar{\nu}_e + \nu_\mu$  (**Background**)
- 61 % Capture :**  $\mu + N \rightarrow \nu_\mu + N'$  (**Normalization**)
- The Signal :**  $\mu + N \rightarrow e + N$  (**Conversion**)



- Signal is monoenergetic electron consistent with:

$$E_e = m_\mu - E_{recoil} - E_{1S B.E.}, \text{ e.g. For Al: } E_e = 104.97 \text{ MeV.}$$

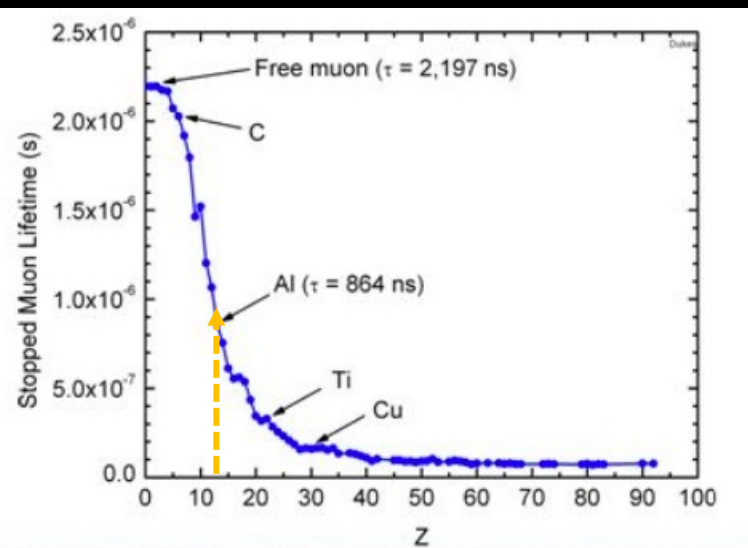
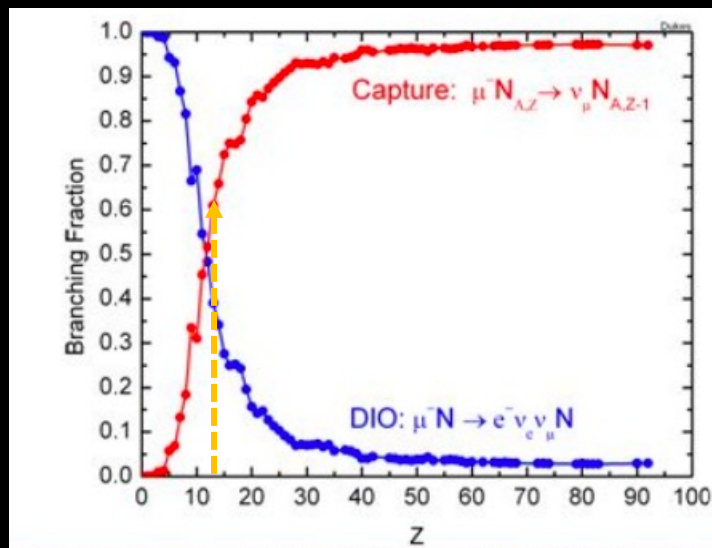
- Will be smeared by detector and stopping target effects.
- Nucleus coherently recoils off outgoing electron; it does not break-up!



# Why Aluminum?



Practical Advantages	Physics Advantages
Chemically Stable	Conversion energy such that only tiny fraction of photons produced by muon radiative capture.
Available in required size/shape/thickness	Muon lifetime long compared to transit time of prompt backgrounds.
Low cost	Conversion rate increases with atomic number, reaching maximum at Se and Sb, then drops. Lifetime of muonic atoms decreases with increasing atomic number.
	Lifetime of muonic atom sits in “goldilocks” region i.e. neither longer than 1700 ns pulse spacing and greater than our pionic live gate.



The lifetime of a muon in a muonic atom decreases with increasing atomic number.

Mu2e gets 8kW, 8GeV Protons from the Fermilab booster:

- Mu2e will acquire  $\vartheta$  ( $10^{20}$ ) Protons on Target to achieve design goal



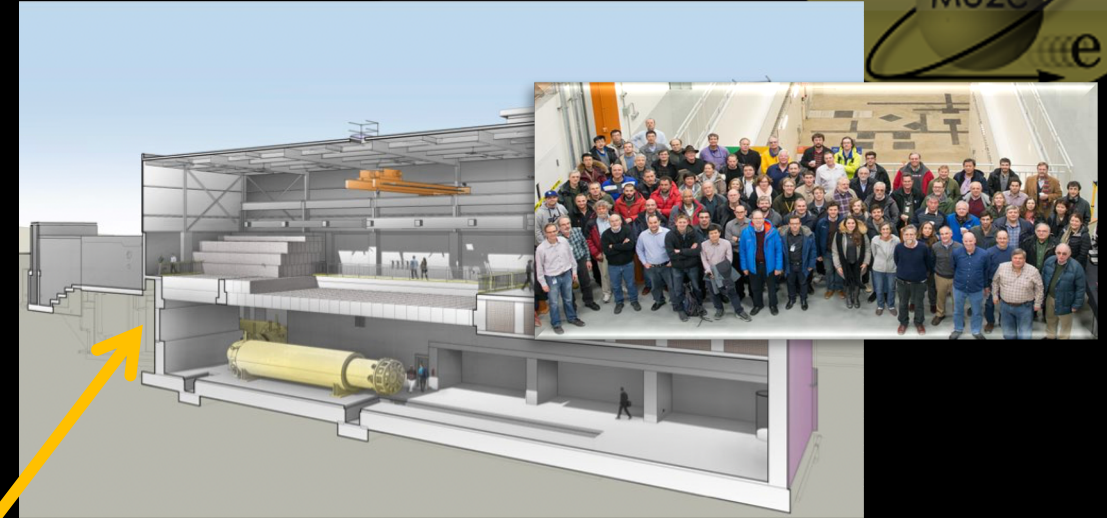


Mu2e gets 8kW, 8GeV Protons from the Fermilab booster:

- Mu2e will acquire  $\vartheta$  ( $10^{20}$ ) Protons on Target to achieve design goal



Mu2e building:

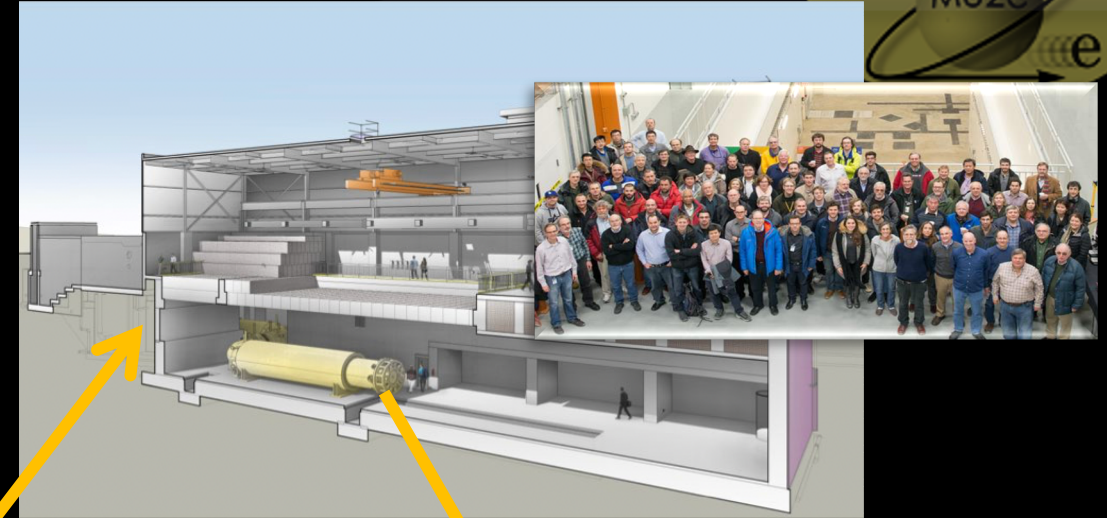


Mu2e gets 8kW, 8GeV Protons from the Fermilab booster:

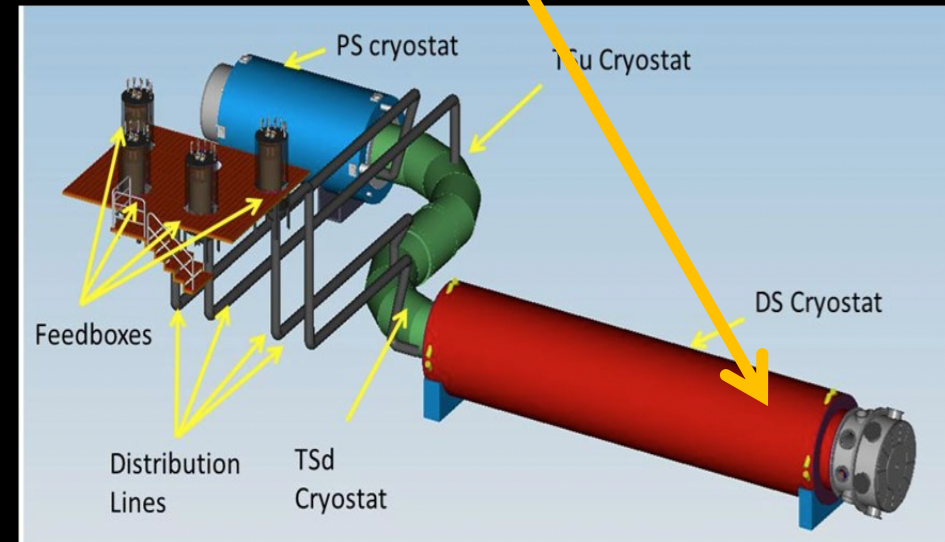
- Mu2e will acquire  $\vartheta$  ( $10^{20}$ ) Protons on Target to achieve design goal



Mu2e building:



Mu2e:





# The Mu2e Experiment

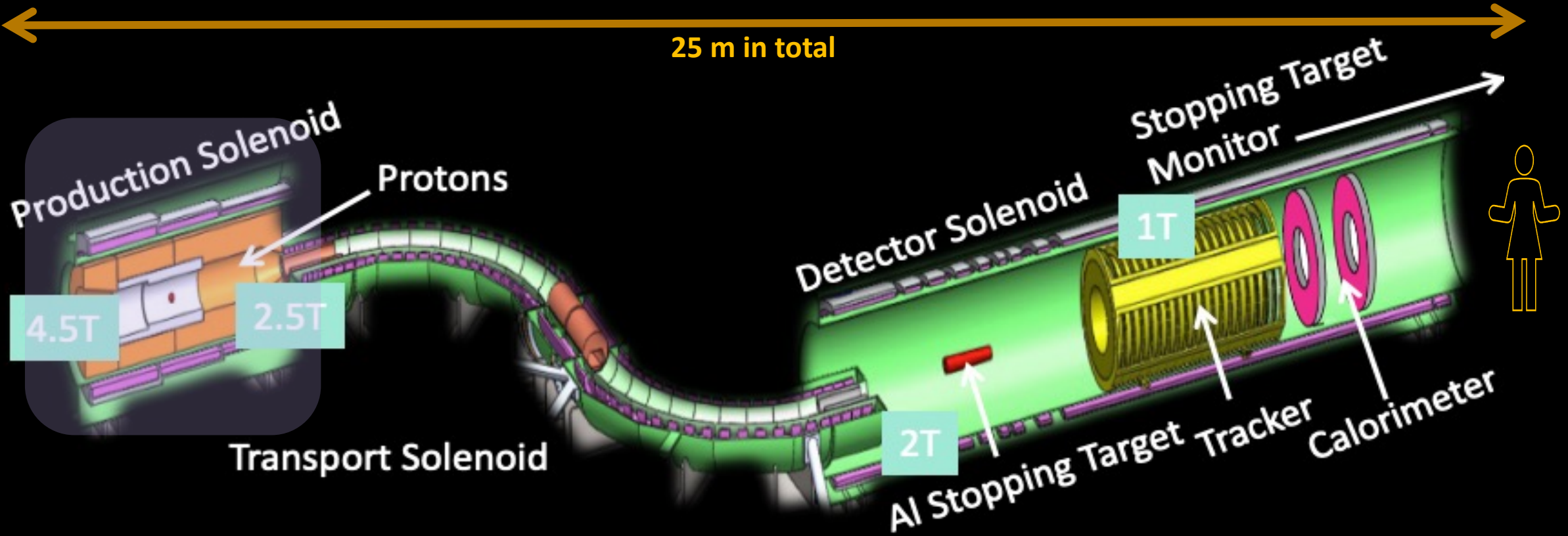
V. Lobashev & R. Djilkibaev (Sov. J. Nucl. Phys. 49(2), 384 (1989))



## Production Solenoid:

- 8 GeV Protons enter, pions produced, decay to muons
- Graded magnetic field reflects pions/muons to transport solenoid

25 m in total



# The Mu2e Experiment

V. Lobashev & R. Djilkibaev (Sov. J. Nucl. Phys. 49(2), 384 (1989))



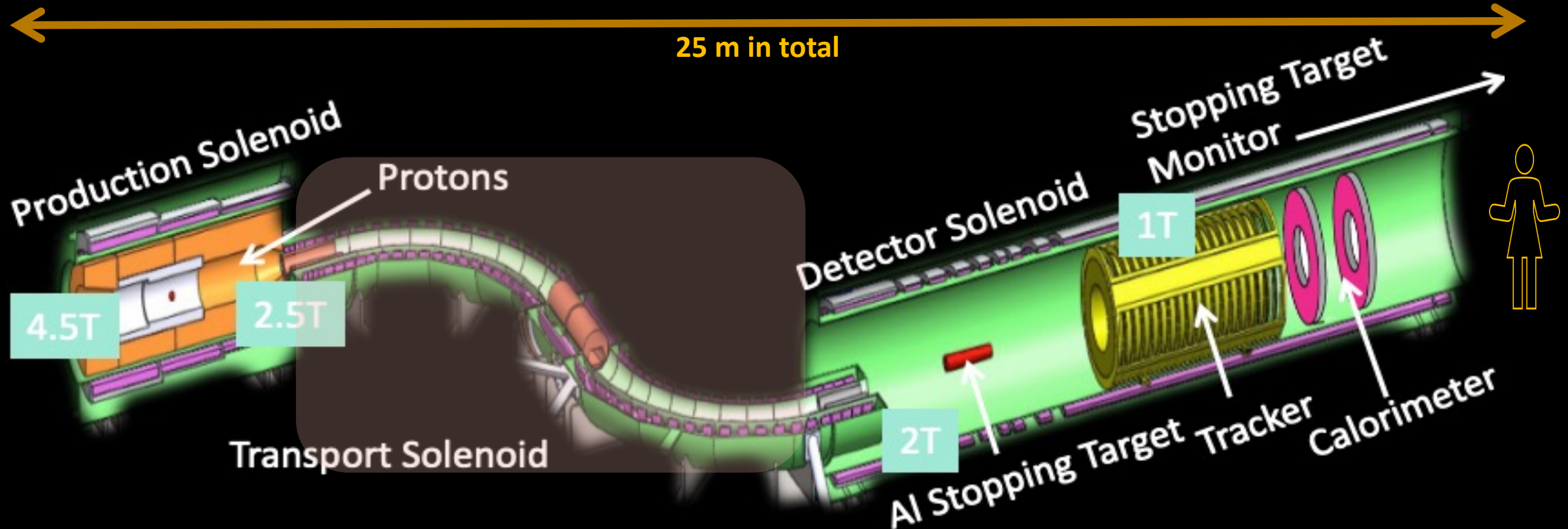
## Production Solenoid:

- 8 GeV Protons enter, pions produced, decay to muons
- Graded magnetic field reflects pions/muons to transport solenoid

## Transport Solenoid:

- “S” shape removes line of sight backgrounds
- Windows remove anti-protons
- Collimators help select low momentum, negative muons and “focus” on detector solenoid aperture.

25 m in total



# The Mu2e Experiment

V. Lobashev & R. Djilkibaev (Sov. J. Nucl. Phys. 49(2), 384 (1989))



## Production Solenoid:

- 8 GeV Protons enter, pions produced, decay to muons
- Graded magnetic field reflects pions/muons to transport solenoid

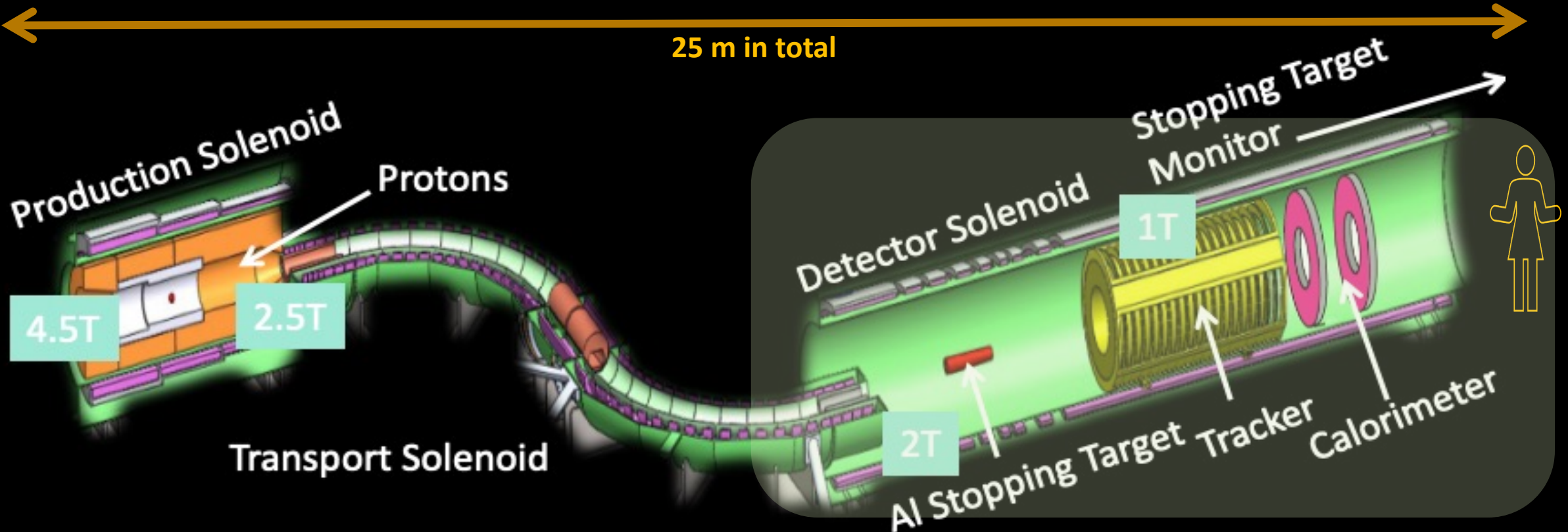
## Transport Solenoid:

- “S” shape removes line of sight backgrounds
- Windows remove anti-protons
- Collimators help select low momentum, negative muons and “focus” on detector solenoid aperture.

## Detector Solenoid:

- Al Stopping Target made of thin foils captures the muons
- Graded magnetic field “focusses” electrons on tracker
- Straw tracker and calorimeter measure momentum

25 m in total







# Beamline & Solenoids: Status

What is the current status of the beamline components?

# Beamline: Status

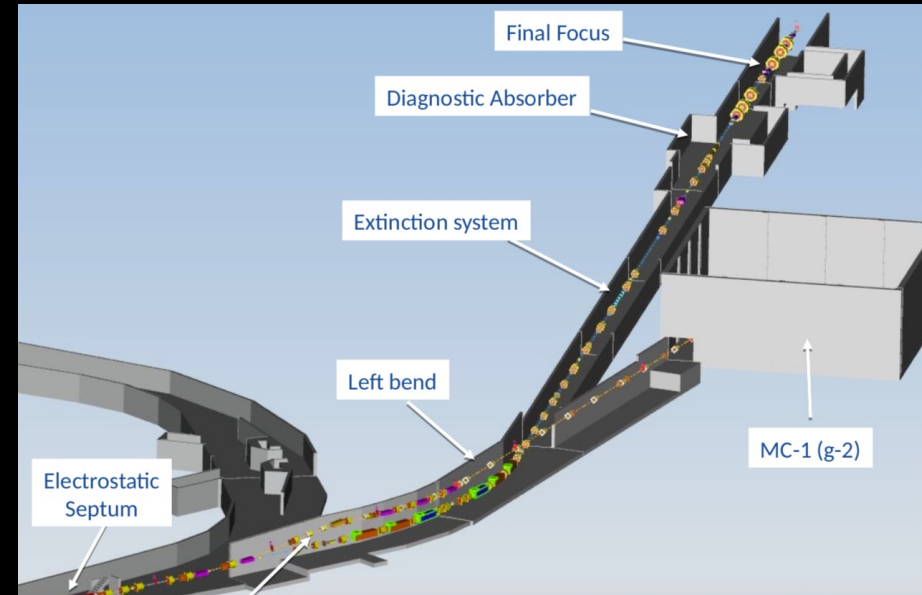
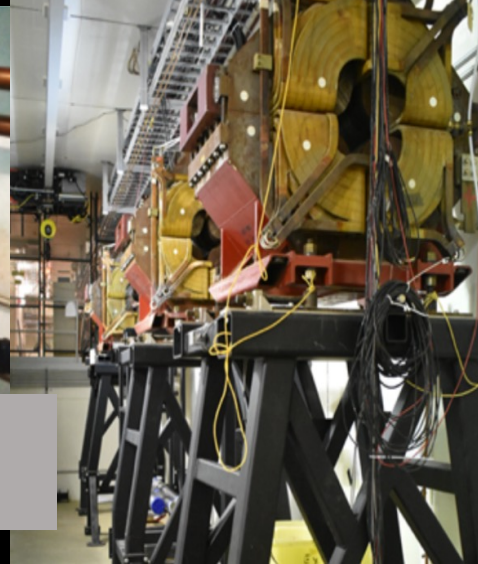


Magnets installed along M4 beamline



Quadrupole in Delivery Ring used for resonant extraction

Final Focus magnets are in place



The beamline installation is almost complete:

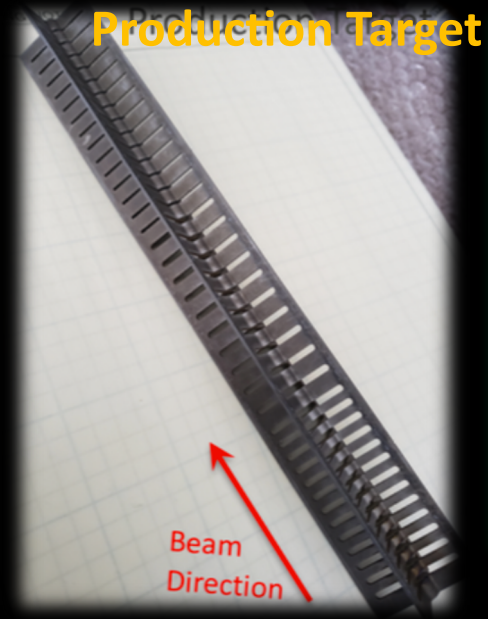
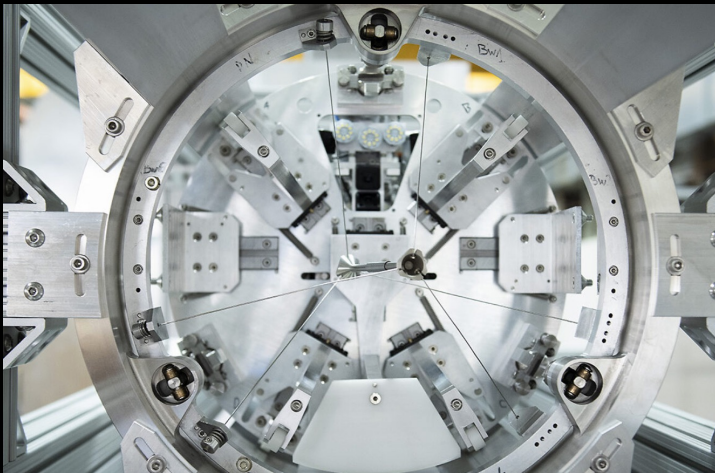
- Vacuum System installed
- Instrumentation upstream of diagnostic absorber in progress



# Production Target: Status

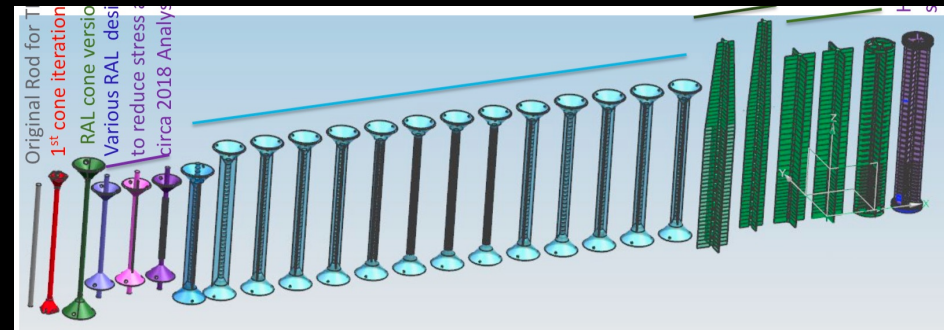
- Made of tungsten, completed in April 2021 - 10% of beam power into the target ,
- Heats up to 1700 °C (~3100 F),
- Production Solenoid must be radiatively cooled,
- Average power density ~150 MW/m<sup>3</sup>

## Production Target & Frame



Production Target in support

## Many iterations



<https://www.symmetrymagazine.org/article/a-robot-ballet>

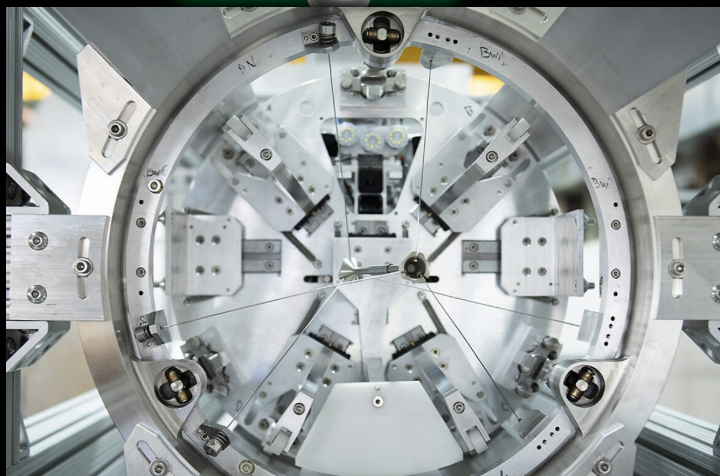
Nice video of robotic extraction of target

Mu2e: Searching for  $\mu N \rightarrow e N$  at Fermilab - Sophie Middleton -  
smidd@caltech.edu

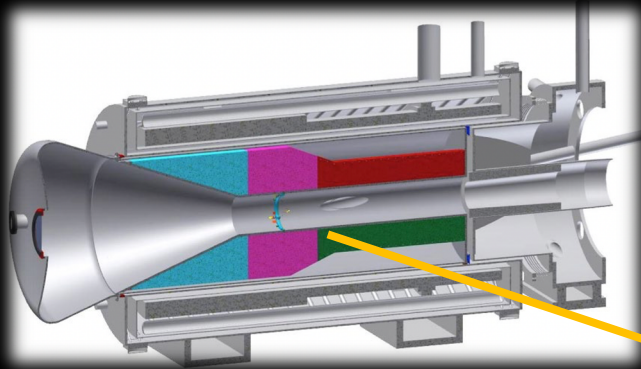
26 October 2021

52

# Production Solenoid: Status



Production Target & Frame



All 3 coils fabricated, under-going tests at vendor



Heat & Radiation Shield



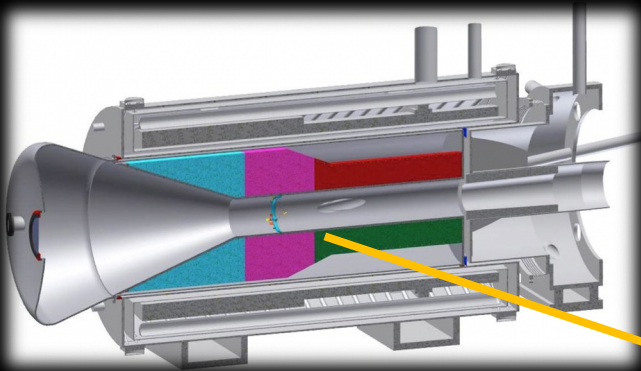
<https://www.symmetrymagazine.org/article/a-robot-ballet>

Nice video of robotic extraction of target

Mu2e: Searching for  $\mu \rightarrow e \gamma$  at Fermilab - Sophie Middleton -  
smidd@caltech.edu



# Production Solenoid: Status

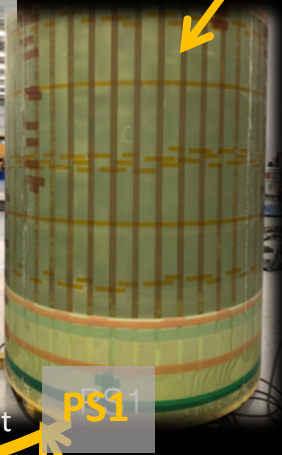


All 3 coils fabricated, under-going tests at vendor

Heat & Radiation Shield



Production Target & Frame



<https://www.symmetrymagazine.org/article/a-robot-ballet>

Nice video of robotic extraction of target

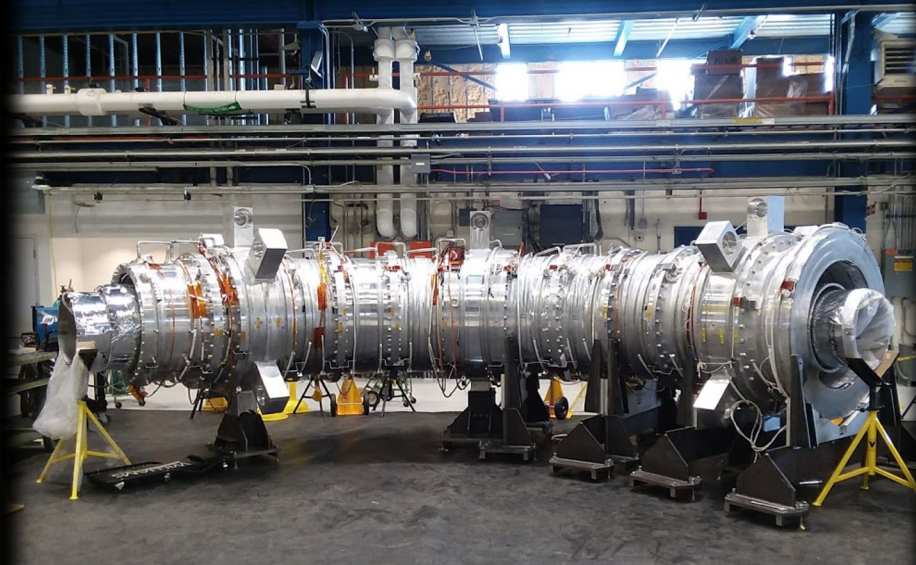
Mu2e: Searching for  $\mu N \rightarrow e N$  at Fermilab - Sophie Middleton - smidd@caltech.edu



# Transport Solenoid: Status



Thermal shield shown next to TSu



TS coldmass at Fermilab awaiting final tests.



- All coils of the TS are now at Fermilab.
- TSu and TSd cold-masses assembled.
- Testing almost complete
- Outer thermal shield will be split and re-assembled around the TSu cold-mass alongside in image.



TSd vacuum vessel, awaiting leak check



TSu vacuum vessel, leak tight

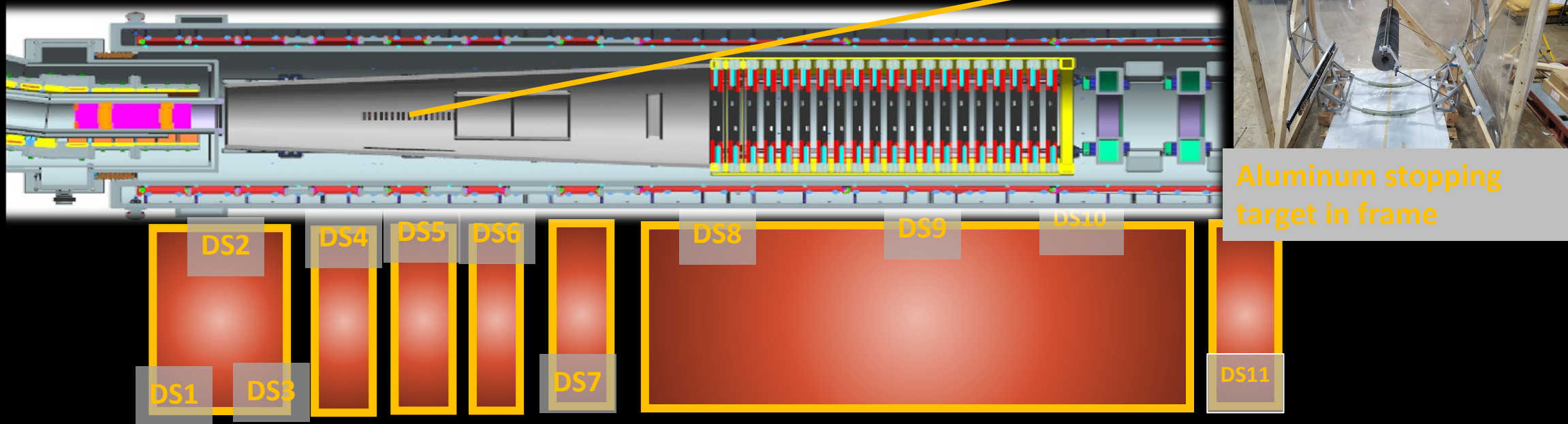




Nice video of the TS being lifted at FNAL in July:

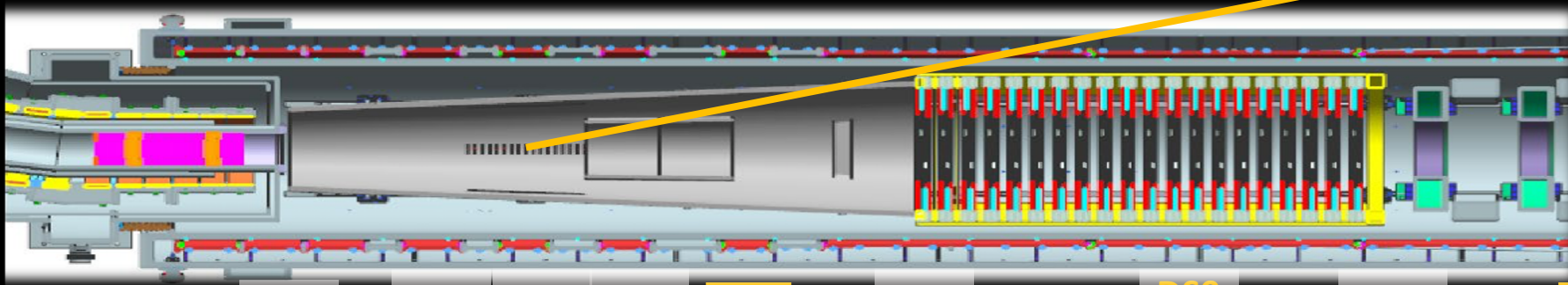


# Detector Solenoid: Status

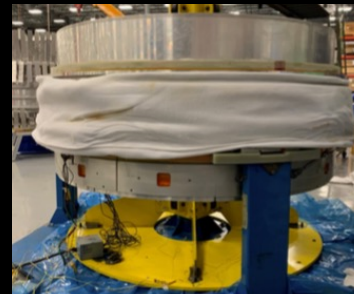
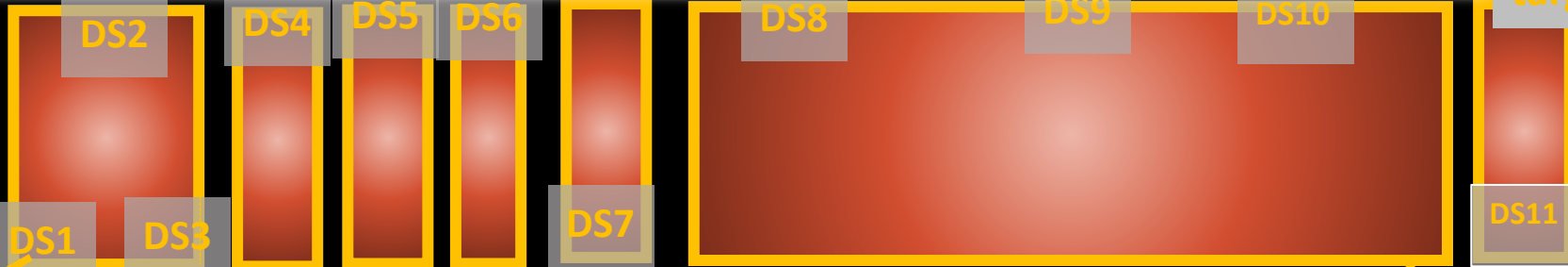




# Detector Solenoid: Status



Aluminum stopping target in frame



DS10

4/11 coils fabricated, tests on going  
Others being wound

for  $\mu N \rightarrow e N$  at Fermilab - Sophie Middleton -  
smidd@caltech.edu



# “Background free” design

How do we ensure Mu2e is “background free”?  
Why have we designed our detectors in this way?



# Removing Backgrounds

Beam delivery and detector systems optimized for high intensity, pure muon beam – must be “background free”:

- Intrinsic :
  - Scale with number of stopped muons.
- Late arriving :
  - Scale with number of late protons/ extinction performance

Type	Source	Mitigation	Yield (over lifetime of experiment)
Intrinsic	Decay in Orbit (DIO)	Tracker Deign/ Resolution	$0.144 \pm 0.028$ (stat) $\pm 0.11$ (sys)
Late Arriving	Pion Capture	Beam Structure /Extinction	$0.021 \pm 0.001$ (stat) $\pm 0.002$ (sys)
	Pion Decay in Flight	-	$0.001 \pm < 0.001$
Other	Anti-proton	Thin Absorber Windows	$0.04 \pm 0.022$ (stat) $\pm 0.020$ (sys)
	Cosmic Rays	Active Veto System	$0.209 \pm 0.0022$ (stat) $\pm 0.055$ (sys)

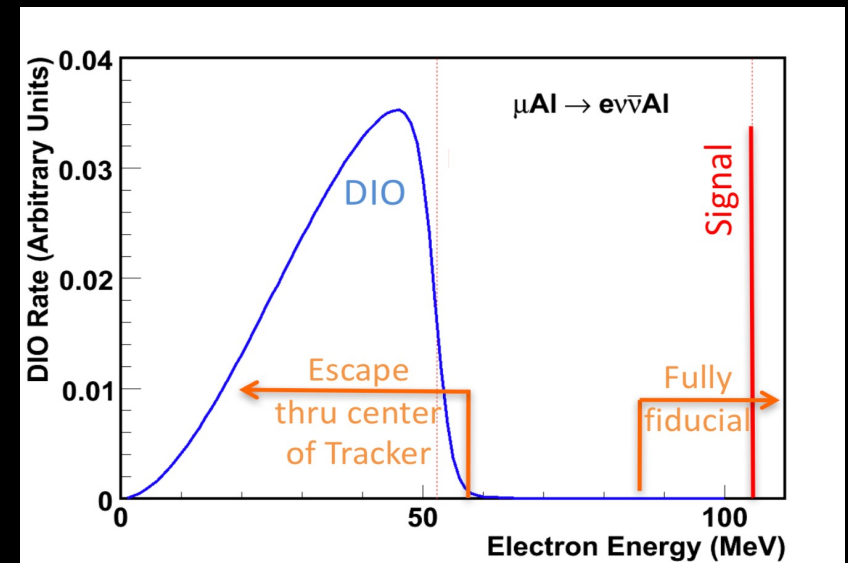


# Muon Decay-in-Orbit (DIO) Backgrounds



In Aluminium 39% of stopped muons will decay in orbit (DIO):

- Free muon decay: peak electron energy far below our signal energy (peaks 52.8 MeV).

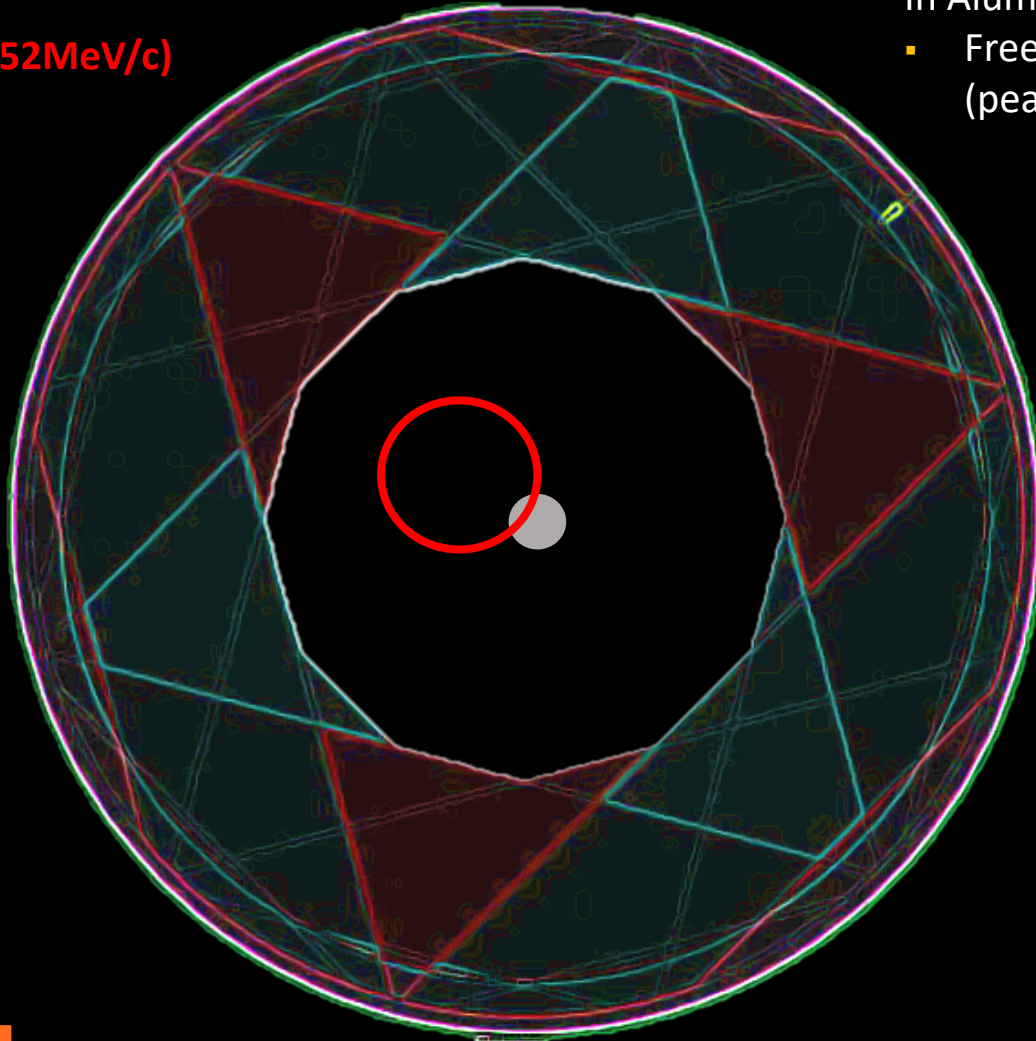


# Muon Decay-in-Orbit (DIO) Backgrounds



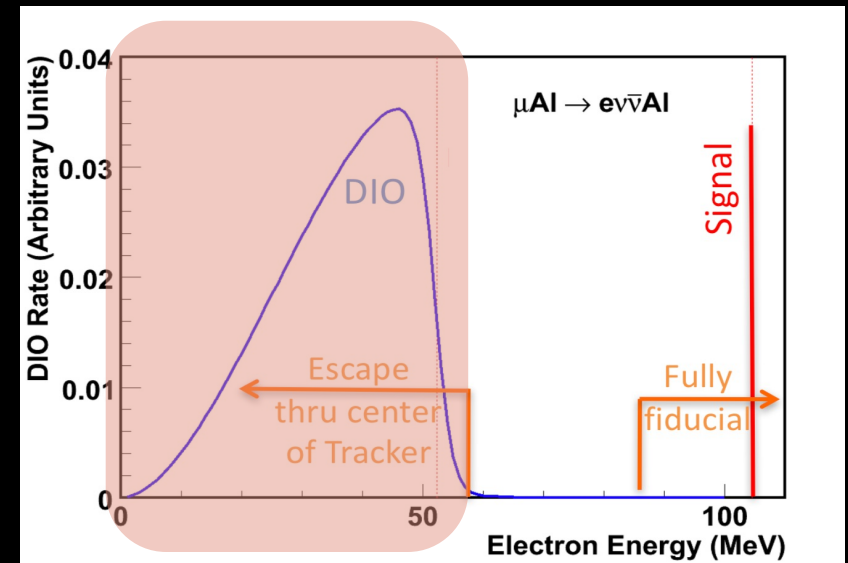
## Transverse Plane

- Michel Electron (52MeV/c)



In Aluminium 39% of stopped muons will decay in orbit (DIO):

- Free muon decay: peak electron energy far below our signal energy (peaks 52.8 MeV).

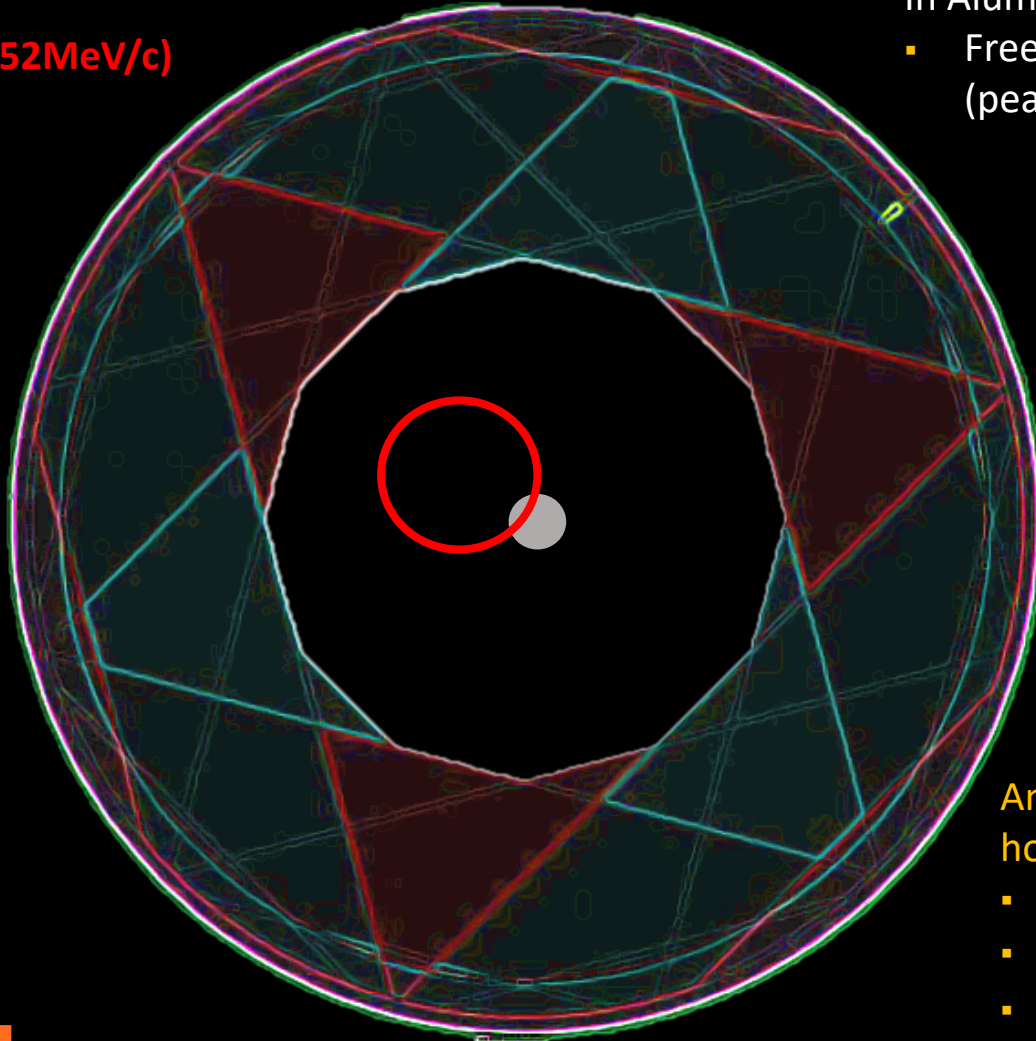


# Muon Decay-in-Orbit (DIO) Backgrounds



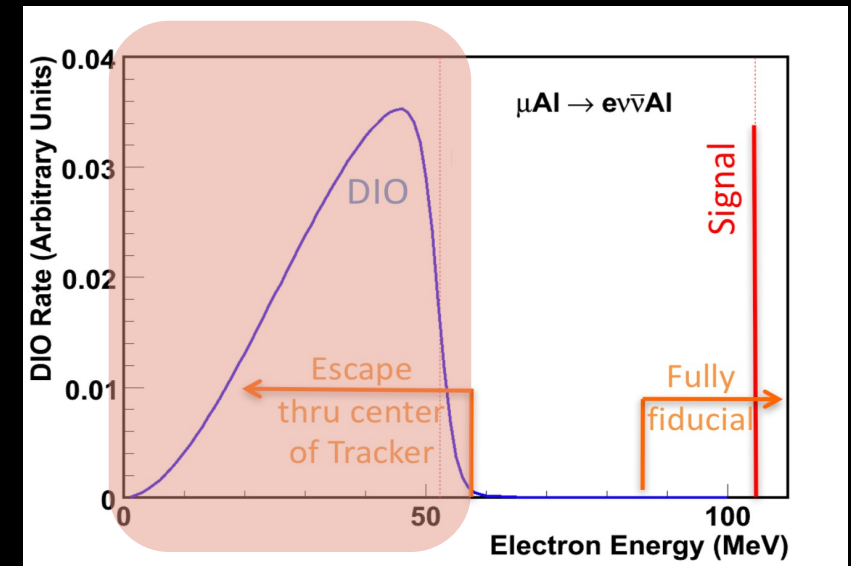
## Transverse Plane

- Michel Electron (52MeV/c)



In Aluminium 39% of stopped muons will decay in orbit (DIO):

- Free muon decay: peak electron energy far below our signal energy (peaks 52.8 MeV).



Annular Design → Excludes low momentum electrons via hollow centre:

- Inner 38 cm un-instrumented .
- Reduces need to reject  $\sim 10^{18}$  to  $\sim 10^5$ .
- Blind to  $> 99\%$  of DIO spectrum.

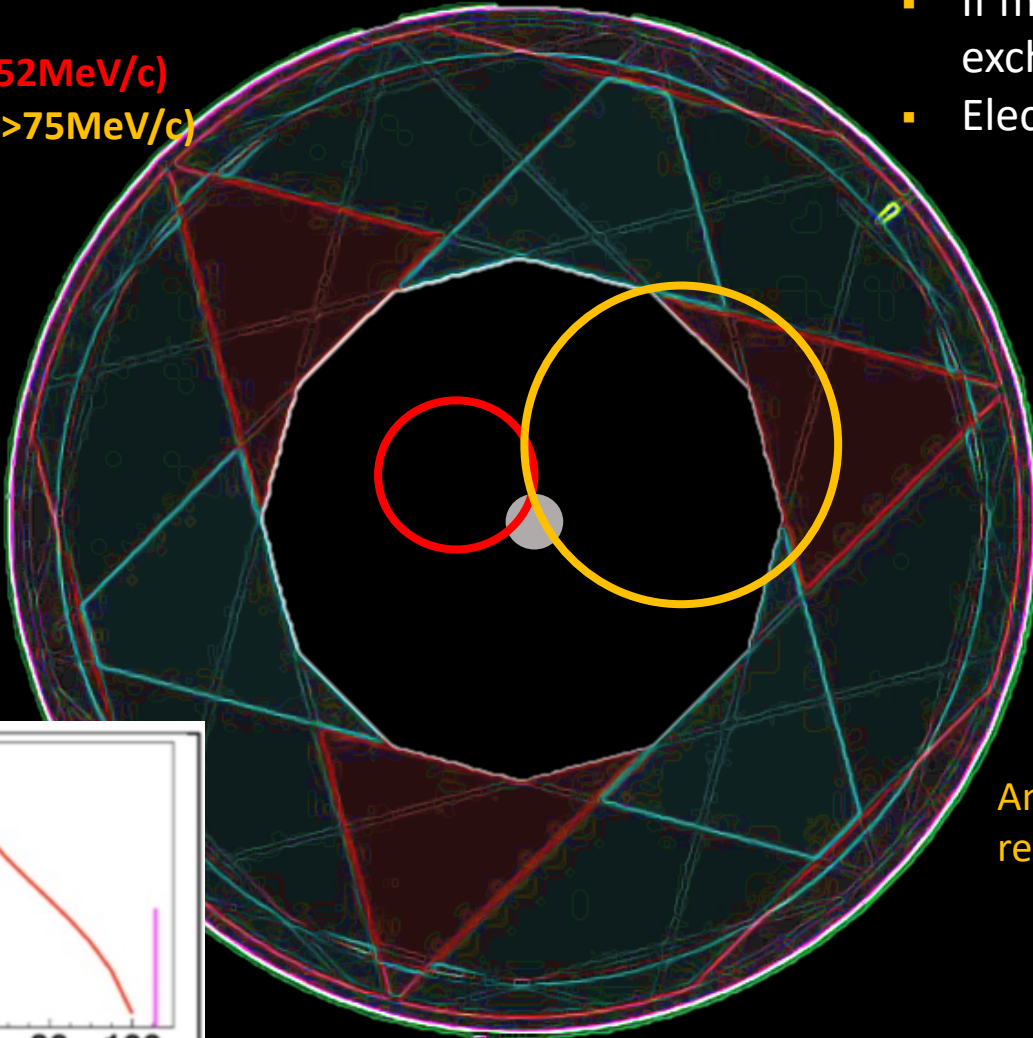
# Muon Decay-in-Orbit (DIO) Backgrounds



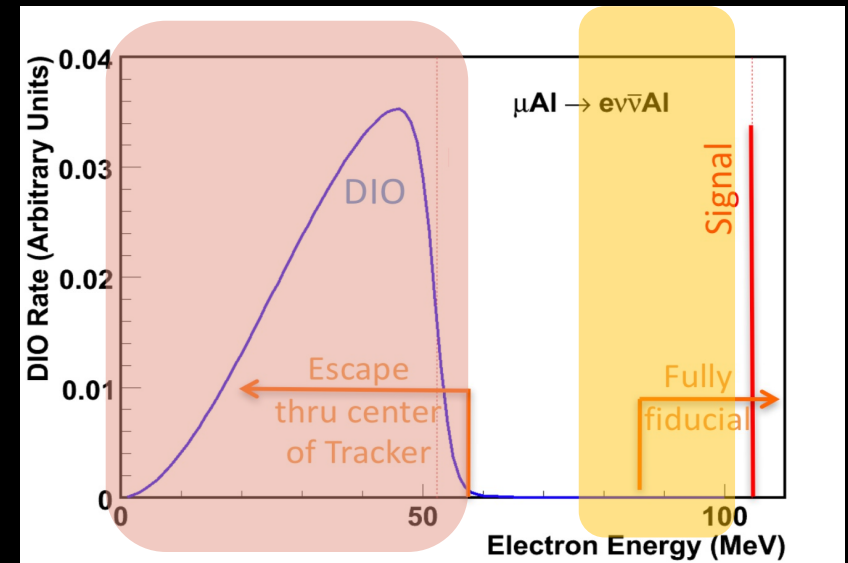
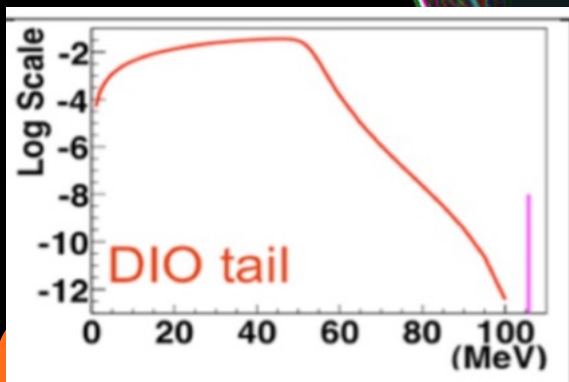
## Transverse Plane

- Michel Electron (52MeV/c)
- Problematic Tail (>75MeV/c)

- If muon bound in atomic orbit, the outgoing electron can exchange momentum with the nucleus.
- Electron could have energy close to signal.



Recoil tail:



Annular Design → cannot fully exclude electrons in the recoil tail.

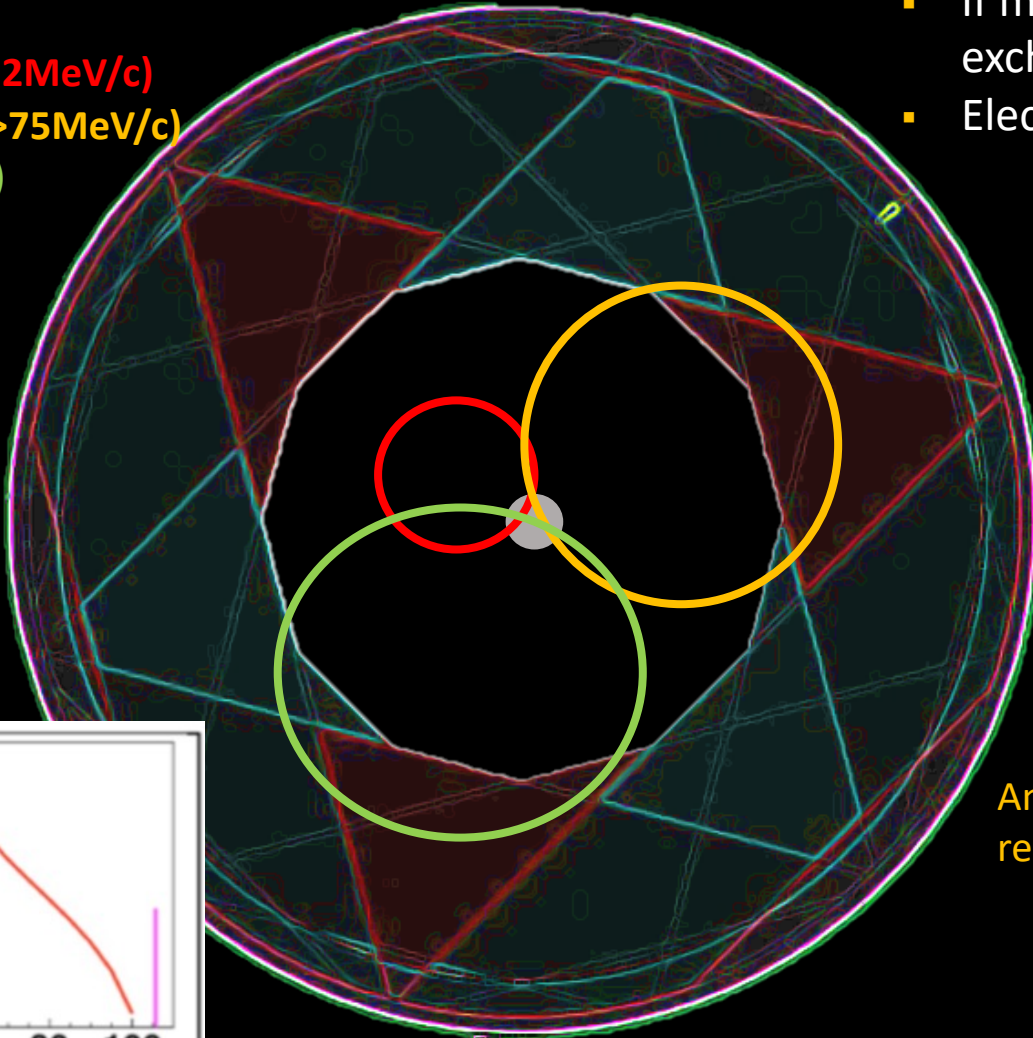


# Muon Decay-in-Orbit (DIO) Backgrounds

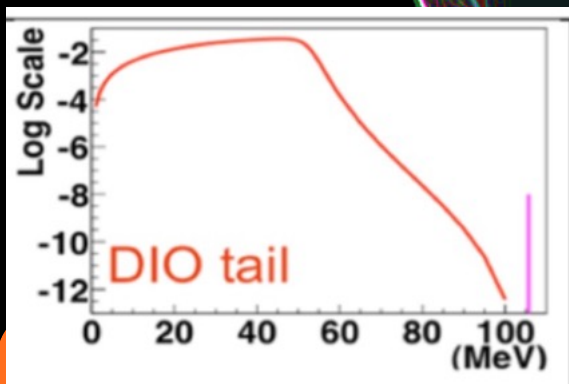


## Transverse Plane

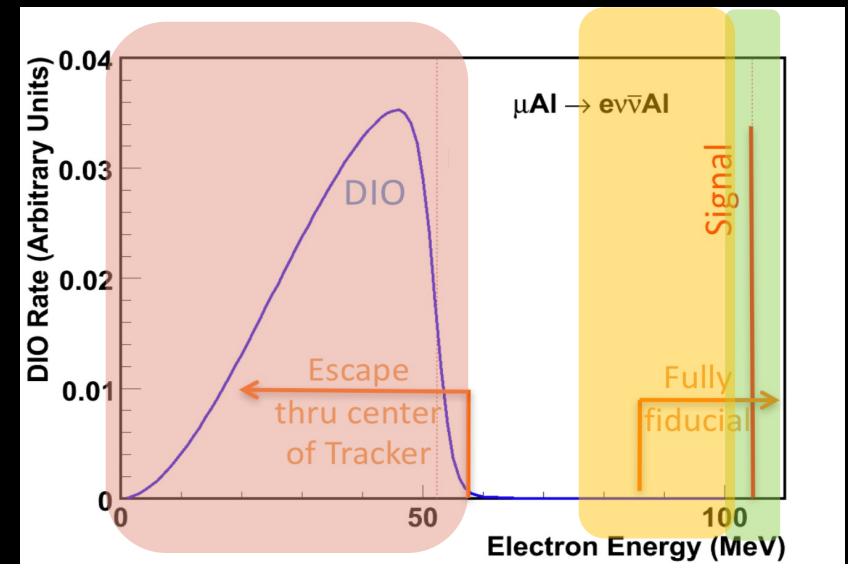
- Michel Electron (52MeV/c)
- Problematic Tail (>75MeV/c)
- Signal (105MeV/c)



Recoil tail:



- If muon bound in atomic orbit, the outgoing electron can exchange momentum with the nucleus.
- Electron could have energy close to signal.



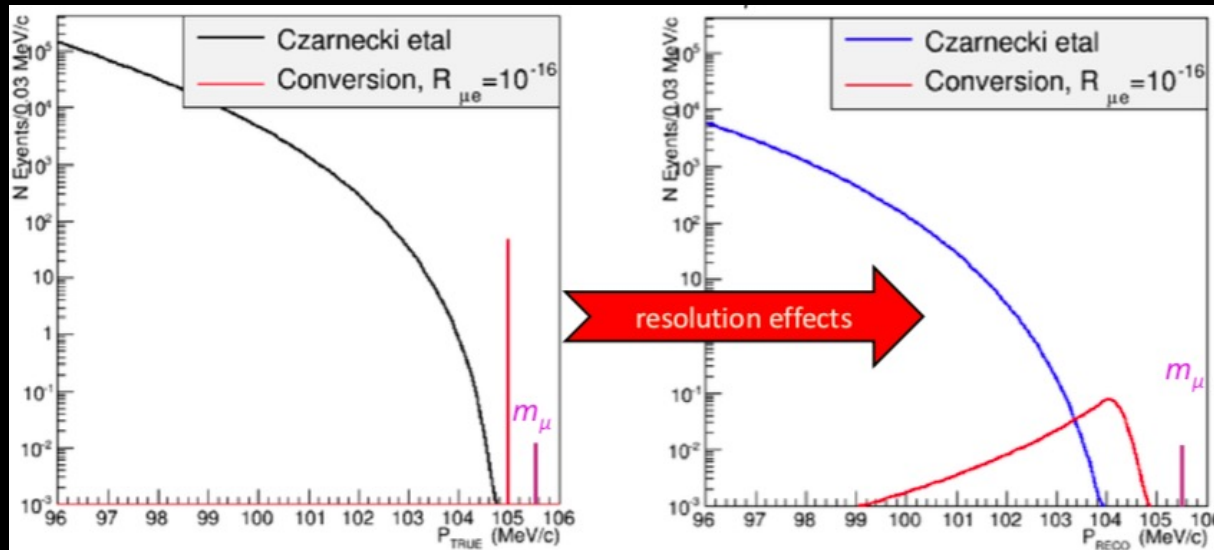
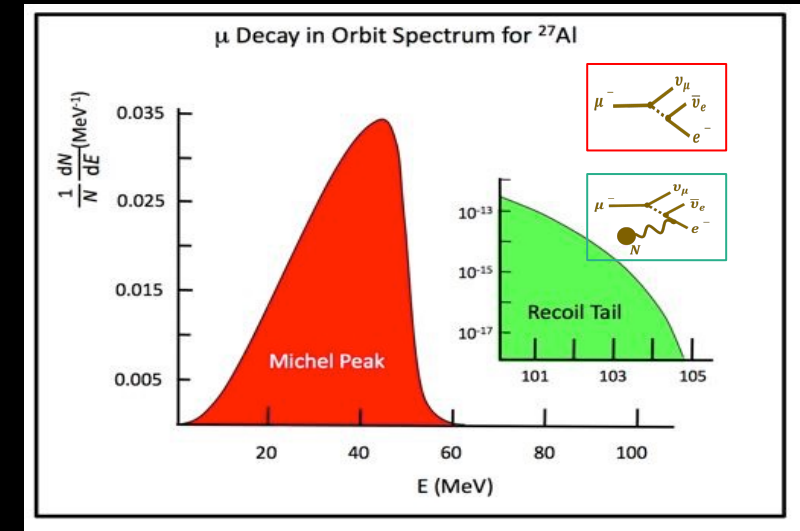
Annular Design → cannot fully exclude electrons in the recoil tail.

# Muon Decay-in-Orbit (DIO) Backgrounds



The differential energy spectrum of DIO electron spectrum has been parameterized in A. Czarnecki et al., “Muon decay in orbit: Spectrum of high-energy electrons,” Phys. Rev. D 84 (Jul, 2011) .

- Necessitates tracker resolution of better than 200 KeV/c





# Rejecting DIO Backgrounds



- To remove remaining DIOs momentum resolution  $< 200$  KeV/c achieved by:

# Rejecting DIO Backgrounds



- To remove remaining DIOs momentum resolution  $< 200 \text{ KeV/c}$  achieved by:
  1. **Low Mass  $\rightarrow$  Minimizes scattering and energy loss :**
    - Entire Detector Solenoid held under vacuum ( $\sim 10^{-4}$  torr).
    - Ultra low mass tracker.

# Rejecting DIO Backgrounds



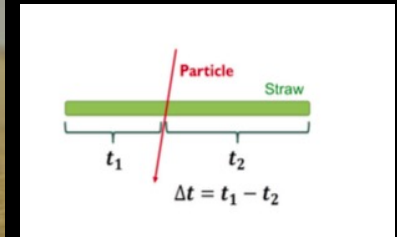
- To remove remaining DIOs momentum resolution  $< 200 \text{ KeV/c}$  achieved by:
  1. **Low Mass  $\rightarrow$  Minimizes scattering and energy loss :**
    - Entire Detector Solenoid held under vacuum ( $\sim 10^{-4}$  torr).
    - Ultra low mass tracker.
  2. **Segmented  $\rightarrow$  Handle high rates and provide high-precision momentum measurements.**

# The Tracker: Design

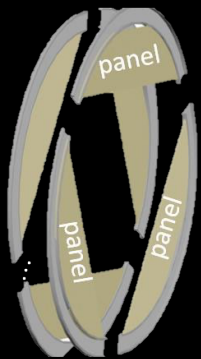


- Tracker is constructed from self-supporting panels of low mass straws tubes detectors
- 18 stations, 2 planes per station, 6 panels per plane, 96 straws per panel.
- Straw drift tubes aligned transverse to the axis of the Detector Solenoid.
  - 1m, 5 mm diameter straw
  - Walls: 12 mm Mylar + 3 mm epoxy
  - 25 mm Au-plated W sense wire
  - 33 – 117 cm in length
  - 80:20 Ar:CO<sub>2</sub> with HV < 1500 V
  - Straw wall thickness of 15  $\mu\text{m}$  has never been done before
- Charged particles ionize gas – drift to wire – detect signals!

## The Straws:



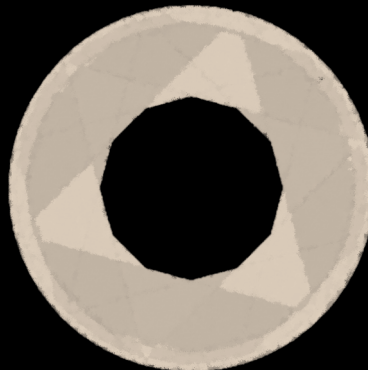
6 Panels



2 Plane

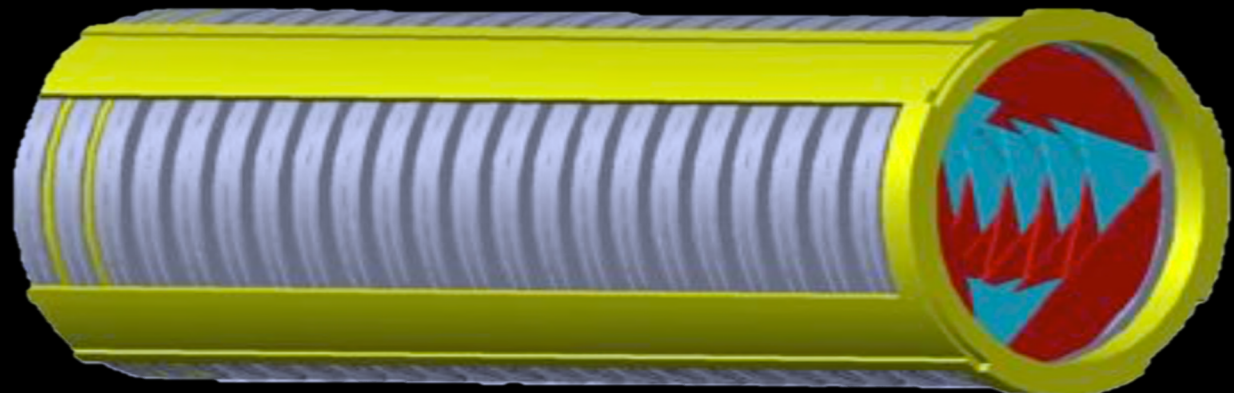


1 Station



Tracker: 18 stations

~ 3m, 1 T field



# Rejecting DIO Backgrounds

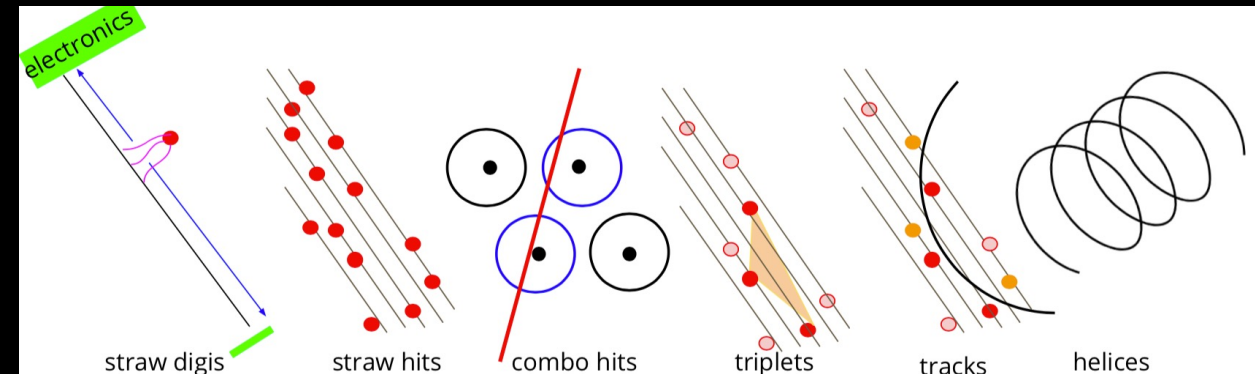


- To remove remaining DIOs momentum resolution  $< 200 \text{ KeV}/c$  achieved by:
  1. **Low Mass  $\rightarrow$  Minimizes scattering and energy loss :**
    - Entire Detector Solenoid held under vacuum ( $\sim 10^{-4}$  torr).
    - Ultra low mass tracker.
  2. **Segmented  $\rightarrow$  Handle high rates and provide high-precision momentum measurements.**

# Rejecting DIO Backgrounds



- To remove remaining DIOs momentum resolution  $< 200 \text{ KeV/c}$  achieved by:
  1. **Low Mass**  $\rightarrow$  **Minimizes scattering and energy loss** :
    - Entire Detector Solenoid held under vacuum ( $\sim 10^{-4}$  torr).
    - Ultra low mass tracker.
  2. **Segmented**  $\rightarrow$  **Handle high rates and provide high-precision momentum measurements.**
  3. **Sophisticated reconstruction algorithm** containing:
    1. hit construction,
    2. time clustering,
    3. tracking via pattern recognition,
    4. refinement via Kalman fitting,
    5. background rejection via Machine Learning



M. Devilbiss, UMich  
FERMILAB-SLIDES-20-100-V



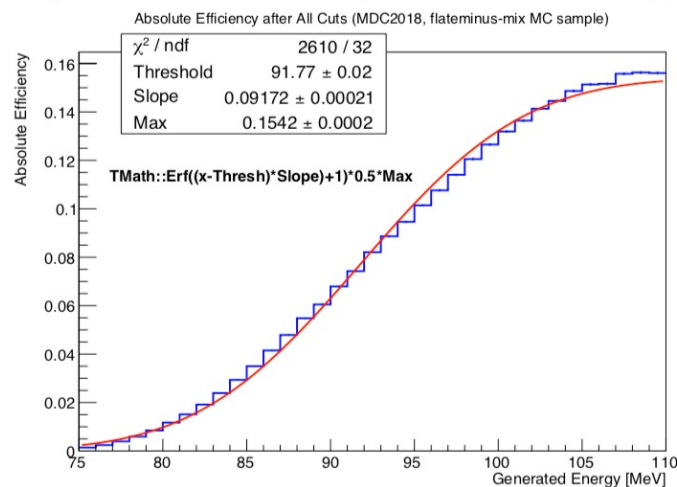
# Acceptance & Response

Paper documenting our Machine Learning analysis.  
<https://arxiv.org/abs/2106.08891>



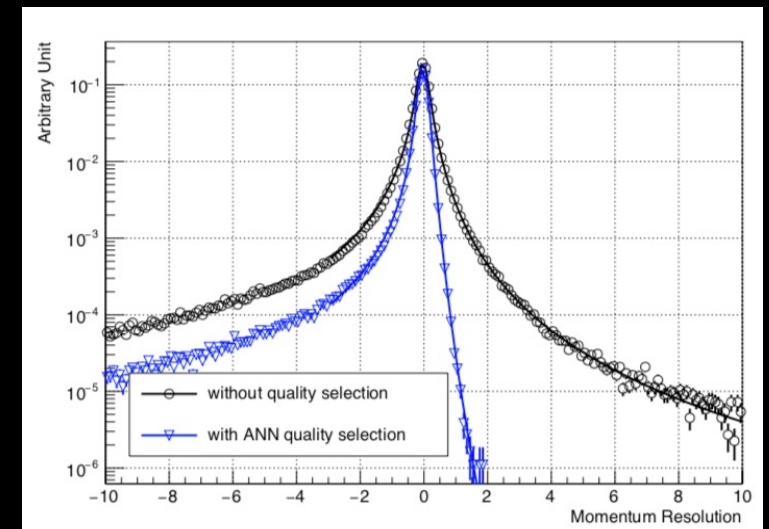
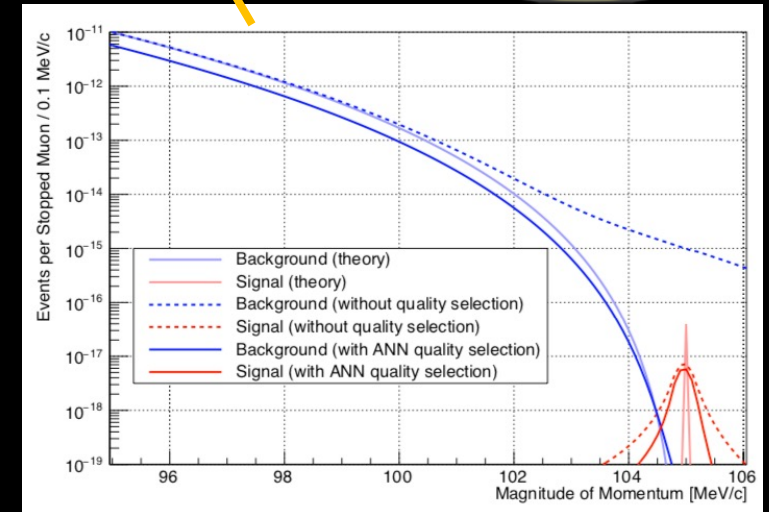
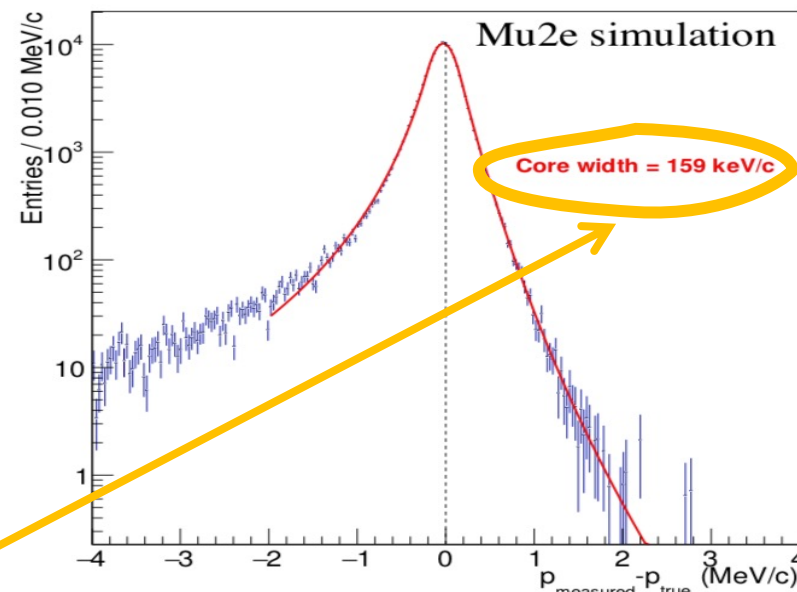
- Experiment is “blind” to anything with energy < 75 MeV.
- Tracking resolution improved by use of ANN.

## Absolute Efficiency (as function of generated energy)



Well within our requirement!

## momentum resolution at start of tracker (simulation)





# Removing Backgrounds

Beam delivery and detector systems optimized for high intensity, pure muon beam – must be “background free”:

- Intrinsic :
  - Scale with number of stopped muons.

- Late arriving :
  - Scale with number of late protons/ extinction performance

Type	Source	Mitigation	Yield (over lifetime of experiment)
Intrinsic	Decay in Orbit (DIO)	Tracker Deign/ Resolution	$0.144 \pm 0.028$ (stat) $\pm 0.11$ (sys)
Late Arriving	Pion Capture	Beam Structure /Extinction	$0.021 \pm 0.001$ (stat) $\pm 0.002$ (sys)
	Pion Decay in Flight	-	$0.001 \pm < 0.001$
Other	Anti-proton	Thin Absorber Windows	$0.04 \pm 0.022$ (stat) $\pm 0.020$ (sys)
	Cosmic Rays	Active Veto System	$0.209 \pm 0.0022$ (stat) $\pm 0.055$ (sys)

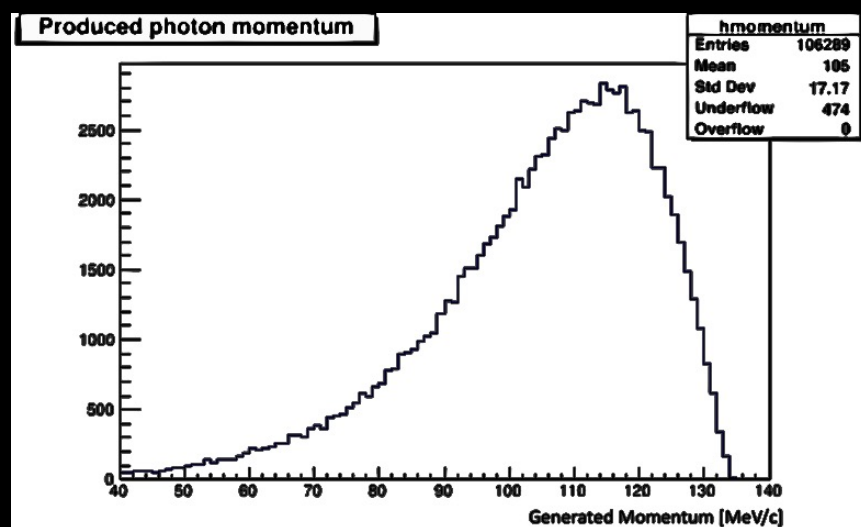


# Pion Backgrounds

J.A. Bistirlich, K.M. Crowe et al., Phys Rev C5, 1867 (1972)

- Radiative Pion Capture occur when a pion is captured by a nucleus at our Stopping Target. The resulting photon produces an outgoing electron and positron pair. Pair production can be internal or external of atom.
- For simulation studies Mu2e uses the work of Bistirlich et al to parameterize the photon energy. The closest material analyzed in data is Magnesium. The work of Kroll-Wada-Joseph is used to calculate outgoing LorentzVectors of positron and electron:

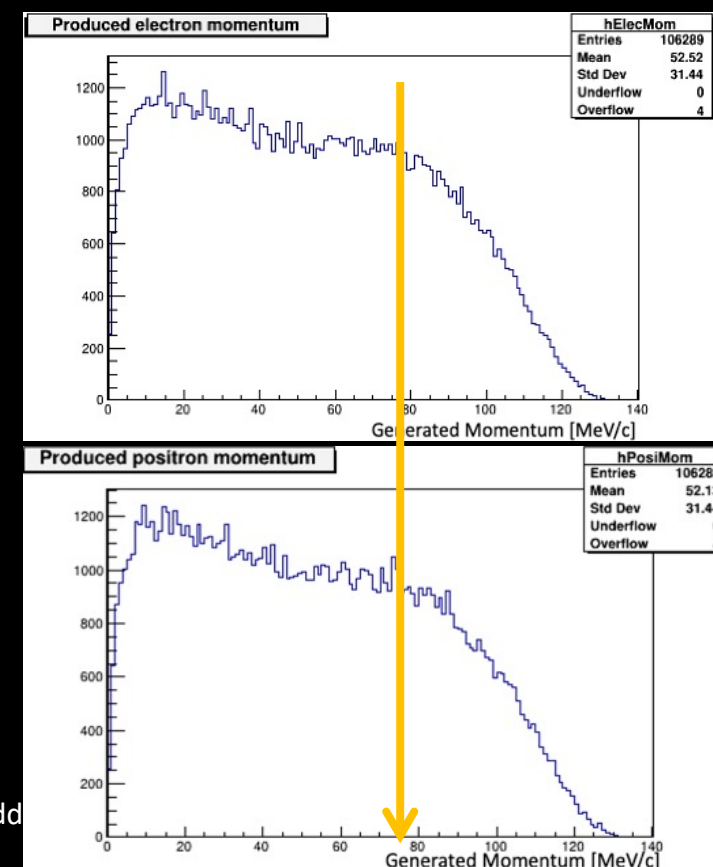
The annular tracker means we are “blind” to large fraction of  $e^-/e^+$  from RPC – even without time cuts!



$e^-$

$e^+$

Photon can be virtual (internal) or not (external)



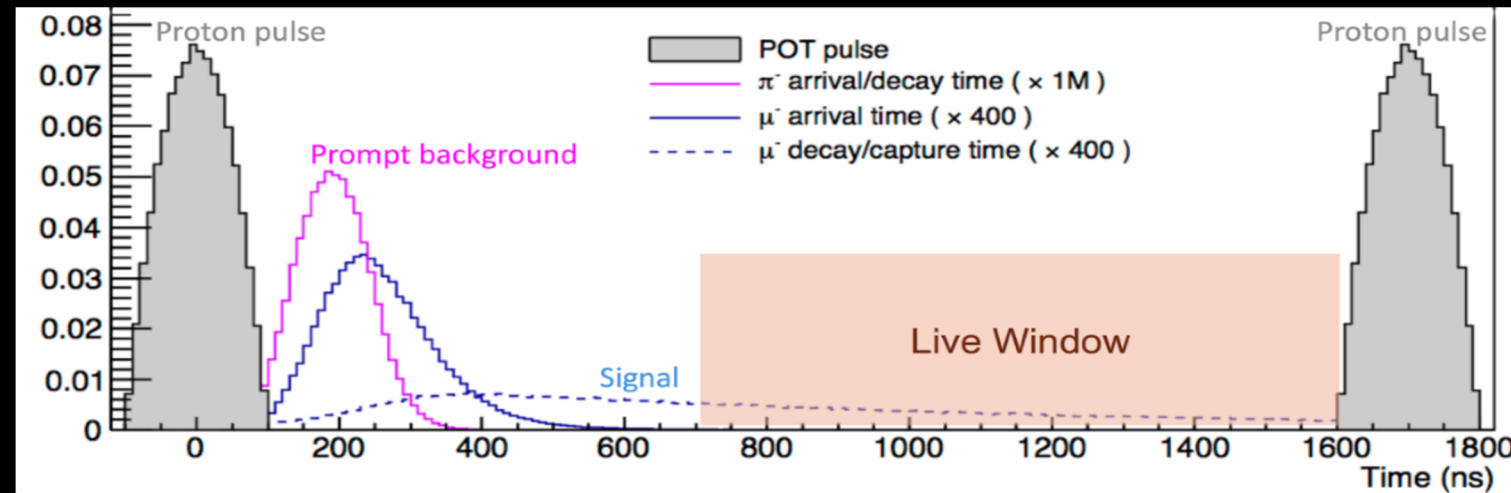
\*shape templates



# Pion Backgrounds

**Most importantly:** a delayed “livegate” is enforced:

- Pions – have a free lifetime of 26ns. They decay to produce muons (and neutrinos). Muons can further decay and produce backgrounds.
- Eliminate prompt backgrounds using a primary beam of short proton pulse. Use a delayed measurement window ( $\sim 700$  ns after proton pulse at target). Before this point we ignore any tracks we see in our detector systems.

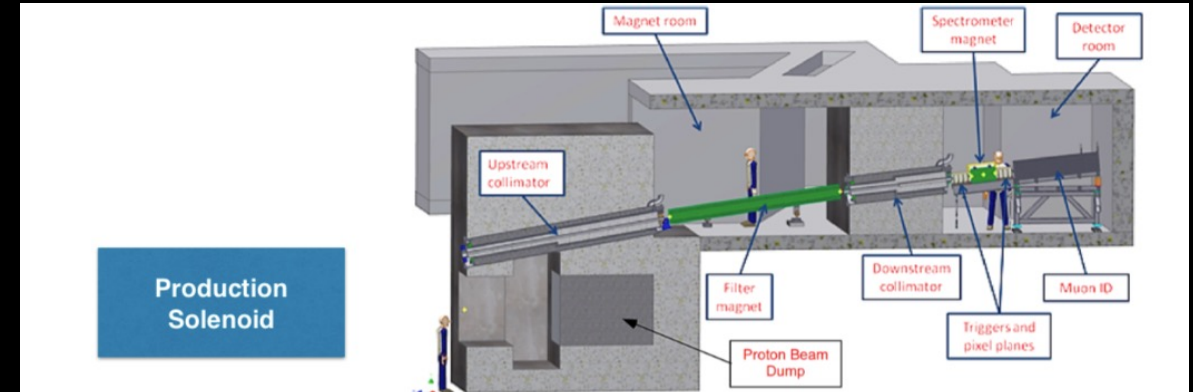
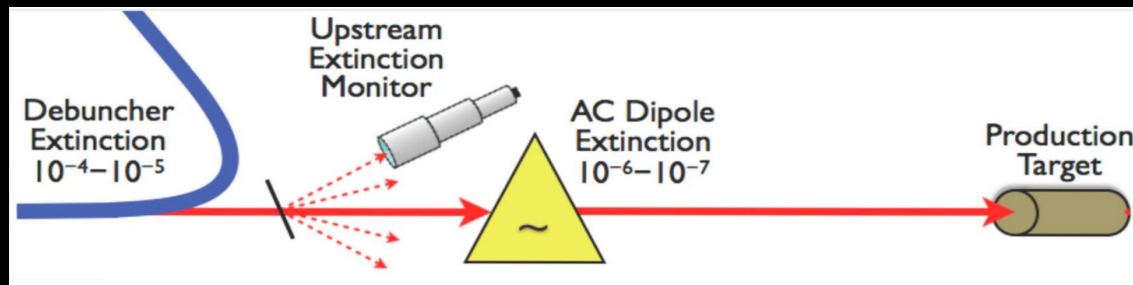


- Out-of-time pions could fall inside “livegate” but are eliminated by excellent extinction in our proton beam.

# Removing out-of-time protons



- Must have out-of-time : in-time proton ratio must be kept  $< 10^{-10}$  to remove potential backgrounds.
- 2 phase process:
  - Fast “kicker” which transfers the proton beam from the Recycler to the Delivery Ring preserves extinction.
  - Extinction of  $10^{-5}$  is expected as the proton beam is extracted and delivered.
  - The beam line from the Delivery Ring to the production target has a set of AC oscillating dipoles that sweep out-of-time protons into a system of collimators. This should achieve an additional extinction of  $10^{-7}$  or better.
- Extinction measured using a detector system: Si-pixel + sampling EMC .







# Removing Backgrounds

Beam delivery and detector systems optimized for high intensity, pure muon beam – must be “background free”:

Type	Source	Mitigation	Yield (over lifetime of experiment)
Intrinsic	Decay in Orbit (DIO)	Tracker Design/Resolution	$0.144 \pm 0.028$ (stat) $\pm 0.11$ (sys)
Late Arriving	Pion Capture	Beam Structure /Extinction	$0.021 \pm 0.001$ (stat) $\pm 0.002$ (sys)
	Pion Decay in Flight	-	$0.001 \pm < 0.001$
Other	Anti-proton	Thin Absorber Windows	$0.04 \pm 0.022$ (stat) $\pm 0.020$ (sys)
	Cosmic Rays	Active Veto System	$0.209 \pm 0.0022$ (stat) $\pm 0.055$ (sys)

Scales with livetime!

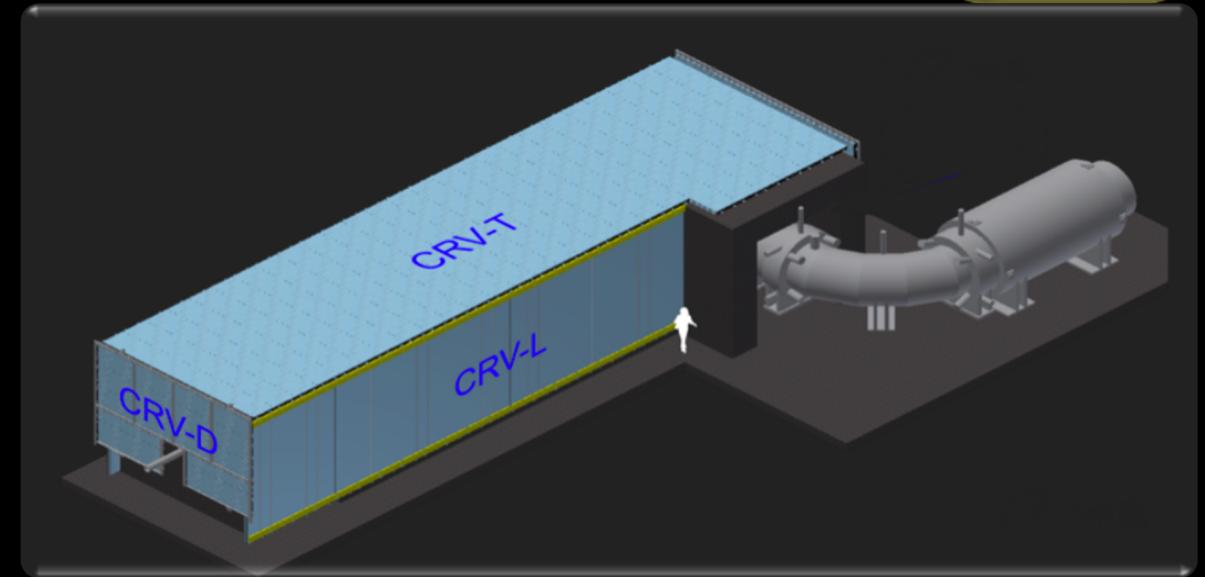
# Cosmic Ray Backgrounds

Each day,  $\sim 1$  conversion-like electron is produced by cosmic rays

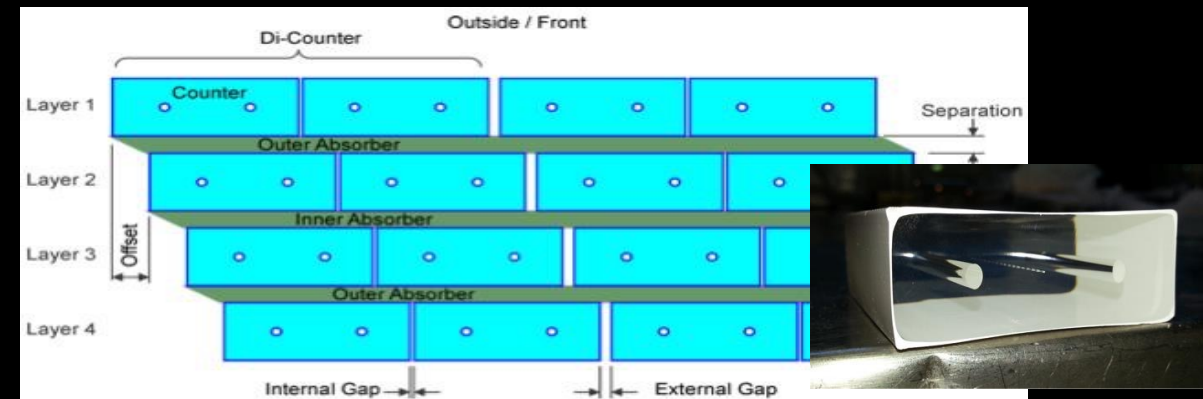


Cosmic Ray Veto will prevent cosmic muons faking a signal:

- Cosmic-ray muons can initiate 105 MeV particles that appear to emanate from the stopping target:
  - Electrons and positrons through secondary and delta-ray production in the material within the solenoids,
  - Electrons from muon decay-in-flight,
  - Muons themselves can be misidentified as electrons.
- Remove using active veto (CRV) + overburden and shielding concrete surrounding the Detector Solenoid.



Each panel is composed of  $5 \times 2 \times 450 \text{ cm}^3$  scintillator bars:



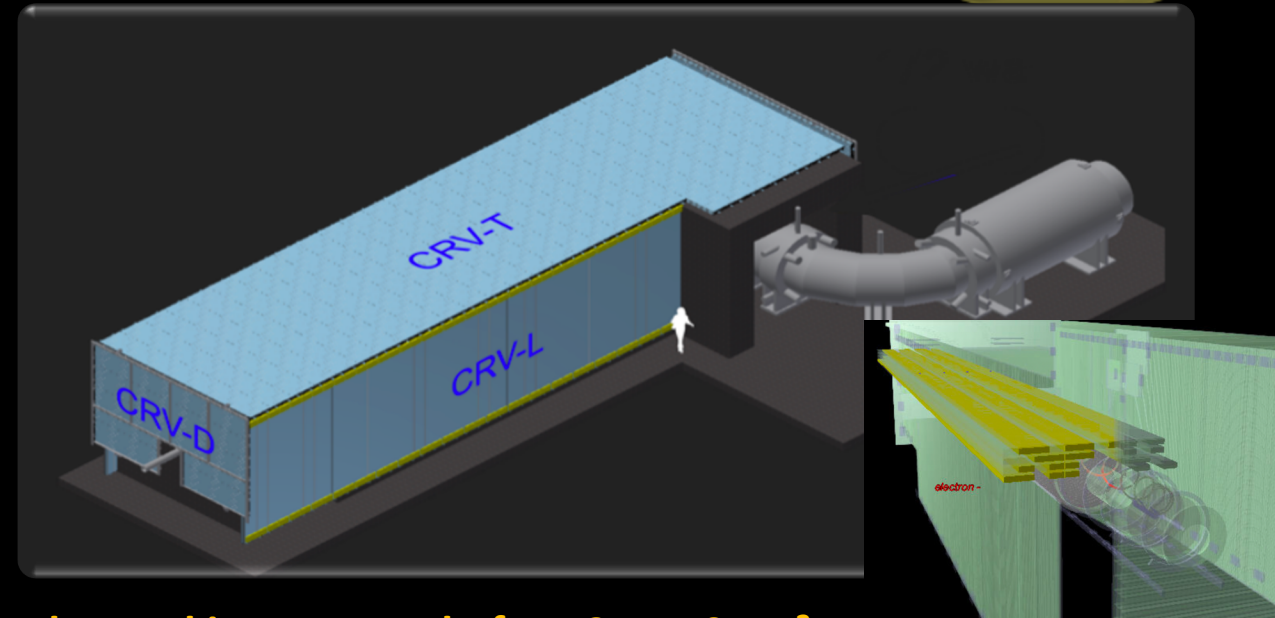
# The Cosmic Ray Veto

Each day,  $\sim 1$  conversion-like electron is produced by cosmic rays

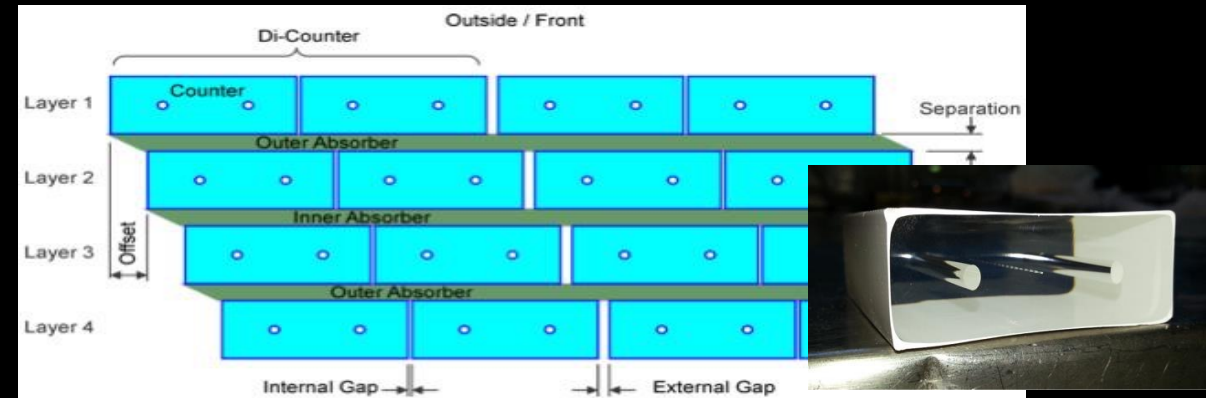


Cosmic Ray Veto will prevent cosmic muons faking a signal:

- 4 layers of extruded polystyrene scintillator counter.
- Surrounds the top and sides of DS and the downstream end of the Transport Solenoid.
- Remove Cosmic-ray candidates:
  - A track stub consisting of at least three adjacent hit strips in different layers within a 5 ns time window signals the presence of a cosmic-ray muon.
  - Signal candidates within 125 ns of such a track stub are assumed to be produced by a cosmic-ray muon and is vetoed.
  - 99.99% efficiency requirement!\*
- CRV in intense radiation environment:
  - Neutrons produced at the production target, stopping target, and muon beam stop;
  - Gammas produced largely from neutron capture.
- These can make hits in CRV, faking cosmic ray muons, increasing the dead-time.



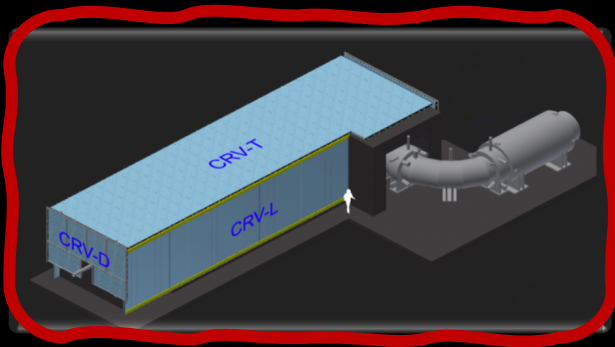
Each panel is composed of  $5 \times 2 \times 450 \text{ cm}^3$  scintillator bars:





# Removing Backgrounds

Beam delivery and detector systems optimized for high intensity, pure muon beam – must be “background free”:



Active veto system surrounds detector region

Type	Source	Mitigation	Yield (over lifetime of experiment)
Intrinsic	Decay in Orbit (DIO)	Tracker Deign/ Resolution	$0.144 \pm 0.028$ (stat) $\pm 0.11$ (sys)
Late Arriving	Pion Capture	Beam Structure /Extinction	$0.021 \pm 0.001$ (stat) $\pm 0.002$ (sys)
	Pion Decay in Flight	-	$0.001 \pm < 0.001$
Other	Anti-proton	Thin Absorber Windows	$0.04 \pm 0.022$ (stat) $\pm 0.020$ (sys)
	Cosmic Rays	Active Veto System	$0.209 \pm 0.0022$ (stat) $\pm 0.055$ (sys)



# Building our Detectors

How are our detectors constructed?  
Where are they constructed?  
What is the current status of each system?  
When will Mu2e be ready?



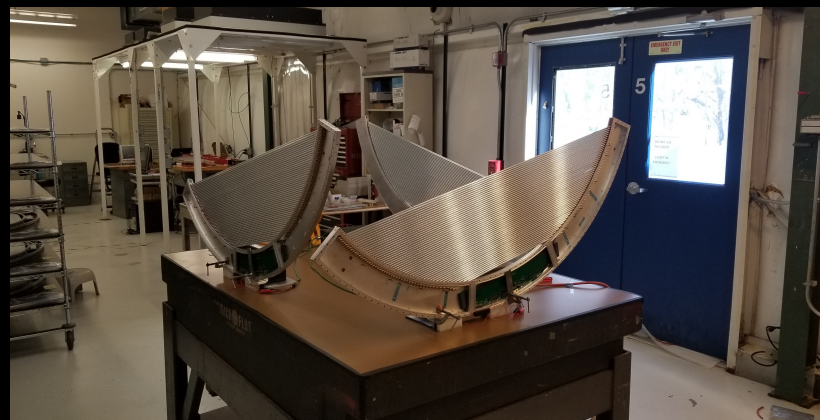
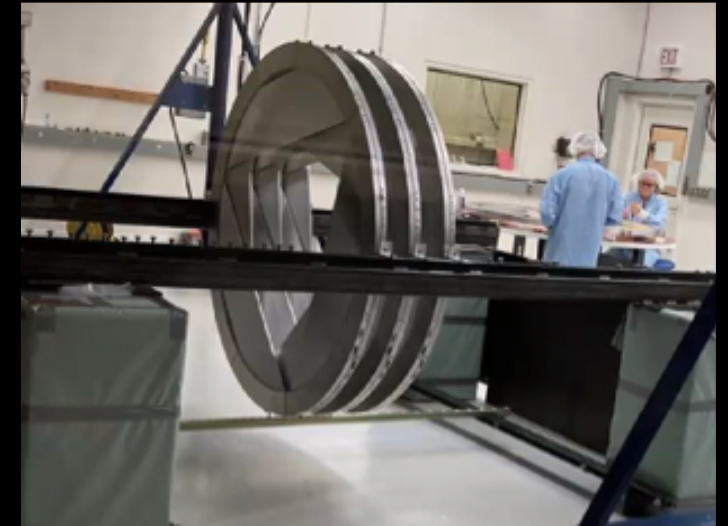
# The Tracker: Progress



2020: Production at University of Minnesota, testing at Duke Uni., → Over 60% of panels fabricated, testing on going

2021: Assembly at FNAL

→ 7/36 planes so far assembled on site



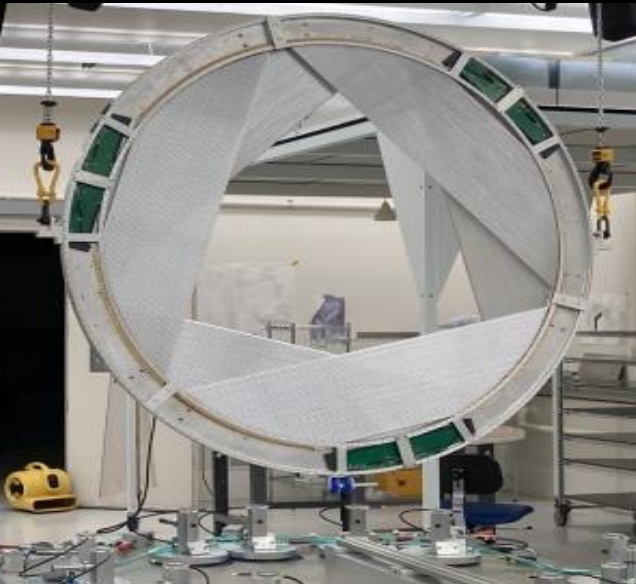
Vacuum tests at FNAL, here for single panel.



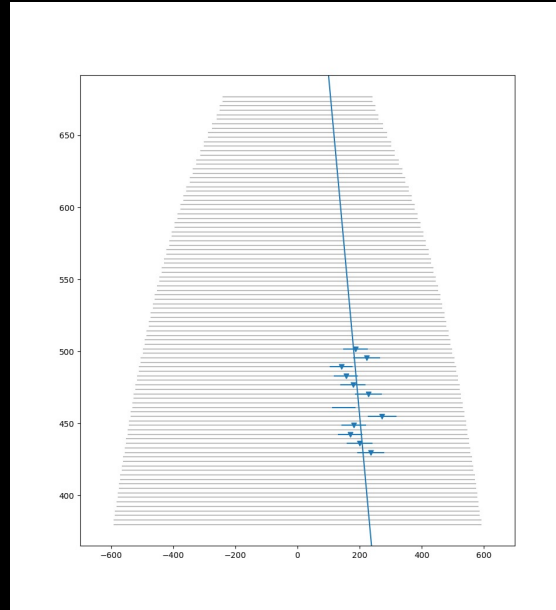


# The Tracker: Progress

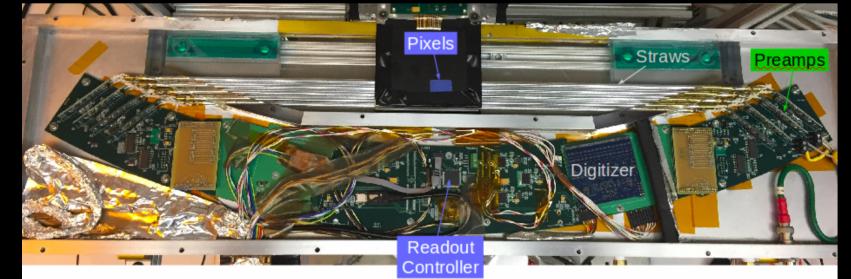
2020: Vertical Slice Test begins at FNAL



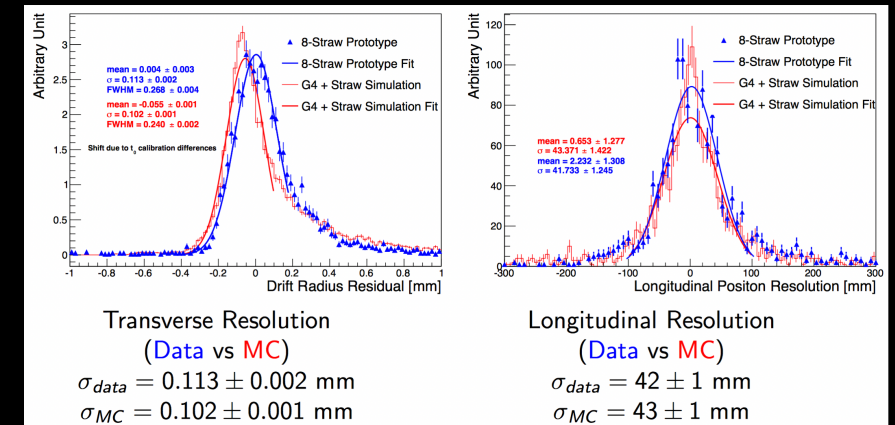
- Use Cosmic Rays.
- Use information gained to update MC.
- Measured performance and resolutions.
- First test with real data.



2017-2018: Electronics prototype produced at LBNL



Measured gain, crosstalk, resolution...



8 channel prototype

→ Good agreement between MC/Data

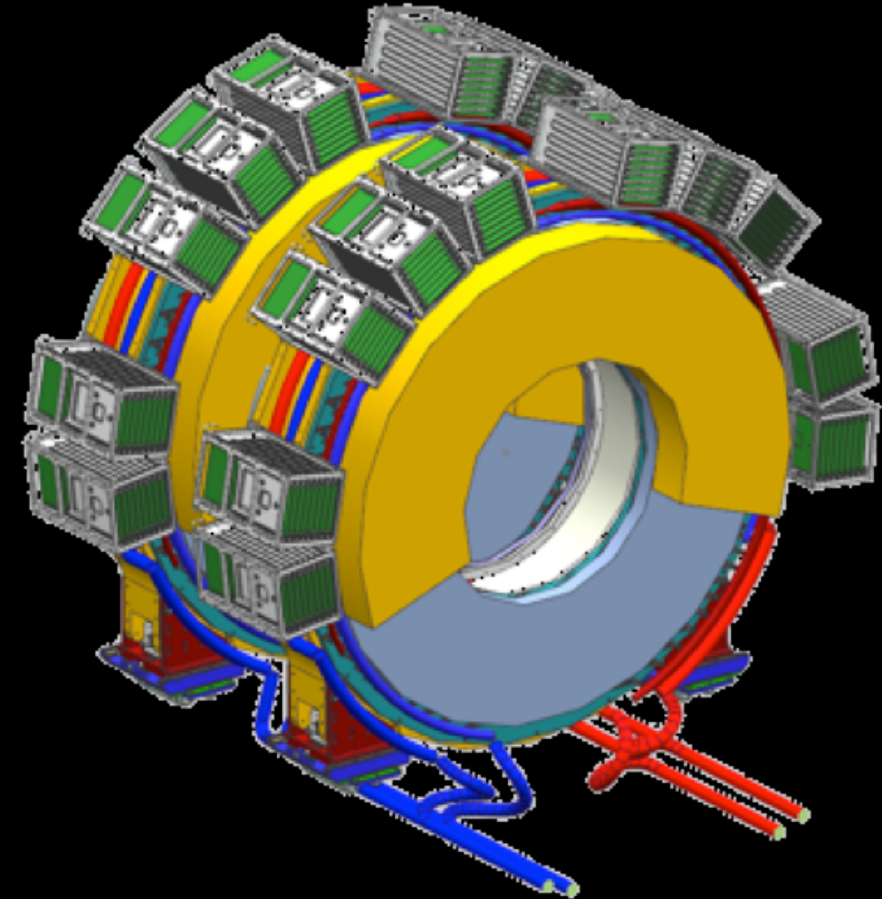
→ Resolution can be achieved

Read about the prototype:  
<https://arxiv.org/abs/1710.03799>

# The Calorimeter: Purpose



- The calorimeter is vital for providing:
  - Particle identification,
  - Fast online trigger filter,
  - Accurate timing information for background rejection
  - Seed for track reconstruction.
- The Mu2e Calorimeter must:
  - Have a large acceptance;
  - Provide time resolution  $< 0.5$  ns;
  - Energy resolution  $< 10\%$ ;
  - Position resolution of 1 cm.;
  - Function in region with radiation exposure up to 20Gy/crystal/year and with neutron flux  $10^{11}$  /cm<sup>2</sup>.
- Annular shape and 2 disks – the separation of disks is  $\frac{1}{2}$  the pitch of the mu2e signal helix, means that we cannot miss a conversion electron.
- Each disk = 674 CsI crystals





# The Calorimeter

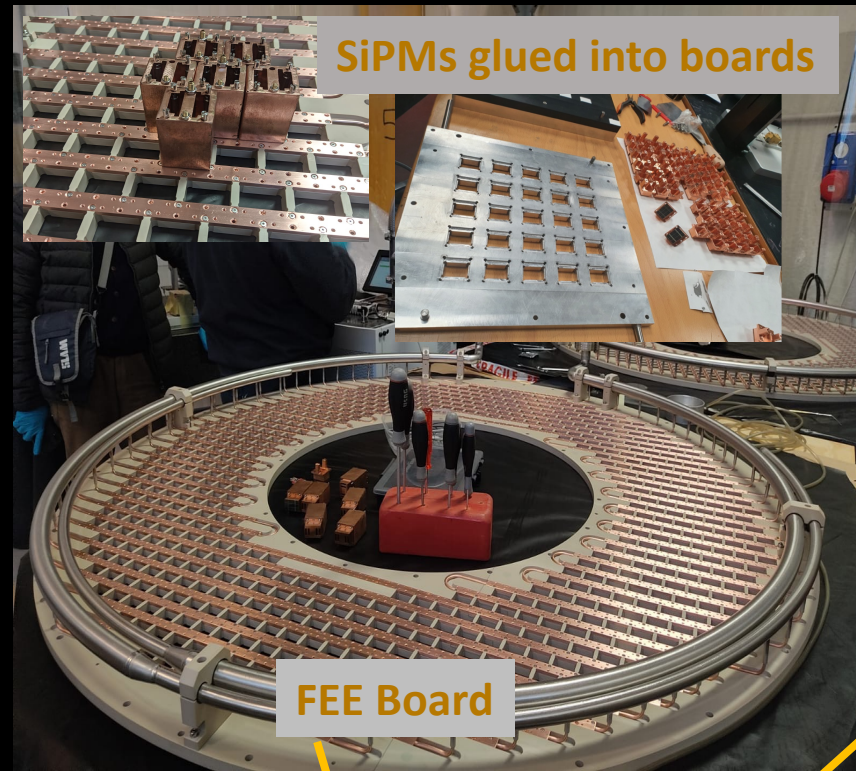
All parts ready  
Assembly beginning now



Inner Ring



Outer Ring



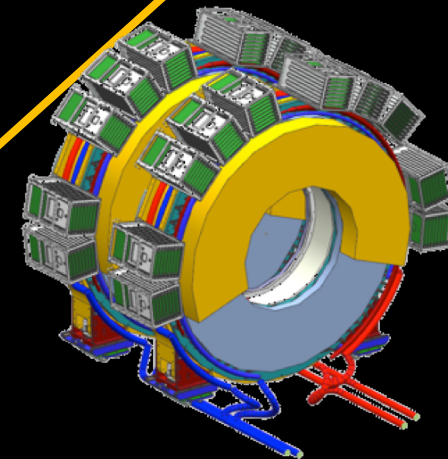
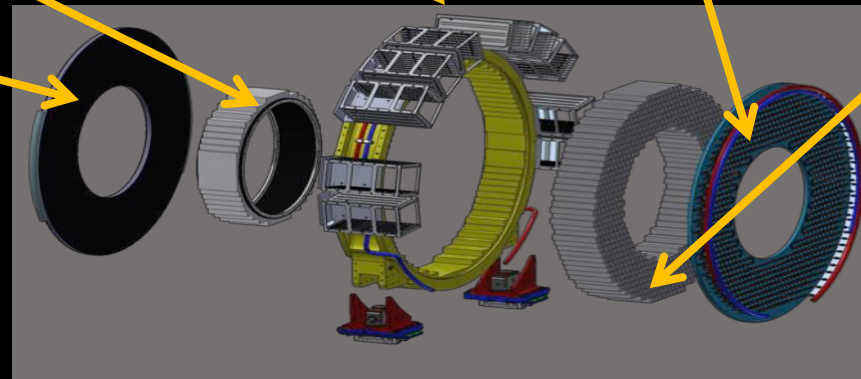
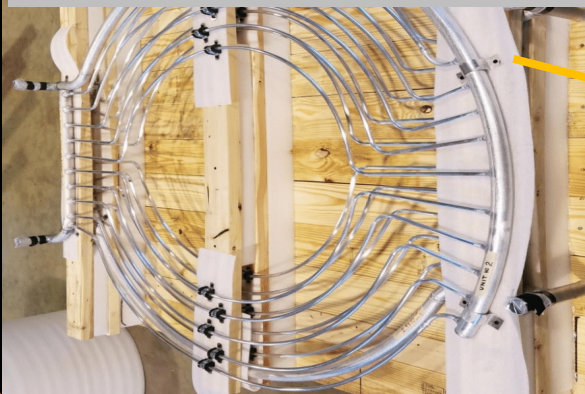
FEE Board

SiPMs glued into boards



Crystals at  
FNAL in sealed  
cupboard after  
QA.

Source Calibration System



Me at FNAL –  
finishing  
crystals QA  
(2020)



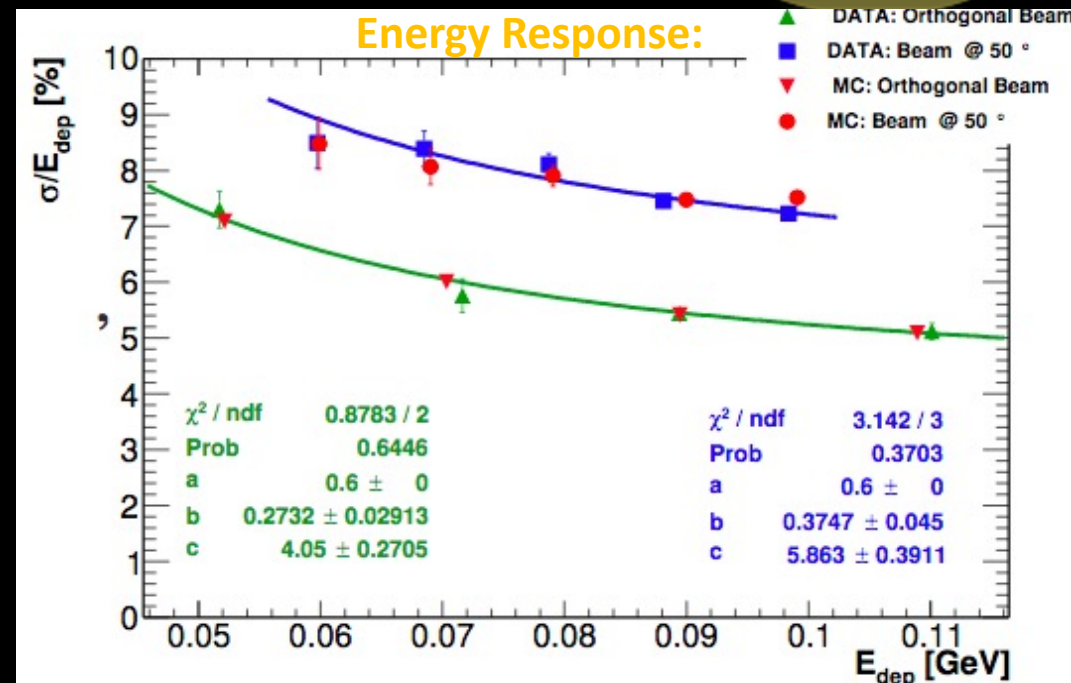
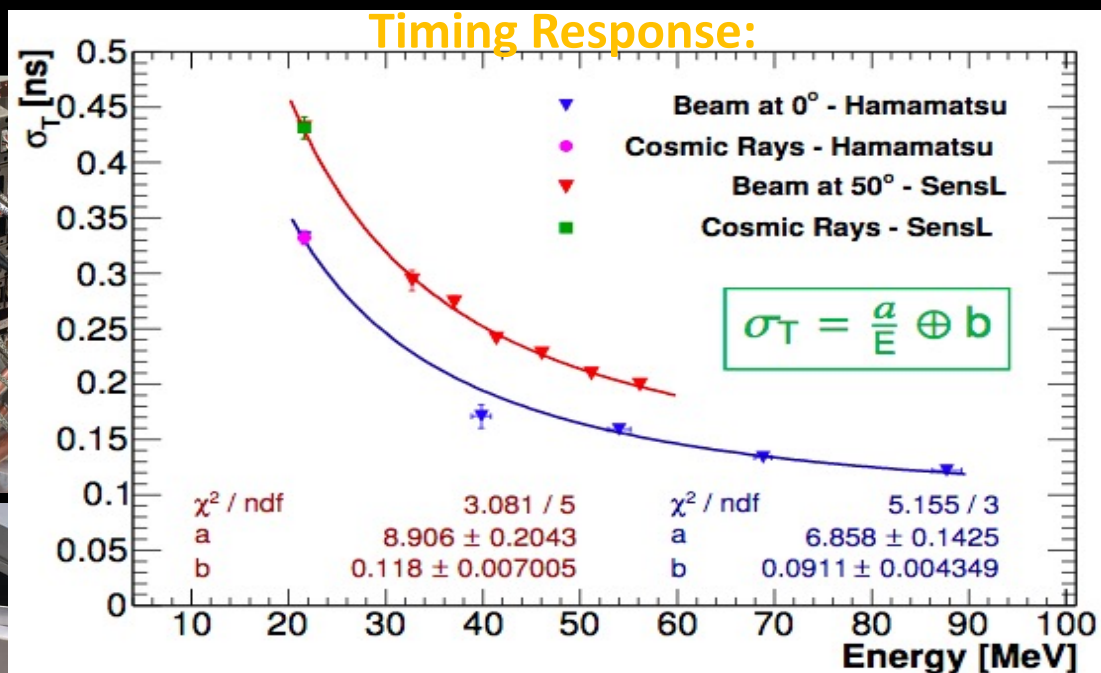
# The Calorimeter: Progress

- R&D and Prototyping successfully completed.
- 51 crystals + 102 SiPM + 102 FEE boards

Read about the test beam results:  
<https://www.osti.gov/pages/biblio/1523418>



2018:



- Test beam with  $e^-$  with  $E = 60\text{-}120$  MeV .
- Good agreement between MC/Data!
- Meets energy and timing performance requirements!

Typical time resolution  
 $E_{\text{beam}} @ 100 \text{ MeV}$   
 $\sigma_{T1} \sim 130 \text{ ps}$



# The Cosmic Ray Veto System

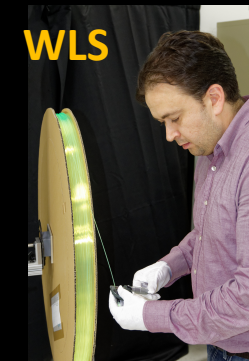
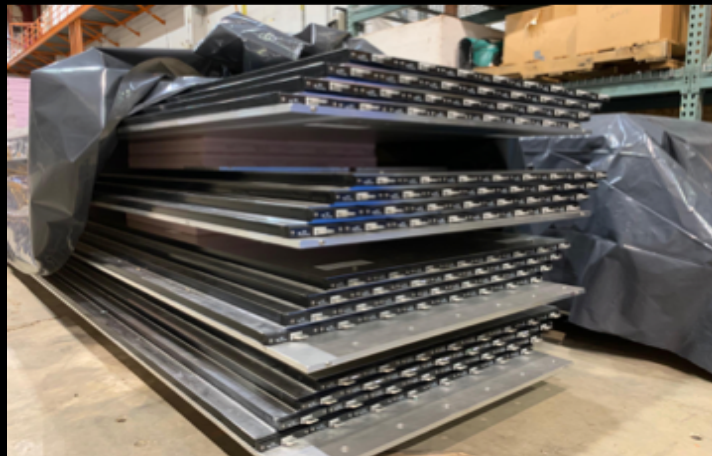


Modules at Argonne

- 56/83 modules fabricated at UVA
- Electronics production underway
- Front-End-Boards produced KSU
- Vertical slice test underway



2020: Vertical Slice Test at UVA



# The Stopping Target Monitor (STM)



- Need an accurate measure of total number of stopped muons in the target (within 10%) .
- Placed far downstream of Detector Solenoids (~34 m from target).
- STM uses HPGe and LaBr<sub>3</sub> detectors to measure X/gamma-rays produced by stopped muons in Al target:
  1. Prompt X-ray emitted from muonic atoms at 347keV;
  2. Delayed gamma ray at 844keV;
  3. Semi-prompt gamma ray at 1.809MeV.

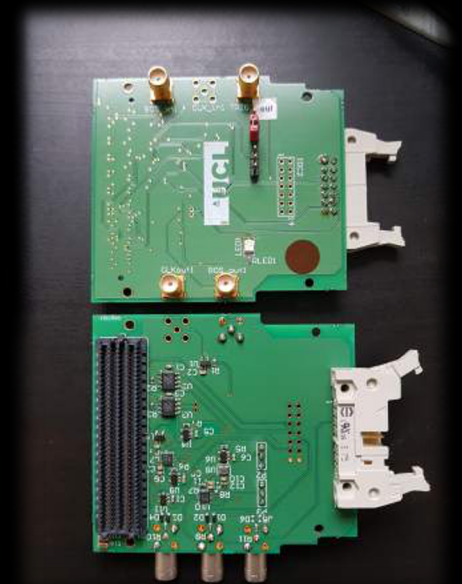
**HPGe and LaBr detectors procured**

$$R_{\mu e} = \frac{\Gamma(\mu^- + A(Z, N) \rightarrow e^- + A(Z, N))}{\Gamma(\text{all} - \text{captures})} < 7 \times 10^{-13} (90\% \text{C.L})$$



**Test beam at ELBE this year.... results being analyzed**

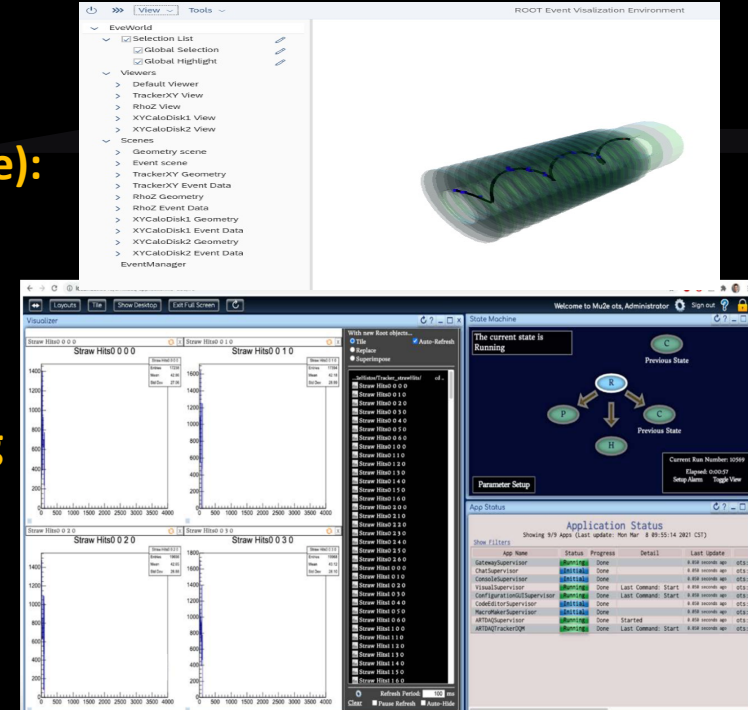
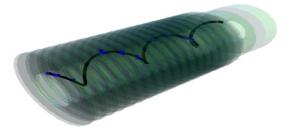
**2019: Test stands setup to begin DAQ development**





# Trigger & DAQ

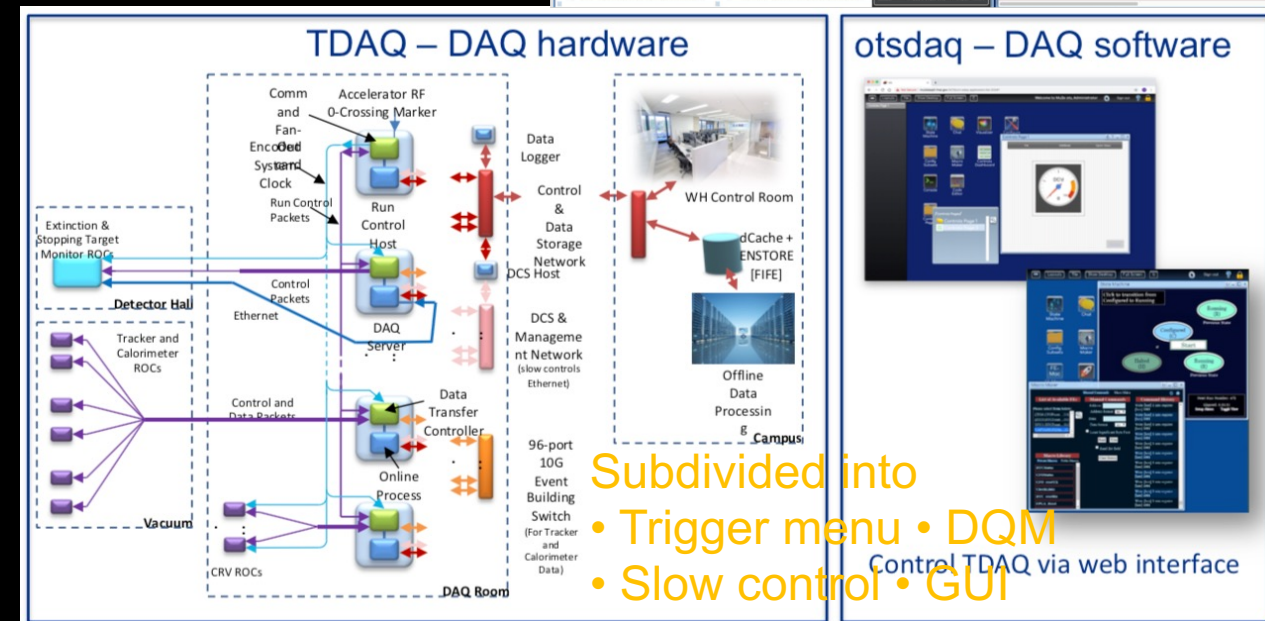
Event Display (REve):



DQM being developed:

TDAQ must:

- provide efficiency > 90% on the signal;
- keep the trigger rate < a few kHz ( $\approx 7$  PB/year);
- achieve a processing < 5 ms/event.



Infrastructure detailed in:  
<https://arxiv.org/abs/2010.16208>

Mu2e: Searching for  $\mu \rightarrow e \gamma$  at Fermilab - Sophie Middleton -  
 smidd@caltech.edu

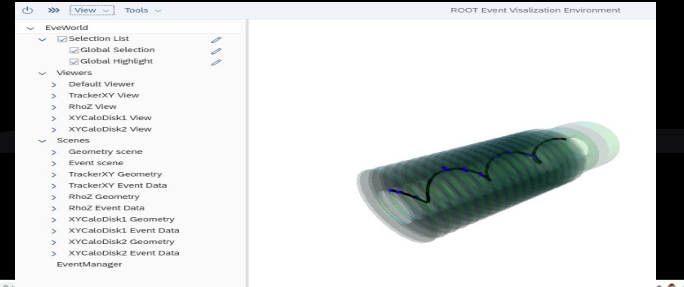
26 October 2021

90



# Trigger & DAQ: Progress

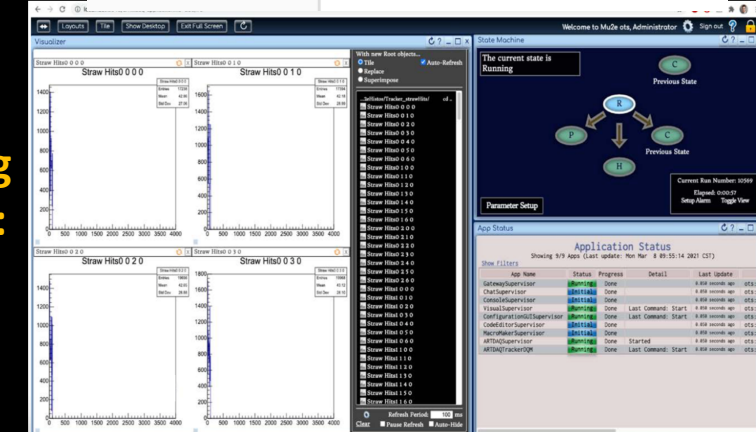
## Event Display (REve):



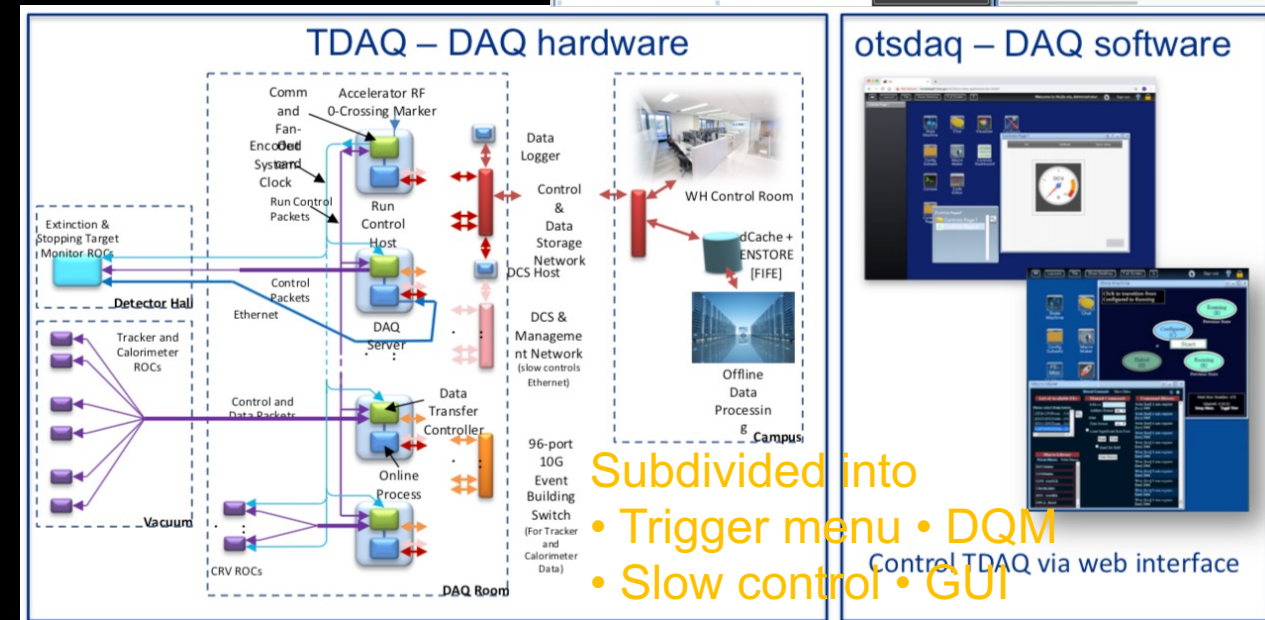
Lots of progress over last few years:

- In 2019: Test stand set up at FNAL
  - A joint platform (OTSDAQ) has been set up to allow compatibility between trackers, calorimeter and STM interfaces.
- In 2020: DQM development, event display developed using cutting edge EVE-7, event builder prototyped.
- In 2021: Horizontal slice test this summer.

## DQM being developed:



Infrastructure detailed in:  
<https://arxiv.org/abs/2010.16208>



# Mu2e: Timeline



**2022 → Transition to installation**

**2023 → Start Commissioning with beam**

**Late 2022 → Start Detector commissioning**  
(e.g. in situ cosmic ray data taking)

**Sept. 2021 Mu2e construction is nearly complete:**

- Beamline is finished.
- TS on-site and finalizing testing, PS and DS testing and fabrication on-going at vendor.
- Tracker straws, FEE prototypes, calorimeter crystals and SiPMs, STM detectors, and CRV counters are complete.
- Assembly and testing of these detector components is on-going.

**End of 2024 – onwards**

**→ Physics data taking:**

- Run 1: Until 2026 ( $O(10^{-16})$ ).
- Run2: After LBNF Shutdown ( $O(10^{-17})$ ).

# Mu2e Sensitivity

*Paper published soon.*



Run 1:

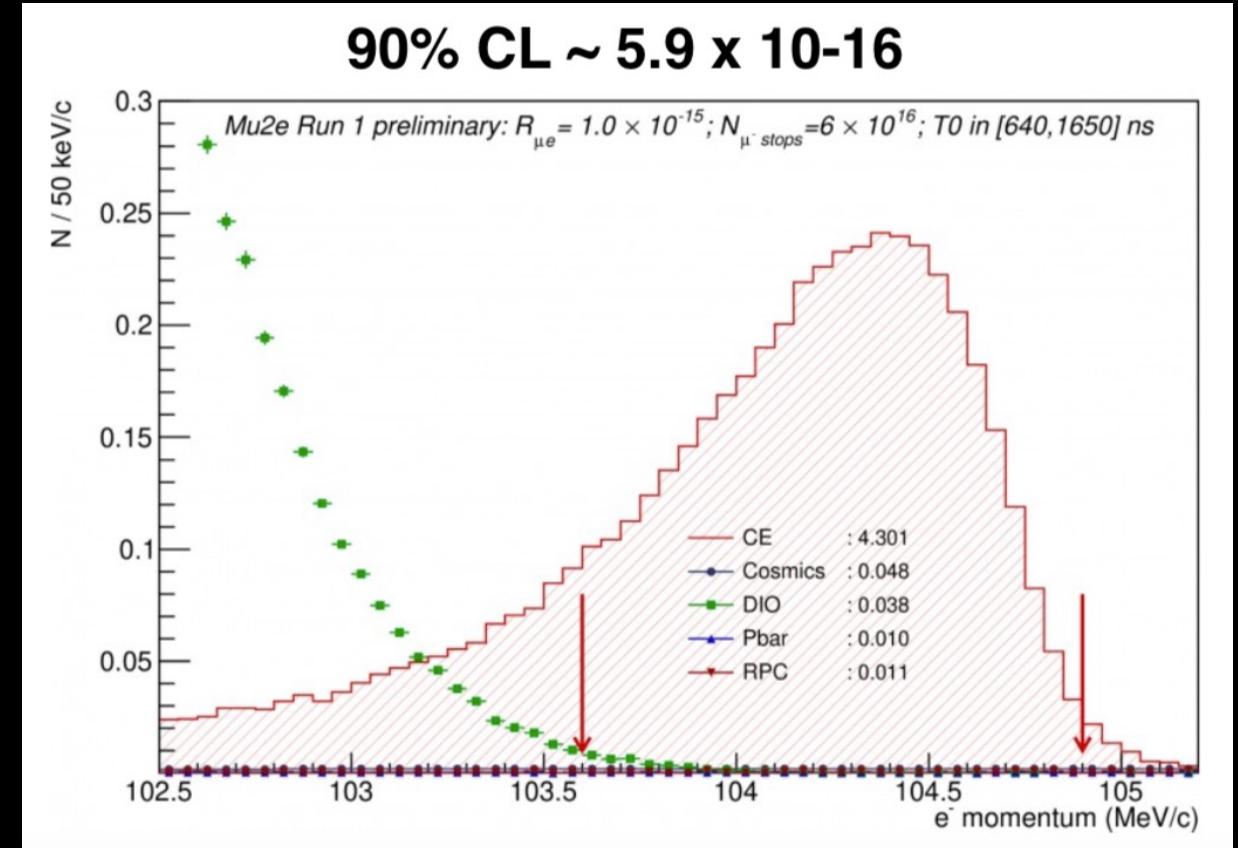
- Beam on target in late by 2024

## Run1: 2025-2026:

- $10^3$  improvement over SINDRUM-II 90% CL limit
- PIP-II/LBNF shutdown scheduled for end of 2026

## Run2: Data-taking resumes early 2029

- The goal is a  $\times 10^4$  improvement over SINDRUM-II: (90% CL)





# Extended Mu2e into the PIP-II Era: Mu2e-II

What happens if we see at Mu2e signal?  
What happens if we don't?



# Mu2e-II

*Mu2e-II aims to improve the sensitivity ( $R_{\mu e}$ ) to the neutrinoless conversion of a muon-to-an-electron in the field of a nucleus by a further order of magnitude than Mu2e i.e.  $SES \sim \mathcal{O}(10^{-18})$*



- There are 2 possible outcomes from Mu2e:
  1. **Conversion not observed** - motivates pushing to higher mass scales .
  2. **Conversion observed** - motivates more precise measurements with different targets.
- Either way Mu2e-II is well motivated!

## Mu2e-II would:

- Be based at Fermilab. Will utilize the (nominal) 100kW beam from Proton Improvement Plan II (PIP-II).
  - Start a few years after the end of Mu2e run with an expected 3+1 years of physics running.
  - Salvage and refurbish as much of Mu2e infrastructure as possible.
  - Upgrade Mu2e components where required to handle higher beam intensity.
- 
- Mu2e-II has a support from muon physics community and Fermilab's PAC
  - If approved, Mu2e-II expects to start data taking at the end of the decade
  - Large effort to write White Paper for Snowmass 2022!

See here for overview: <https://arxiv.org/pdf/1802.02599>

# The PIP-II Project

- The project received CD-1 approval from the U.S. Department of Energy in July 2018.
- PIP-II will power both DUNE and other experiments like Mu2e-II.
- PIP-II is planned to deliver beam in the next decade.
- Groundbreaking ceremony took place in 2019.



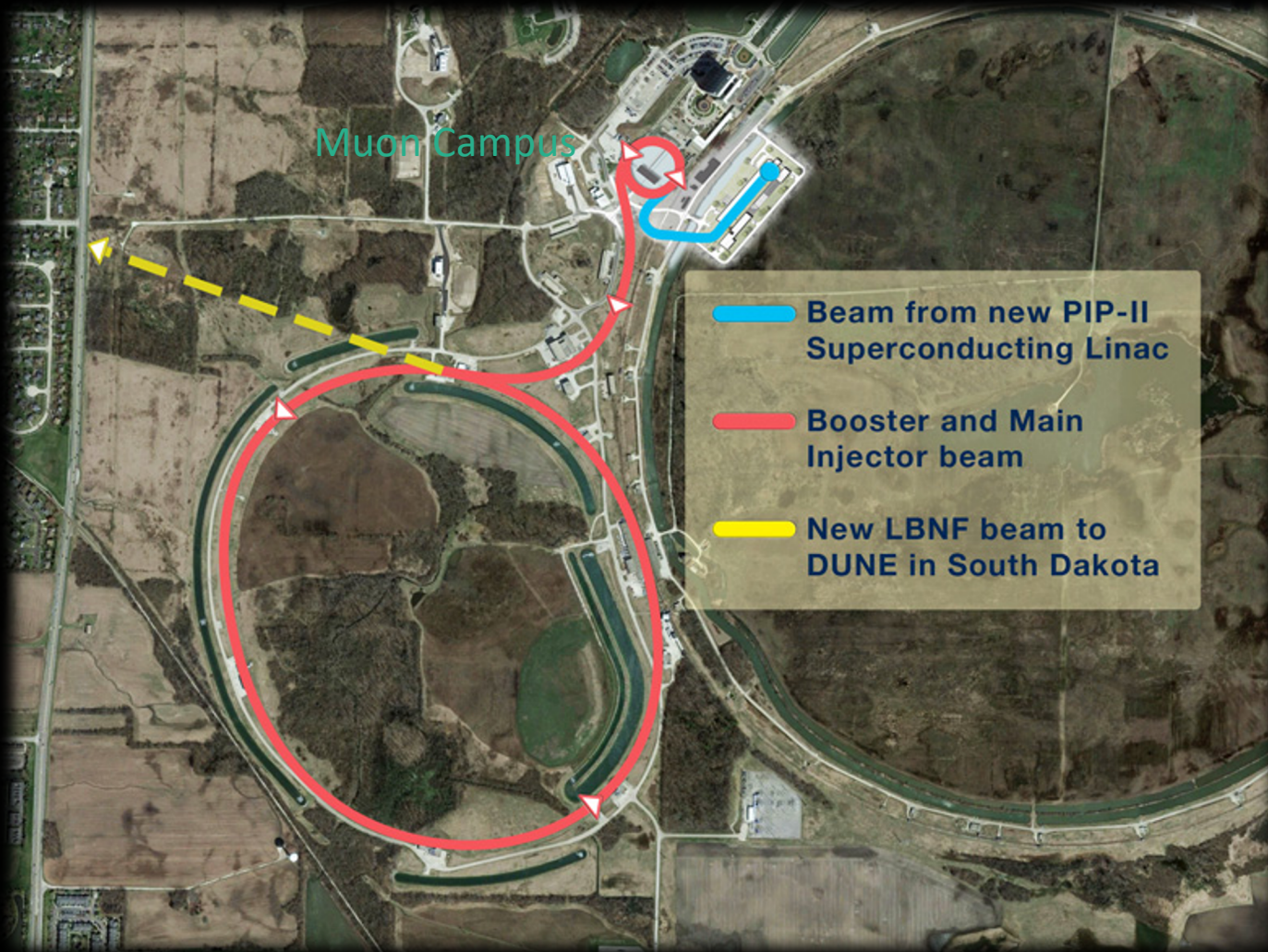
2021



2025



# PIP-II



- PIP-II designed to deliver 800 MeV H<sup>-</sup> beam to the Booster.
- Capable of running in CW mode with 2 mA average current at 1.6 MW .
- Mu2e-II will get a beam at upstream end of transfer line to Booster:
  - Need to build a beamline to deliver beam to M4 enclosure



# Production Target

*LDRD Project on-going to investigate production target choice*

*Front runner is Conveyor design. But made out of W or C?*

	Tungsten/WC	Lower-density bent (Carbon)
Rotated	Requires a large hardware in HRS	Too large to fit HRS
Fixed granular	DPA is too high	DPA is high; lower pion production
Conveyor	Thermal analysis is ongoing	Lower pion production; thermal analysis is ongoing

## Prioritizing designs

- Constraint: compatibility with the current HRS design (inner bore=20 (25) cm)

### Rotator



**Pros:** radiation damage can be distributed over many rods  
**Cons:** its hardware would require a significant space inside the bore (complicates cooling and muon flow)

### Granular



**Pros:** small space required  
**Cons:** peak DPA (MARS15) >300/yr; gas cooling cannot be performed efficiently

### Conveyor



**Pros:** small space required; He gas could be used for both cooling and moving elements inside conveyor; radiation damage can be distributed; **Cons:** technical complexity (prototyping needed)



(btofoylbiu8 ueeqeq)  
tecmuic9j comblexig  
qisatiputeq: **Cons:**  
qaw986 c9u p6  
couleloj: l9q9tjou

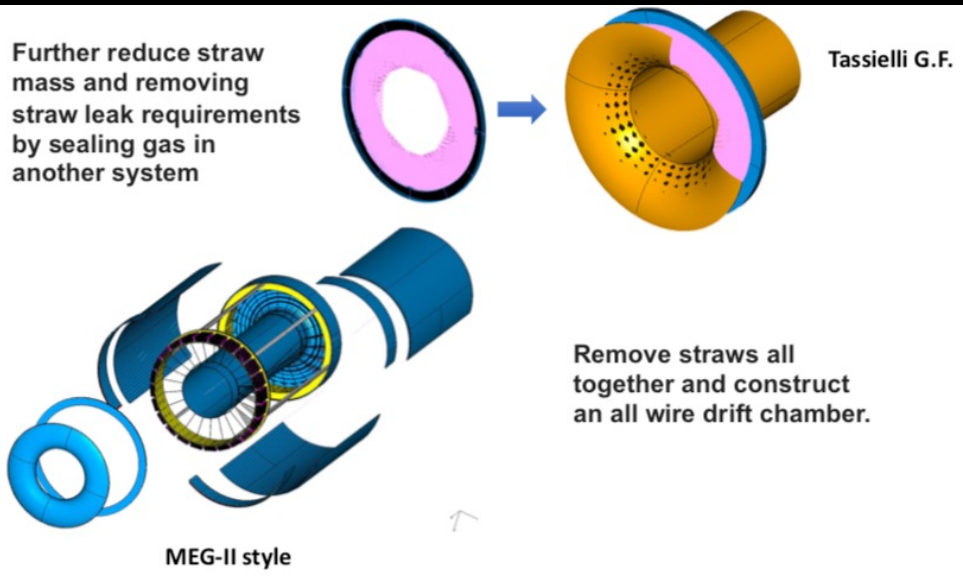
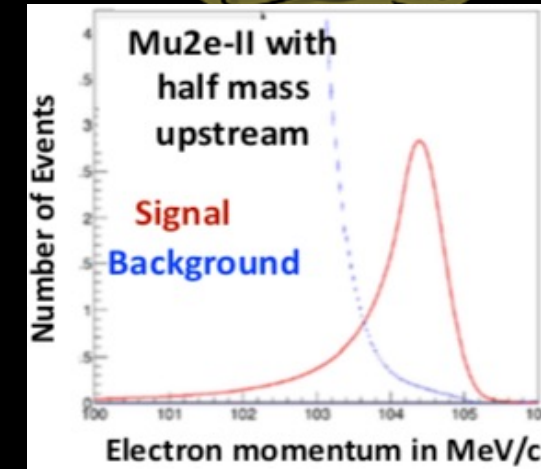
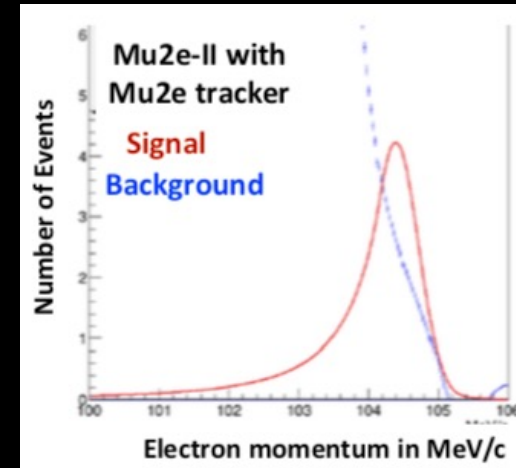
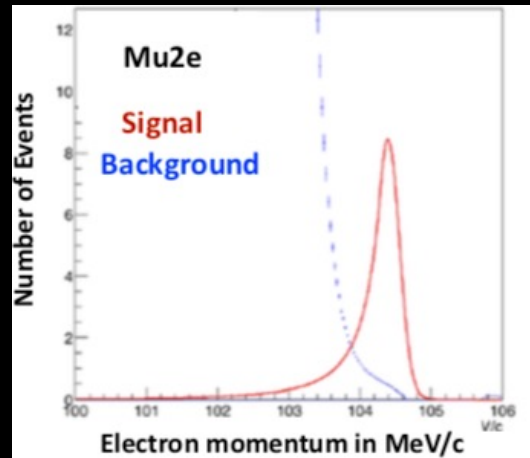


# Tracker Requirements



*DIO background would increase x10 in Mu2e-II.*

*Must improve momentum resolution to suppress DIO.*



**To meet Mu2e-II momentum resolution/background separation goals:**

**Reduce total Tracker Mass:**

- Thinner straws ( $8\mu\text{m}$ )
- Remove the 200 angstrom gold layer from inside straw

**Change detector design:**

- Use an ultra light gas vessel to ease straw leakage requirements
- Use different gas
- Consider all wires construction and remove the straws
- Or wires separated by mylar walls

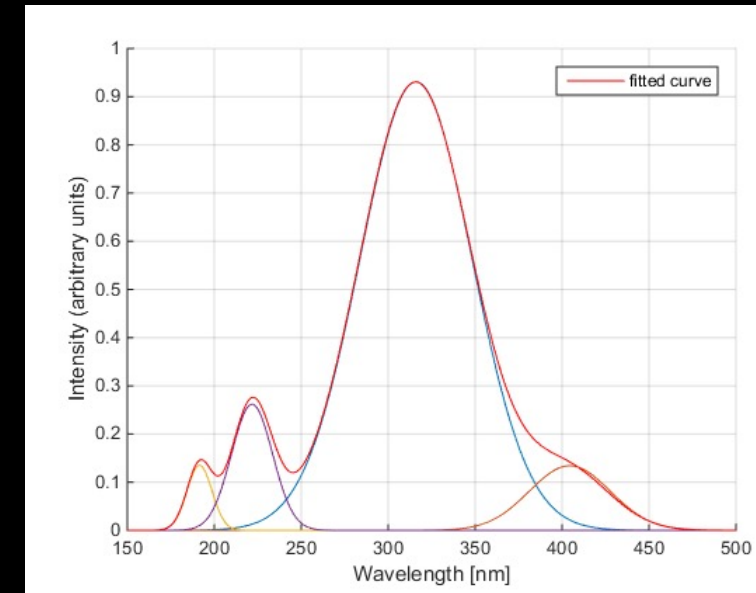
**Increased hit occupancy and timing window:**

- 4x increase in PBI is estimated to reduce reconstruction efficiency by 30%.

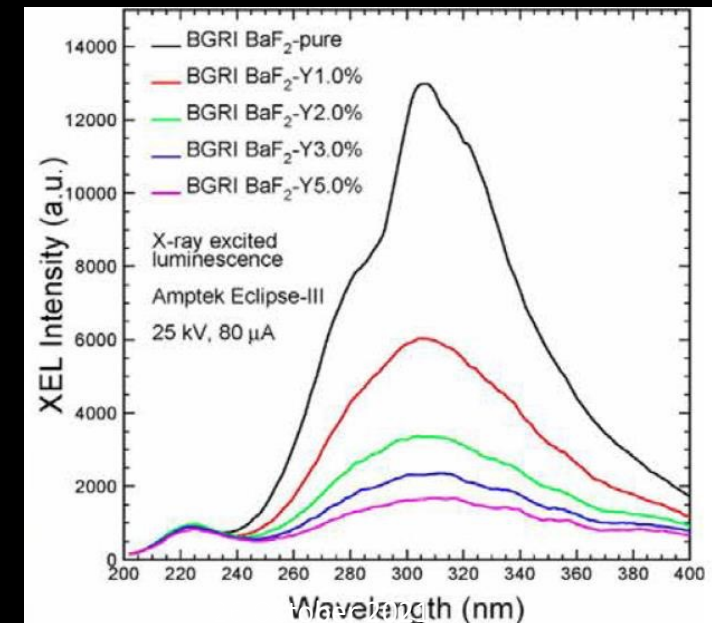
# Barium Fluoride Calorimeter Crystals

- **Radiation doses and rates at Mu2e-II are high for CsI:**
  - Up to 900 krad and  $1E13$  n [ $1\text{MeVeq}/\text{cm}^2$ ]
- **BaF<sub>2</sub> is an excellent candidate for a fast, high rate, radiation-hard crystal for the Mu2e-II calorimeter:**
  - BaF<sub>2</sub> can survive up 100 Mrad
- **Must have way of utilizing 220 nm fast component without interference from the larger 320 nm slow component.**
- **Slow suppression achieved by:**
  1. Rare Earth Doping (Y, La,Ce).
  2. Develop photo-detectors sensitive to UV only:
    - SiPM with an external filter
    - UV-sensitive photocathodes
    - Solar-blind MCP - SiPM “sees” only fast component.

**R&D Collaboration between Caltech, JPL & FBK on-going**



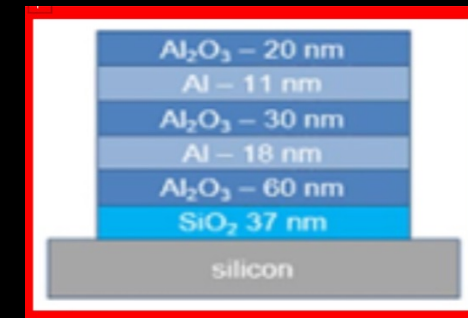
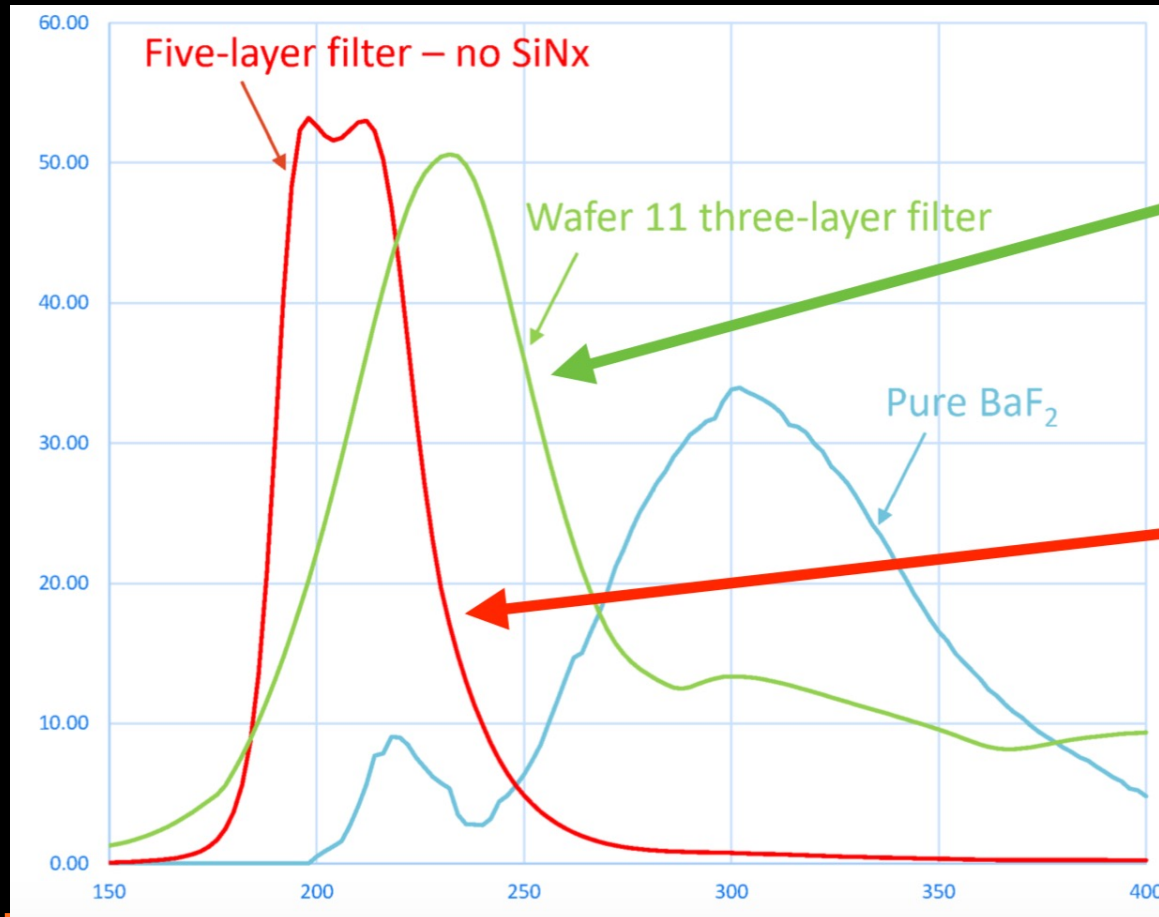
*Actually two fast components ( $t = 0.6$  ns) at 195 and 220 nm and two slow components ( $t = 630$  ns) at 320 and 400 nm .*



# SiPM R&D



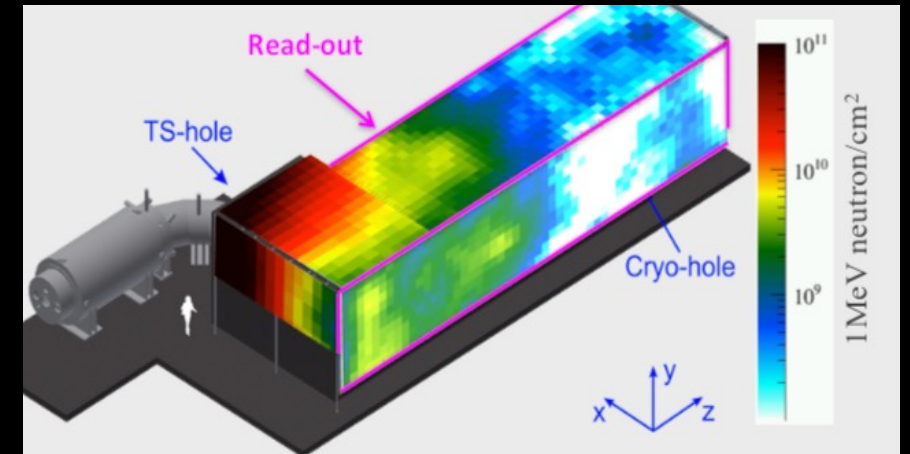
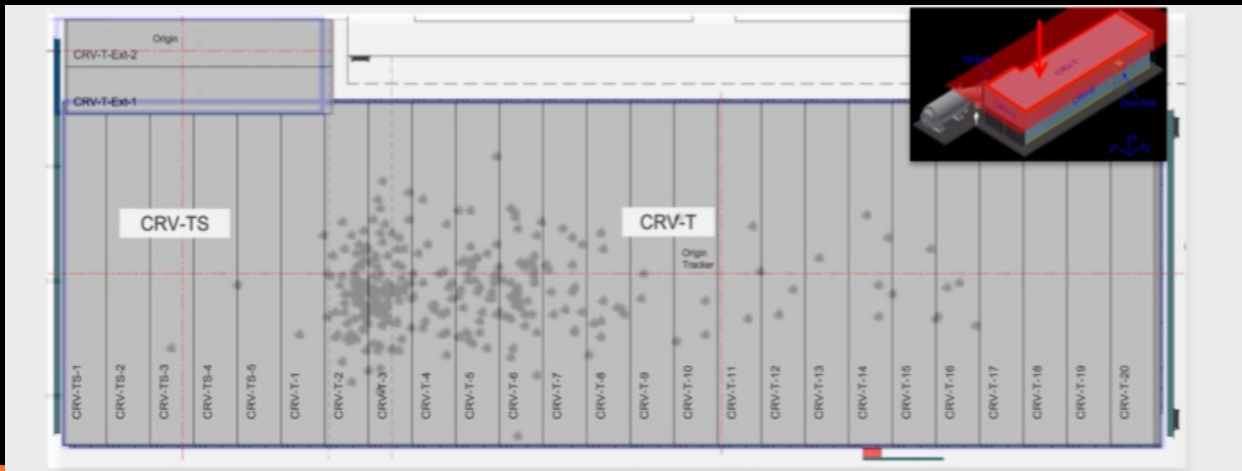
- Caltech-JPL-FBK consortium working on delivering developing a special locating for SiPMs
- Sandwich of Al, SiN<sub>2</sub> and Al<sub>2</sub>O<sub>3</sub> layers deposited on the active material



# The Cosmic Ray Veto System (CRV)



- **Expected live-time and therefore Cosmic Ray backgrounds will be 3 x higher for Mu2e-II**
    - Need to enhance the CRV performance in critical regions
  - **Light Yield degradation impacts CRV performance**
    - Must replace CRV
  - **Higher noise rates (x2-3) these impose challenges:**
    - Higher DAQ rates
    - Radiation damage
    - Induced dead-time
- Enhanced shielding, fine-granular layers, other technologies



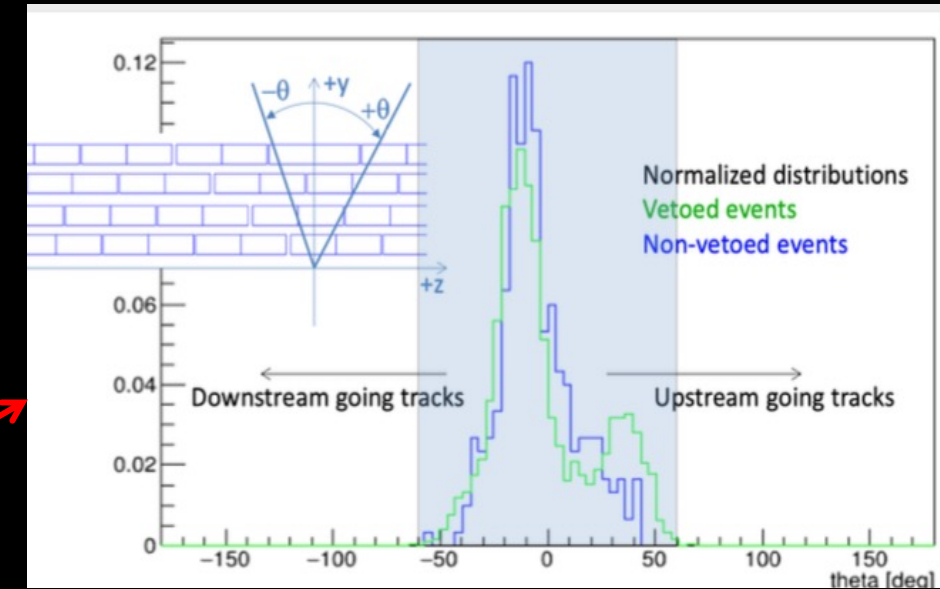
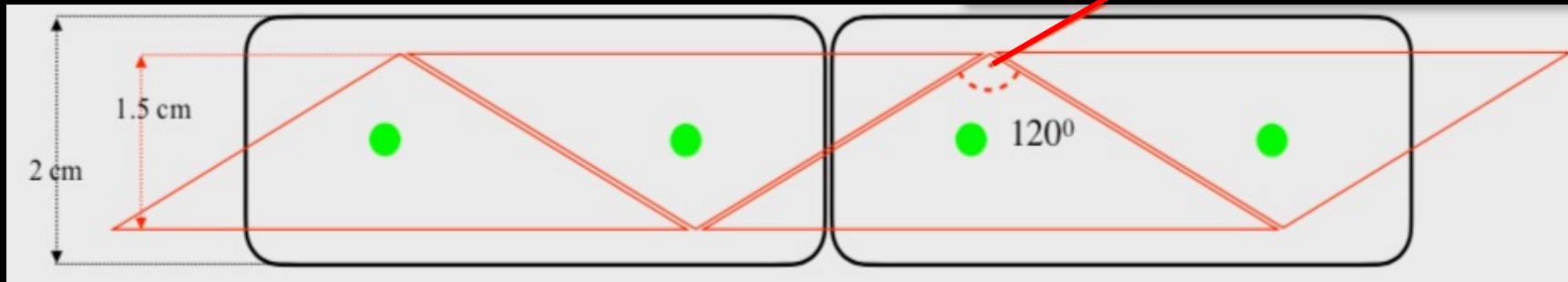


# The Cosmic Ray Veto System



- Gaps between modules and counters and modules impact the CRV performance:
  - Reduce Gaps
  - Change geometry
  - Extra Layers
- **Triangular Bars:**
  - Improved efficiency due to reduced gaps
  - Lower dead time
  - Lower rate per channel
  - Simple design

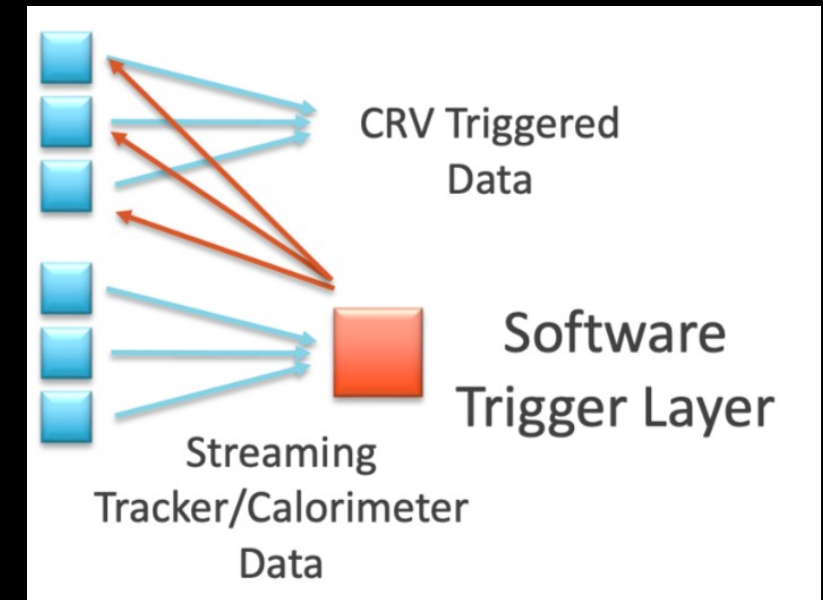
Possible Mu2e-II Design



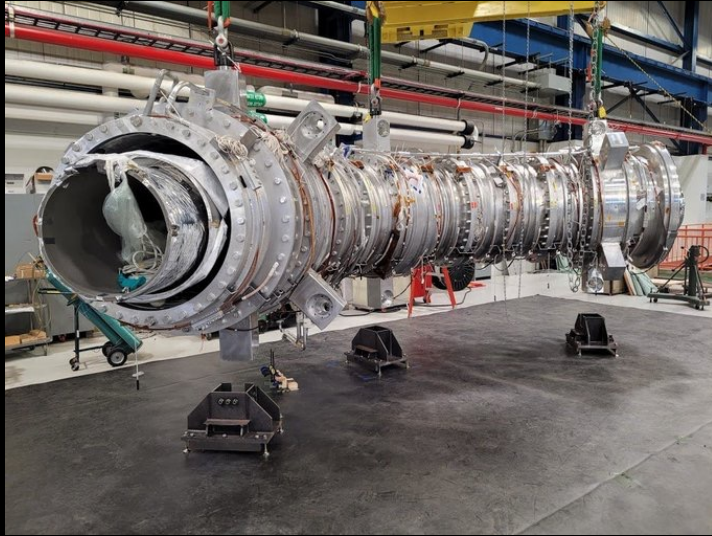
# Trigger & Data Acquisition (TDAQ)



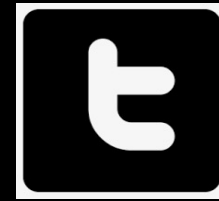
- **Increased data rate, more background and more detector channels:**
  - 10x data rate
  - X3 event size
  - 3000:1 rejection is needed to arrive at 14PB/year
- **Considerations:**
  - Reduced off-spill time to readout large front-end buffers
  - Streaming .v. triggered data taking
  - Radiation tolerances requirements
- **No large buffers for the CRV:**
  - Large CRV buffers + software trigger
  - Small CRV buffers + hardware trigger
- **Solutions:**
  - 2-level TDAQ based on FPGA pre-processing and trigger primitives
  - 2-level TDAQ system based on FPGA pre-filtering
  - TDAQ based on GPU co-processor
  - Trigger-less TDAQ based on software trigger.



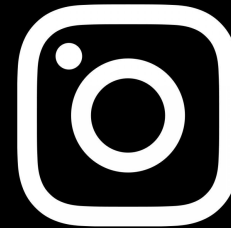
# Follow us



Watch the experiment evolve with frequent videos and images:



<https://twitter.com/Mu2eExperiment>



<https://www.instagram.com/mu2eexperiment/>





# Summary

- Muon CLFV channels offer deep indirect probes into BSM.
- Mu2e is at the forefront of active global CLFV program. Discovery potential over a wide range of well motivated BSM models.
- Muon-to-electron sector complements tau and Higgs collider searches such as:  $\tau \rightarrow e\gamma$  or  $\mu\gamma$  and  $H \rightarrow e\tau, \mu\tau$ , or  $\mu e$ .
- It is important to eliminate Standard Model backgrounds so the experiment is designed to be “background free”:
  - Super conducting solenoids to collect and efficiently transport low momentum muons;
  - Pulsed beam removes backgrounds from pions;
  - Low mass, annular tracker has high resolution to avoid DIO backgrounds;
  - Cosmic Ray Veto surrounds detectors to remove “fake signals” from Cosmic muons.
- Looking further ahead the Mu2e-II experiment will help elucidate any signal and push to higher mass scales (of no signal).
- Large effort on-going to design the Mu2e-II experiment with consideration of requirements introduced due to higher beam intensity.

*Thank You for listening!*





# Useful Resources

1. S. T. Petcov, Sov. J. Nucl. Phys. **25**, 340 (1977); Yad. Fiz. **25**, 1336 (1977) [erratum].
2. S. M. Bilenky, S. T. Petcov, and B. Pontecorvo, Phys. Lett. B **67**, 309 (1977).
3. W. J. Marciano and A. I. Sanda, Phys. Lett. B **67**, 303 (1977).
4. B. W. Lee, S. Pakvasa, R. E. Shrock, and H. Sugawara, Phys. Rev. Lett. **38**, 937 (1977); **38**, 1230 (1977) [erratum].
5. J. Adam *et al.* (EG Collaboration), Phys. Rev. Lett. **110**, 20 (2013).
6. W. Bertl *et al.* (SINDRUM-II Collaboration), Eur. Phys. J. **C47**, 337 (2006).
7. U. Bellgardt *et al.*, (SINDRUM Collaboration), Nucl. Phys. **B299**, 1 (1988).
8. A.M. Baldini *et al.*, “MEG Upgrade Proposal”, arXiv:1301.7225v2 [physics.ins- det].
9. Y. Kuno *et al.*, “COMET Proposal” (2007) see also <https://arxiv.org/abs/1812.09018> for Phase I TDR
10. Mu2e TDR, arXiv:1501.05241
11. Nuclear Physics B - Proceedings Supplements Volumes 248–250, March–May 2014, Pages 35-4
12. A. Czarnecki *et al.*, “Muon decay in orbit: Spectrum of high-energy electrons,” Phys. Rev. D **84** (Jul, 2011) .
13. Sindrum-II “Improved limit of Branching Fraction of  $\mu^- \rightarrow e^+$  in Titanium”, Phys Lett B **422** (1998) 334-338 (1998)



# Radiative Corrections for CE Signal

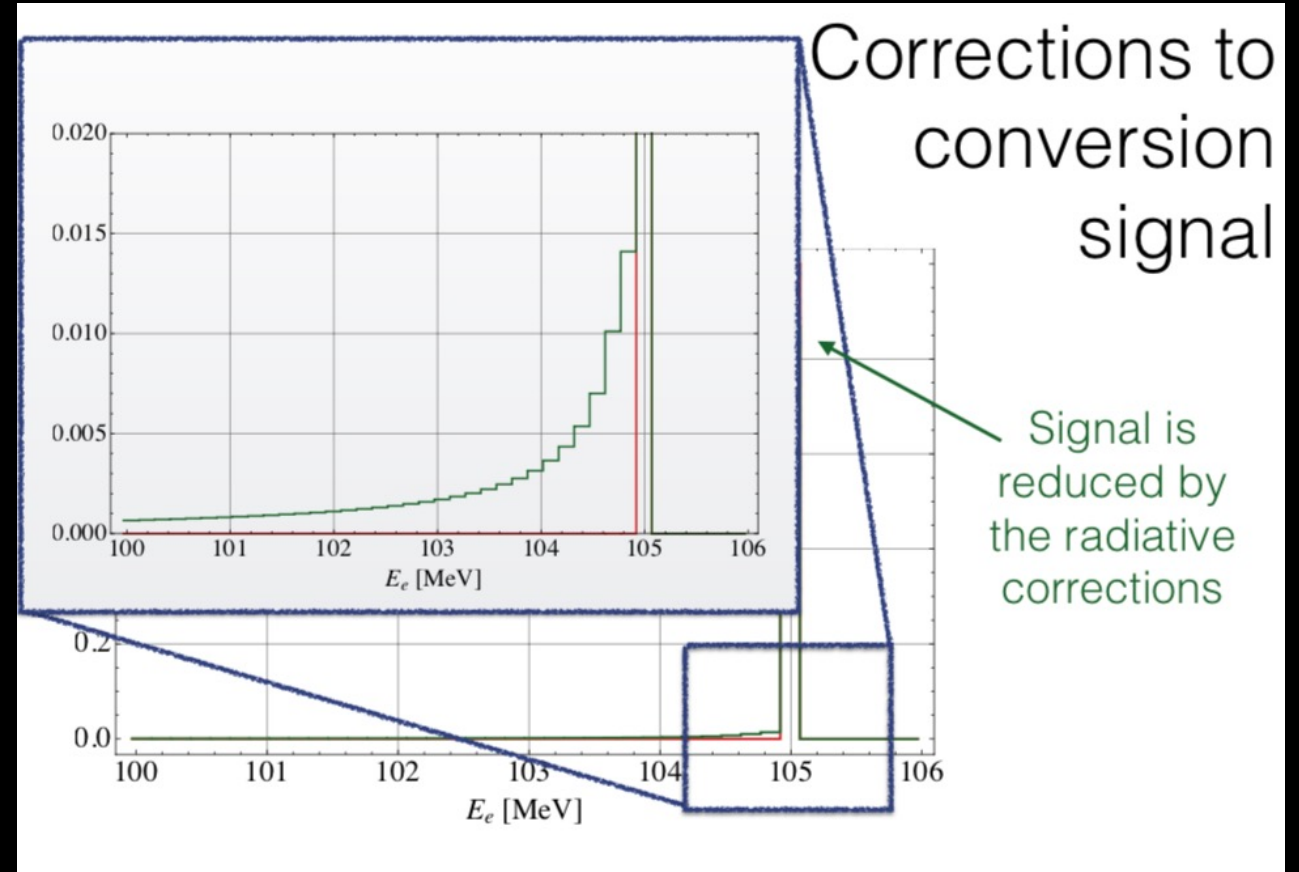
- Our signal also requires radiative corrections:

$$\frac{m_\mu}{\Gamma_0} \frac{d\Gamma}{dE_e} = \frac{\alpha}{2\pi} \left[ \left( \ln \frac{4E_e^2}{m_e^2} - 2 \right) \frac{E_e^2 + m_\mu^2}{m_\mu (m_\mu - E_e)} + P(E_e) \right]_+.$$

Universal part; proportional to the splitting function

Model dependent part (polynomial in electron energy)

Only the leading order in  $Z\alpha$





# g-2 Result: Implications for Mu2e

P. Paradisi / Nuclear Physics B (Proc. Suppl.) 248–250 (2014)

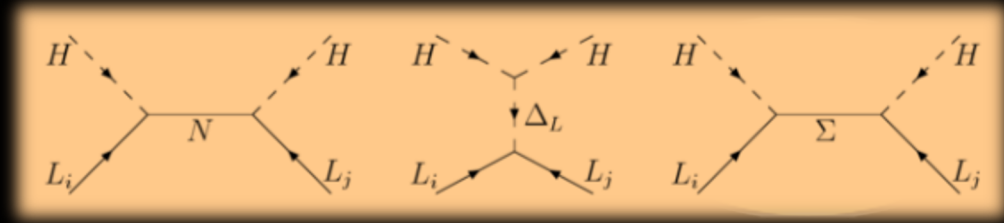
- Dipole transitions  $\mu \rightarrow e\gamma$  in the leptonic sector are accounted for by means of the effective Lagrangian :

$$\mathcal{L} = e \frac{m_\ell}{2} \left( \bar{\ell}_R \sigma_{\mu\nu} A_{\ell\ell'} \ell'_L + \bar{\ell}'_L \sigma_{\mu\nu} A_{\ell\ell'}^* \ell_R \right) F^{\mu\nu},$$

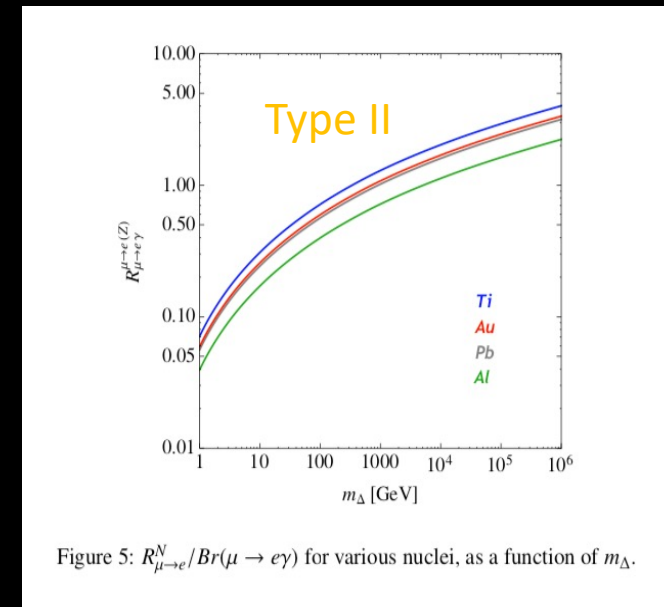
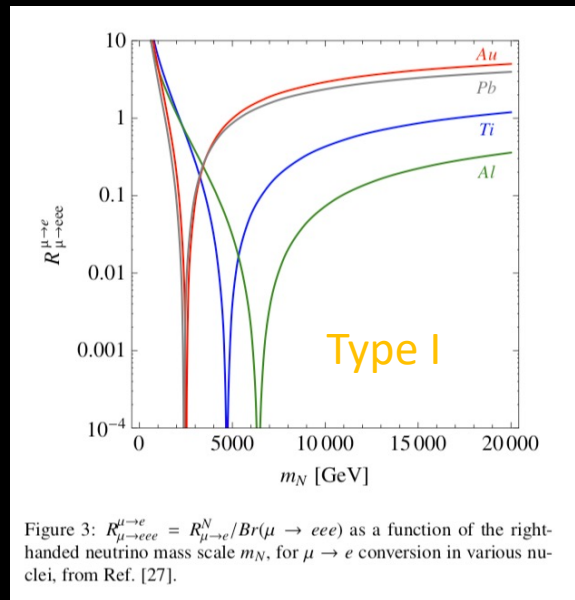
$$\frac{\text{BR}(\ell \rightarrow \ell' \gamma)}{\text{BR}(\ell \rightarrow \ell' \nu_\ell \bar{\nu}_{\ell'})} = \frac{48\pi^3 \alpha}{G_F^2} \left( |A_{\ell\ell'}|^2 + |A_{\ell'\ell}|^2 \right).$$

- The underlying  $\mu \rightarrow e\gamma$  transition can also generate lepton flavor conserving processes like the anomalous magnetic moments ( $\Delta a_\mu$ ) as well as leptonic electric dipole moments (EDMs,  $d_\mu$ ).
- In terms of the effective Lagrangian can write as :
 
$$\Delta a_\ell = 2m_\ell^2 \text{Re}(A_{\ell\ell}), \quad \frac{d_\ell}{e} = m_\ell \text{Im}(A_{\ell\ell}).$$
- On general grounds, one would expect that, in concrete NP scenarios,  $(\Delta a_\mu)$ ,  $d_\mu$  and  $\text{BR}(\mu \rightarrow e\gamma)$ , are correlated. In practice, their correlations depend on the unknown flavor and CP structure of the NP couplings and thus we cannot draw any firm conclusion that we would necessary see CLFV in the next generation, but this is of course a very promising result for muon physics!

# Example: See Saw Mechanisms



- See Saw Models can induce rates which are not suppressed by smallness of these masses.
- There are 3 ways of inducing  $\Delta L = 2$  Majorana neutrino masses from the tree level exchange of a heavy particle:
  - Type I exchange of right-handed neutrinos  $N_i$ ,
  - Type II exchange scalar triplet  $\Delta_L$ ,
  - Type II exchange of fermion triplets  $\Sigma_i$ .
- Knowledge of the neutrino mass matrix is not sufficient to be able to distinguish between the 3 seesaw models  $\rightarrow$  CLFV can help here.





# SUSY SO(10)

Complementary to Muon g-2 and LHC program:

## SUSY SO(10)

Consider SO(10) SUSY GUT model with very massive right-handed neutrinos. Can consider different hypothesis for the neutrino Yukawa couplings. Mu2e will be able to test all PMNS type and most CKM type SO(10).

L. Calibbi et al., JHEP 1211 (2012) 040

L. Calibbi, G. Signorelli arXiv:1709.00294

Muon g-2 results will also be helpful here.

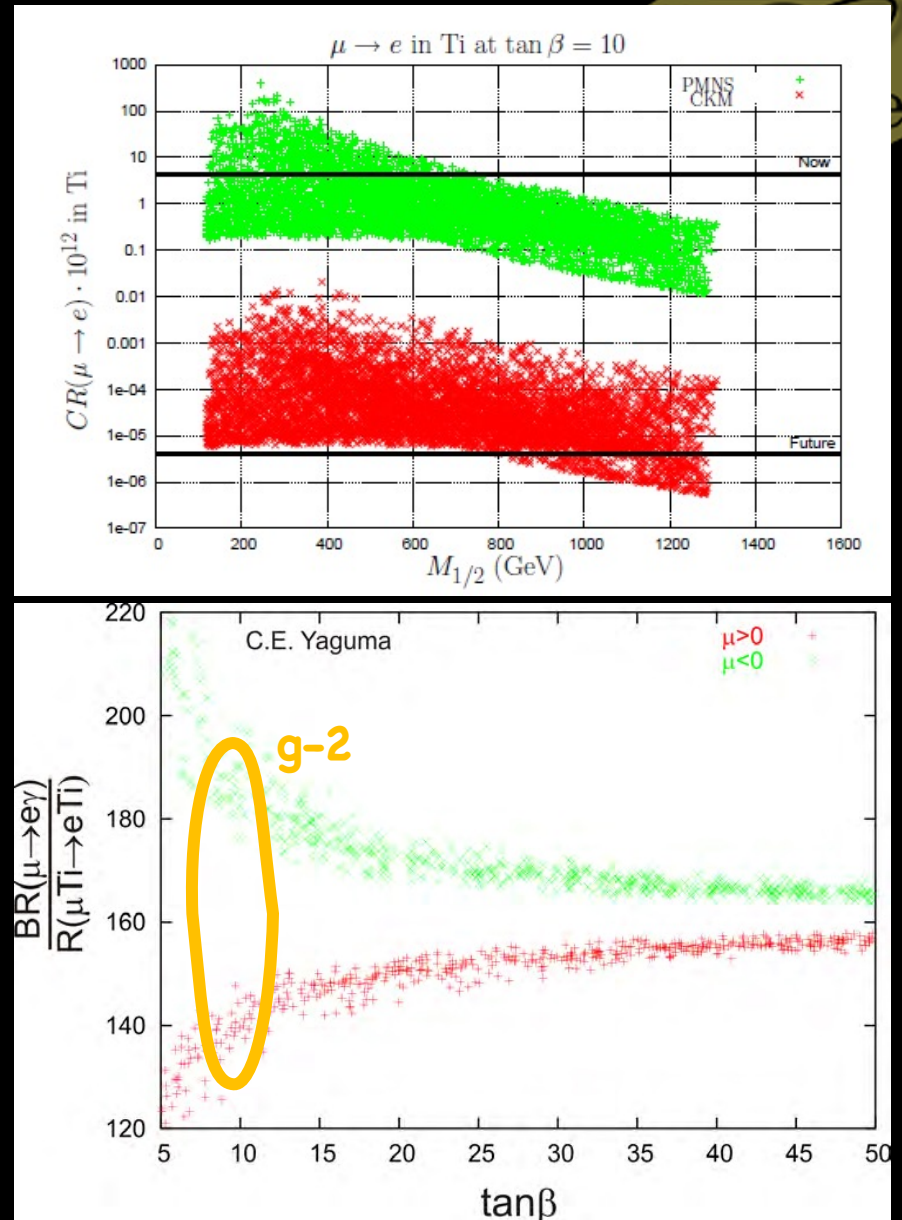
To allow discrimination among different models

Need:

- Observation of CLFV in more than one channel, and/or
- Evidence from LHC and/or g-2

Yaguna, hep-ph/0502014v2

Endo arxiv.org/abs/1303.4256v1 (g-2 SUSY .v. LHC constraints)



# COMET: Phased Implementation

